Tsunami Inundation Assessment for the Gisborne District Council

eCoast Limited
Marine Consulting and Research
P.O. Box 151
Raglan, New Zealand

jose@ecoast.co.nz

<BLANK PAGE>

Tsunami Inundation Assessment for the Gisborne District Council

Report Status

Version	Date	Status	Approved By:
V 1.0	6 June 2018	DRAFT	JCB
V 2.0	29 June 2018	DRAFT FINAL	JCB/CB

It is the responsibility of the reader to verify the currency of the version number of this report.

Jose C. Borrero Ph.D.

Cover Picture: Extents of the Yellow, Orange and Red inundation zones developed in this study compared to the extent of the previous evacuation zone (white line).

<BLANK PAGE>

CONTENTS

TABLE OF FIGURES

TABLE OF TABLES

1 INTRODUCTION

The objective of this work is to produce for the Gisborne District Council a set of tsunami inundation and evacuation zones compliant with guidelines set forth in MCDEM (2008). This publication defines the following three evacuation zones:

Red Zone

The red zone is intended as a shore-exclusion zone that can be designated off limits in the event of any expected tsunami. This represents the highest risk zone and is the first place people should evacuate from in any sort of tsunami warning. People could expect 'activation' of this zone several times during their life.

Orange Zone

The orange zone is intended to be the area evacuated in most if not all distant- and regional source of official warnings (i.e., warnings that extend beyond the red zone, for tsunami from sources more than one hour of travel time away from the mapped location). Local differentiation of this zone can be achieved using terms that are familiar to the community such as street names and key landmarks.

Yellow Zone

The yellow zone should cover all maximum credible tsunami, including the highest impact events. The intention is that the yellow zone provides for local-source maximum credible events, based on locally determined risk. People should evacuate this zone in natural or informal warnings from a local source event.

1.1 Historical Context

The study area for this project extends from Poverty Bay and Gisborne City in the south north to Hick's Bay (see Figure 1.1). This region of the coast sits astride the plate boundary between the Pacific and Australian tectonic plates. Being a subduction type plate interface, this area has the potential to produce large earthquakes and associated tsunami. Furthermore, the east coast of New Zealand faces in to the Pacific Ocean and is vulnerable to tsunami generated from around the Pacific Rim. Numerous reports, studies and scientific papers have been produced on the tsunami vulnerability of New Zealand's East Cape.

This area has experienced the effect of several near, regional and distant source tsunamis. The records of these events have been collected and organized in the "New Zealand Tsunami Database: Historical and Modern Records" which can be accessed at: http://data.gns.cri.nz/tsunami/index.html. This is an excellent resource for evaluation historical tsunami impacts for a region. We have compiled all the available records from this database relevant to the study area and reproduced them in Appendix 1 of this report. This includes all available records for the distant source tsunami of 1868 and 1877 from Peru and Chile, 1952 from the Aleutian Islands and 1960 from southern Chile. We also reproduce the historical information from the near source tsunami of 1946 (March and May) that affected the coast from Gisborne north to Tokomaru Bay.

Figure 1.1 Location map of the study area.

1.2 Prehistoric Tsunami Records

In addition to the historical database mentioned above, there is also a database of prehistoric or 'palaeo' tsunami records available online at: https://ptdb.niwa.co.nz . Data from this source can be viewed in an interactive map and two such maps are reproduced in Figure 1.2 below.

A brief inspection of the available data shows that very few palaeotsunami records are available within our study area. Indeed, of the three data points in our region two are prehistoric and one is 'unknown' with two having poor validity and one only having 'moderate' validity. We note however that the area to the south in and around Hawke's Bay and the Mahia Peninsula, as well as areas to the north west in the Bay of Plenty contain more records of identified potential tsunami evidence. Among the data records in the study site the inferred tsunami heights from the evidence are very small, less than 5 m with

inundation extents of 50 – 100 m. None of these records are clearly associated with any specific or known earthquake or tsunami event.

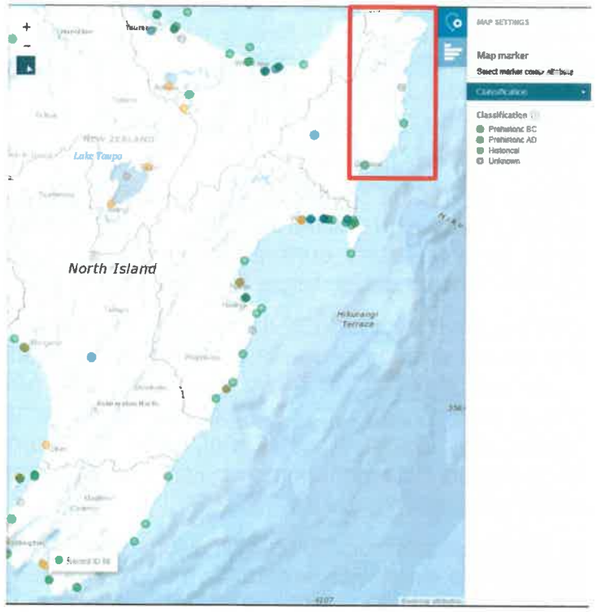

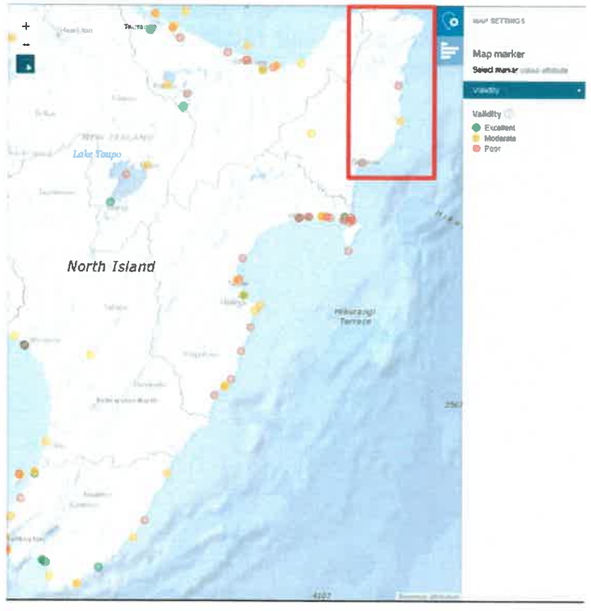

Figure 1.2 Location map of available palaeotsunami data records in and around the study region (red box). The records are colour coded by record type (top) and record validity (bottom).

1.3 The 1947 Gisborne Tsunami(s)

The 1947 Gisborne tsunamis (two tsunamis occurring in March and May of that year) remain rather enigmatic events. The tsunami effects were well documented (Eiby, 1982) and describe tsunami heights of up to 10 m in the March 1947 event with extensive penetration of the tsunami surge up coastal rivers. Later that year, in May, a second earthquake and associated tsunami occurred with somewhat smaller tsunami (~5-6 m) heights affecting ~50 km of the coast. The full available records of this event from the GNS Historical database are reproduced in Appendix 1 of this report.

These events are enigmatic in that the causative earthquakes were relatively weak (~M=7) and were not strongly felt by coastal residents. Most recent assessments attribute the anomalously large wave to a 'tsunami earthquake' the special class of earthquakes responsible for local tsunami that are much larger than the magnitude alone would suggest.

Wang et al. (2009) [described in Power (2013)] modelled the March event and showed that variable slip distribution over fault segments with reduced crustal rigidities (slower rupture velocity) produced a somewhat better fit to the observed data, however, none of the modelling produced results that accurately reproduced the observed 10 m tsunami heights (Figure 1.3). This modelling was updated in Bell et al., (2014) and produced a better fit to the magnitude of the measured data although the along coast location of the modelled maxima did not match the measured or observed data.

It should be noted that based on probabilistic analyses (described in Section 4.1 below) an offshore tsunami height of 10 m would correspond to the 84th percentile tsunami height at recurrence intervals of approximately 300 – 600 years and to a 50th percentile tsunami height at recurrence intervals of approximately 700 – 1600 years. As such, this event sits well below the desired level of 84th percentile, 2500-year recurrence interval desired for defining a maximum credible event type source.

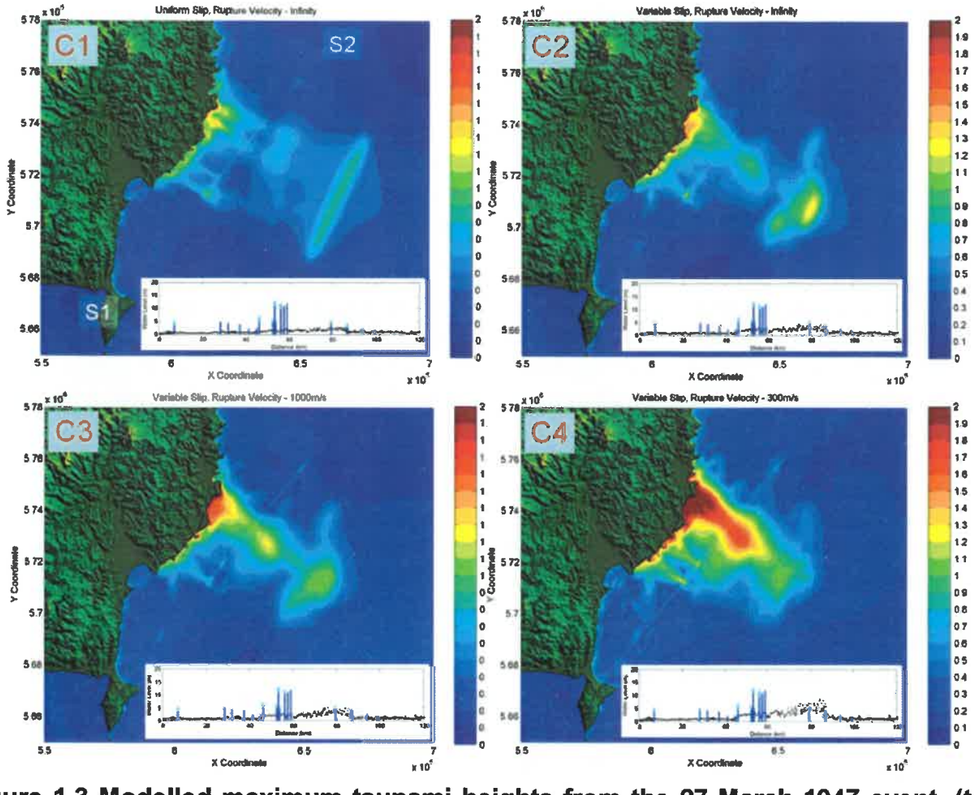

Figure 1.3 Modelled maximum tsunami heights from the 27 March 1947 event. (top left) shows results from uniform slip with instantaneous rupture; (top right) shows variable slip with instantaneous rupture (bottom left) shows variable slip with a rupture velocity of 1000 m/s; and (bottom right) shows variable slip with a rupture velocity of 300 m/s. Inset figure shows comparison between modelled tsunami height (black line) and observed data (vertical bars). (From Wang et al., 2009, reproduced in Power, 2013)

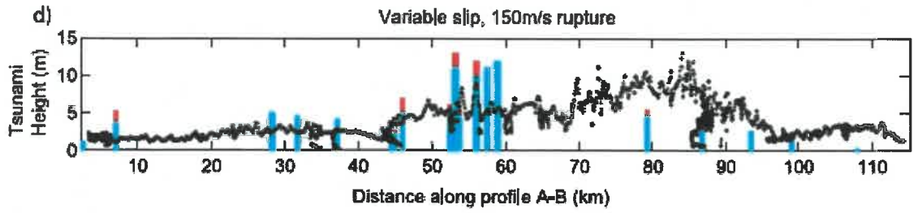

Figure 1.4 Modelled runup results (black) compared to historical data (blue bars) for the March 1947 tsunami (from Bell et al. 2014).

2 MODELLING APPROACH

The numerical modelling presented in this study was carried out using the Community Model Interface for Tsunamis (ComMIT) numerical modelling tool. The ComMIT model interface was developed by the United States Government National Oceanic and Atmospheric Administration's (NOAA) Centre for Tsunami Research (NCTR) at the Pacific Marine Environmental Laboratory (PMEL) following the December 26, 2004 Indian Ocean tsunami as a way to efficiently distribute assessment capabilities amongst tsunami prone countries.

The backbone of the ComMIT system is a database of pre-computed deep-water propagation results for tsunamis generated by unit displacements on fault plane segments (100 x 50 km) positioned along the world's subduction zones. Currently, there are 1,691 pre-computed unit source propagation model runs covering the world's oceans included in the propagation database. Using linear superposition, the deep ocean tsunami propagation results from more complex faulting scenarios can be created by scaling and/or combining the pre-computed propagation results from several unit sources (Titov et al., 2011). The resulting trans-oceanic tsunami propagation results are then used as boundary inputs for a series of nested near shore grids covering a coastline of interest. The nested model propagates the tsunami to shore computing wave height, velocity and overland inundation. The hydrodynamic calculations contained within ComMIT are based on the MOST (**M**ethod **O**f **S**plitting **T**sunami) algorithm described in Titov and Synolakis (1995, 1997, 1998) and Titov and Gonzalez (1997). The ComMIT tool can also be used in conjunction with real time recordings of tsunami waveforms on one or more of the deep ocean tsunameter (DART) stations deployed throughout the oceans to fine tune details of an earthquake source mechanism in real time. An iterative algorithm that selects and scales the unit source segments is used until an acceptable fit to the observed DART data is met.

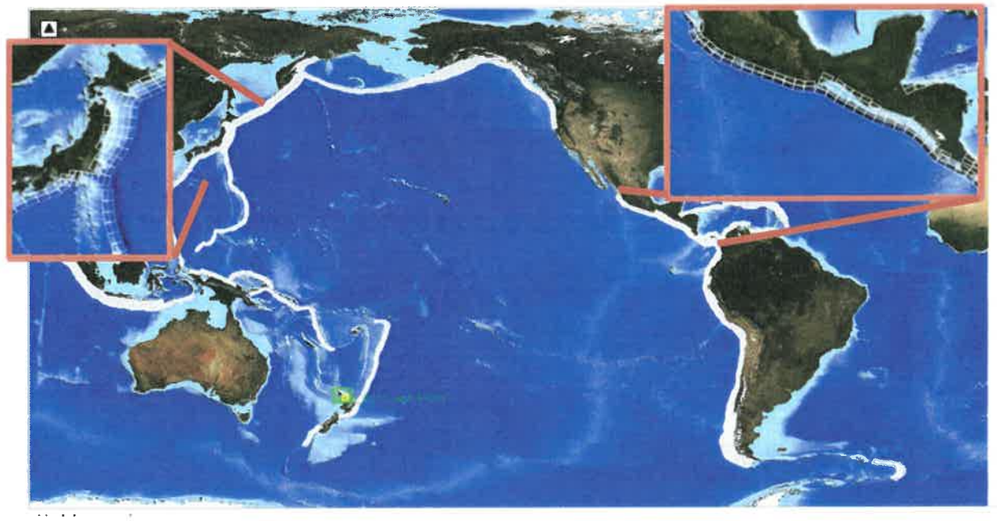

Figure 2.1 The ComMIT propagation model database for tsunamis in the world's oceans. Insets show the details of the source zone discretization in to rectangular sub-faults.

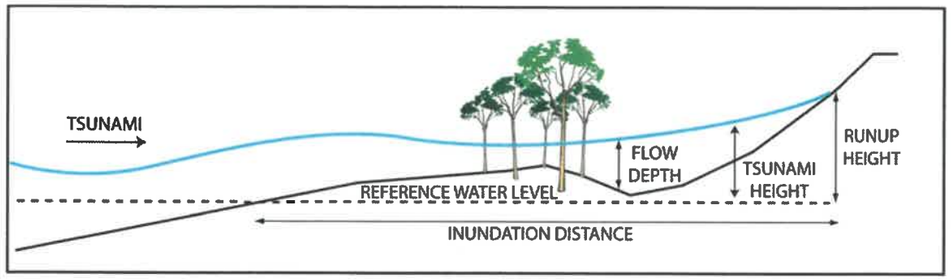

Figure 2.2 Definition sketch for tsunami height, flow depth, runup and inundation distance.

2.1 A Note on Terminology

There is often some ambiguity in the terminology used to describe the size of a tsunami. Generally, the term 'height' is used as defined in the figure above, i.e. the measure of a distance above a particular datum. However, since tsunamis are waves, it is also common to use the term 'amplitude' which is the distance (height) above or below a particular datum. For a perfectly symmetrical sine wave, the 'height' is twice the 'amplitude'.

In Power (2013) he writes:

"TSUNAMI HEIGHT (m) is the vertical height of waves above the tide level at the time of the tsunami (offshore it is approximately the same as the AMPLITUDE). It is far from constant, and increases substantially as the wave approaches the shoreline, and as the tsunami travels onshore. The term "WAVE HEIGHT" is also often used, but there is a potential ambiguity as many scientists define WAVE HEIGHT as the peak-to-trough height of a wave (approximately twice the amplitude). Note that this is a change in terminology from the 2005 Tsunami Hazard and Risk Review, intended to bring greater consistency with international usage of these terms.

And with regards to runup he says:

"TSUNAMI RUN-UP (m), a measure much used in tsunami-hazard assessment, is the elevation of inundation above the instantaneous sea level at the time of impact at the farthest inland limit of inundation. This measure has a drawback in that its relationship with the amplitude of the waves at the shore depends markedly on the characteristics of waves and on the local slopes, vegetation, and buildings on the beach and foreshore areas, so it is highly site-specific."

And finally, with regards to the hazard curves for the National Tsunami Hazard Model he writes:

"in the curves shown here the 'maximum amplitude' should be interpreted as the tsunami height measured at the location within the section where it is highest"

Hence there is a degree of interchangeability in the use of 'height' and 'amplitude'. In this report we use 'height' for the elevation of the water surface above the sea level datum at the start of a model run. When discussing the hazard curves, we use the term 'amplitude' in line with Power (2013), which, as we see above, is used interchangeably with 'height'.

2.2 Numerical Modelling Grids

The Gisborne District Council provided LiDAR topography data for construction of the numerical modelling grids. The data were provided with a reference datum of Gisborne 1926 Vertical Datum and a WGS84 projection. The data were combined with additional data sets covering the regional offshore bathymetry and on land topography. This included the Shuttle Radar Topography Mission (SRTM) 90 m resolution topography, 200 m resolution bathymetry from NIWA, as well as nautical chart data from Land Information New Zealand (LINZ). The coverage areas of the various data sets are shown in Figure 2.3. The data were combined in to a master set of (x, y, z) triplets and then gridded in to different resolutions and coverage areas using a Kriging algorithm. Model grids were set up for mean sea level (MSL).

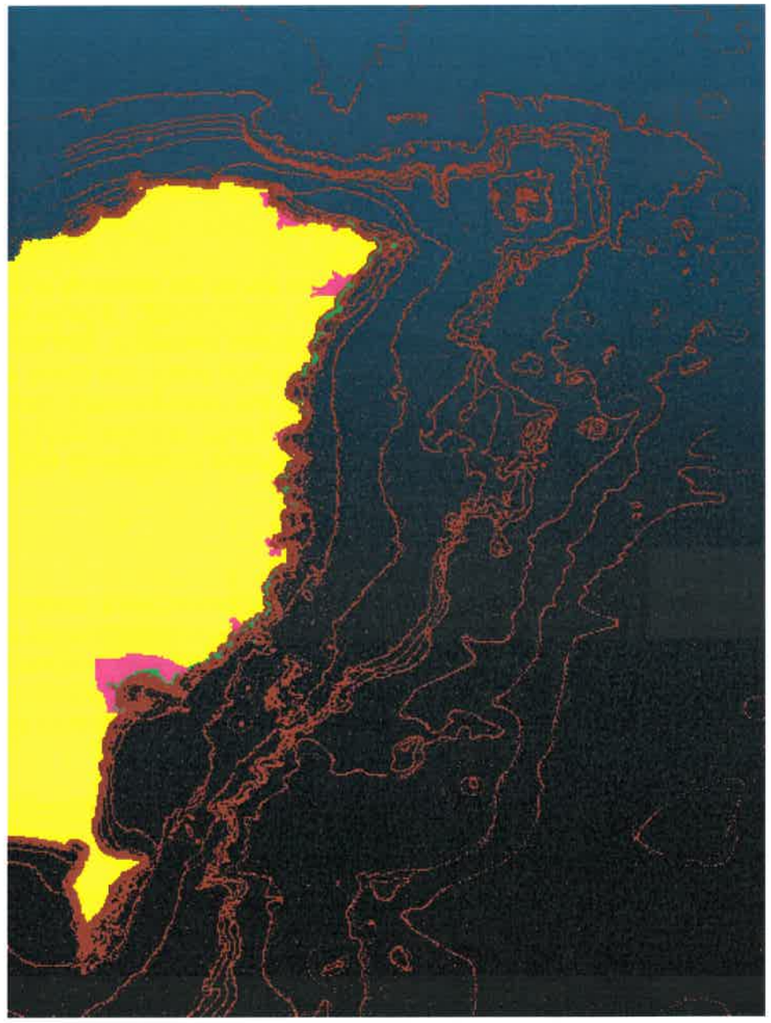

Figure 2.3 Coverage area of the different bathymetry data sets. Yellow: SRTM topography, Pink: GDC supplied LiDAR, RED: LINZ digitised charts contours and sounding points, Green: hand digitized near-shore bathymetry.

Each model run utilized the same A grid. Five separate B level grids were set up (Figure 2.4 and Figure 2.5) along with 14 separate C level modelling grids (Figure 2.5). Details on each of the model grids used in this study are presented in Table 2.1 while plots of the individual grids used in this study are reproduced in Appendix 2.

Table 2.1 The details of the various computational grids used in the study.

Grid	nx (nodes)	ny (nodes)	dx (m)	dy (m)	max dt (sec)
A Grid					
A	97	168	2866	3000	13.14
B Grids					
B0	181	192	200	200	5.61
B1	158	195	200	200	5.21
B2	131	195	200	200	6.37
B3	164	195	200	200	4.67
B4	207	126	200	200	2.57
C Grids					
Hicks 10 m	1050	1154	10	10	0.32
Waiapu 50 m	212	223	50	50	2.20
Whareponga 50 m	150	312	50	50	2.18
Waipiro Bay 50 m	159	223	10	10	2.36
Tokomaru 10 m	788	998	10	10	0.51
Anaura 50 m	176	168	50	50	2.73
Tolaga 10m	831	889	10	10	0.54
Waihau 50 m	176	290	50	50	1.86
Whangara 10 m	437	390	10	10	0.58
Pouawa 50 m	207	198	50	50	2.11
Makorori 10 m	530	389	10	10	0.53
Wainui 10 m	420	620	10	10	0.56
Gisborne: Port and Town 10 m	349	334	10	10	0.74
Poverty Bay 20 m	1001	834	20	20	1.09

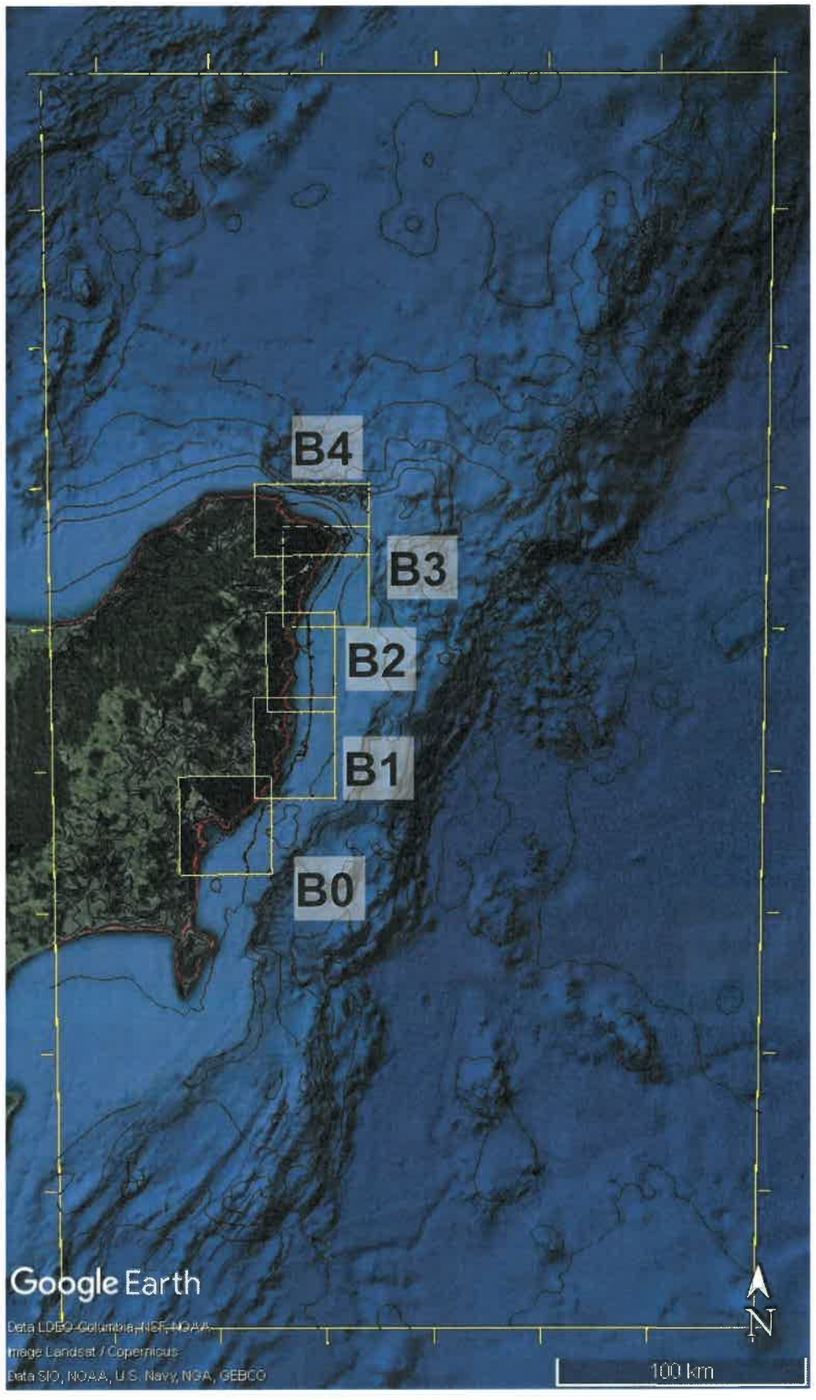

Figure 2.4 Extents of the A and B level modelling grids.

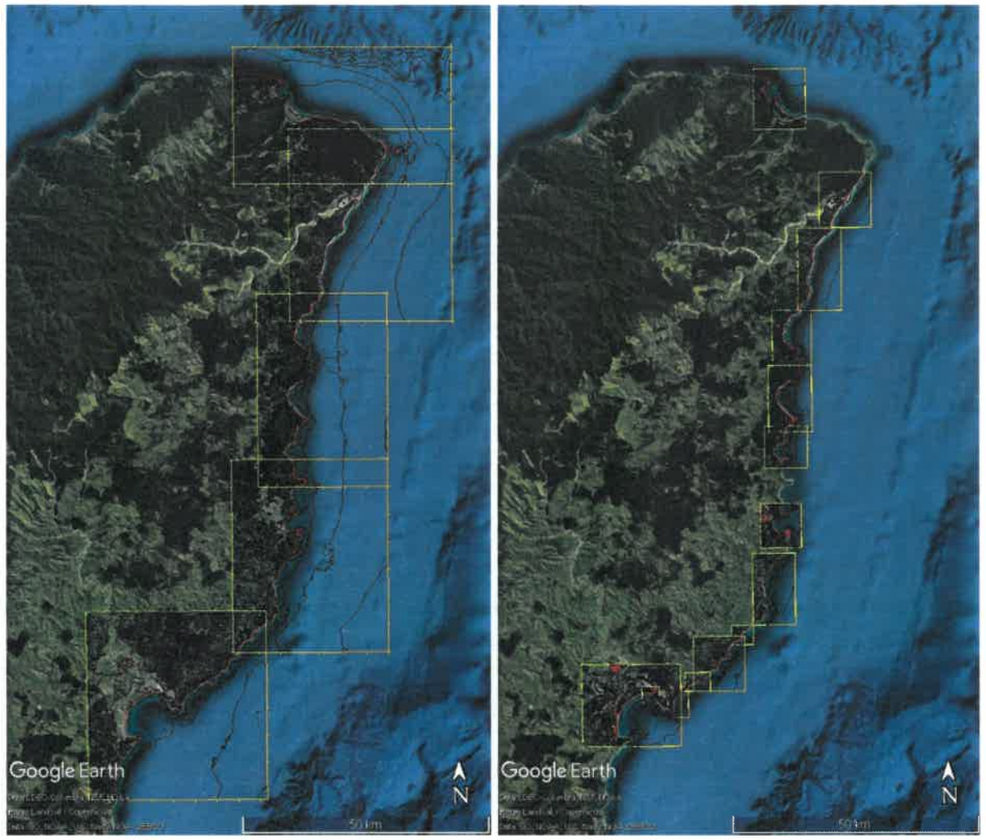

Figure 2.5 Zoomed in view of the extents of the B level (left) and C level (right) modelling grids.

3 VALIDATION OF THE COMMIT TSUNAMI MODEL

The ComMIT model was validated for both a distant source and near source events.

3.1 Case 1: The February 27, 2010 Maule, Chile Earthquake and Tsunami

Two different source models were available for the 2010 Chile tsunami. The first source model, based on real time DART tsunameter inversions, was developed in the hours immediately following the earthquake. This source was later updated to refine the agreement between the numerical model and the DART tsunameter records.

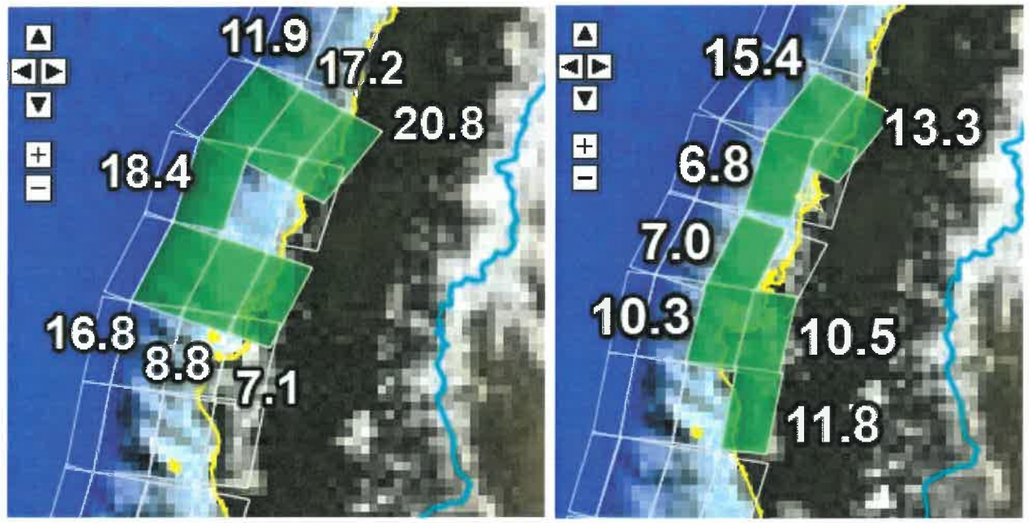

Figure 3.1 The two tsunami sources used to model the 2010 Chile tsunami. The original DART constrained source (left) and the updated source (right). Numbers represent slip amount applied to each fault segment.

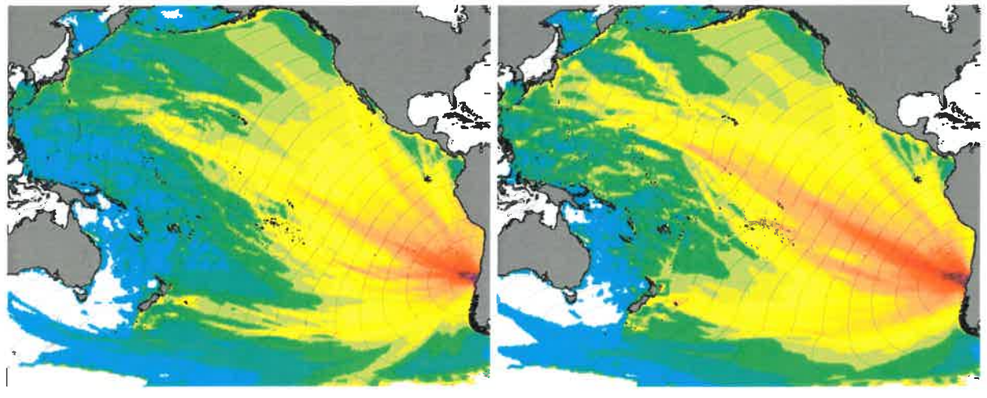

Figure 3.2 Far field propagation patterns for the two tsunami source models shown in Figure 3.1.

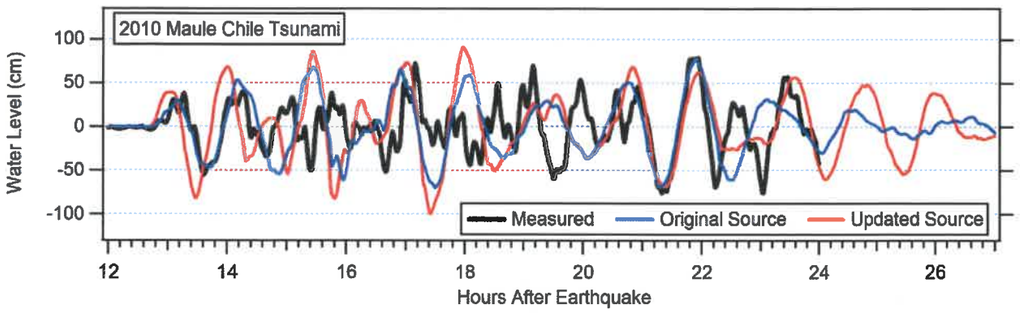

Figure 3.3 Modelled water level time series compared to measured data at the Port Gisborne tide gauge for the 2010 Maule, Chile tsunami.

3.2 Case 2: The March 11, 2011 Tohoku Earthquake and Tsunami

The March 11, 2011 Tohoku earthquake and tsunami presents an excellent case study for the validation of the ComMIT model. The tsunami event was recorded on tide gauges throughout New Zealand with a wealth of data recorded on 5 water level gauges and one current meter in Tauranga Harbour (Lynett et al., 2012, Borrero et al., 2012, Borrero and Greer 2013).

For the validation, the MOST/ComMIT model was initialised using the tsunami source model derived during the Tohoku event using measured tsunami data. The source model is based on 100 x 50 km fault segments with different slip amounts applied to each segment (see Figure 3.4). The use of real-time data from the DART tsunameters, enabled the development and distribution of this source model approximately 1.5 hours after the earthquake. This source was used to make timely threat assessments for communities on the US West Coast (Wei et al., 2013, 2014) and in New Zealand (Borrero et al., 2012). More details on the inversion process and tsunami source can be found in (Percival et al., 2010).

Several months following the event, another tsunami source was developed for the Tohoku tsunami. This featured a different slip distribution and is shown in the right-hand panel of Figure 3.4. Both source models are used to initialise the tsunami model. The far-field propagation patterns are shown in Figure 3.5 and the modelled water level time series at the Port Gisborne tide gauge is presented in Figure 3.6. The results show that both sources do a relatively good job at modelling the tsunami heights throughout the duration of the event, except for a period of overprediction by both models between 15.5 and 17.5 hours after the earthquake.

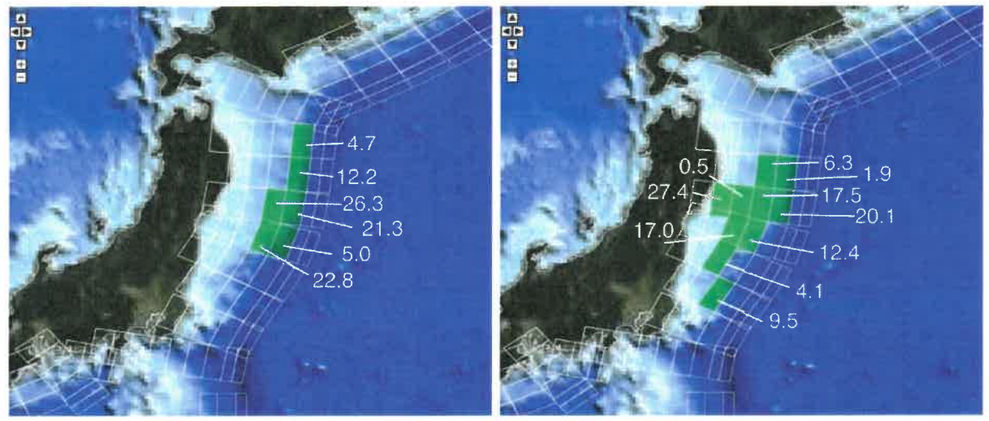

Figure 3.4 Tsunami source models used for the 2011 Tohoku tsunami. The amount of slip on each segment is indicated in white. The left panel is the slip distribution developed in near real-time in the hours following the earthquake and used for real-time forecasting (Wei et al. 2013) while the right panel is the slip distribution developed months after the event.

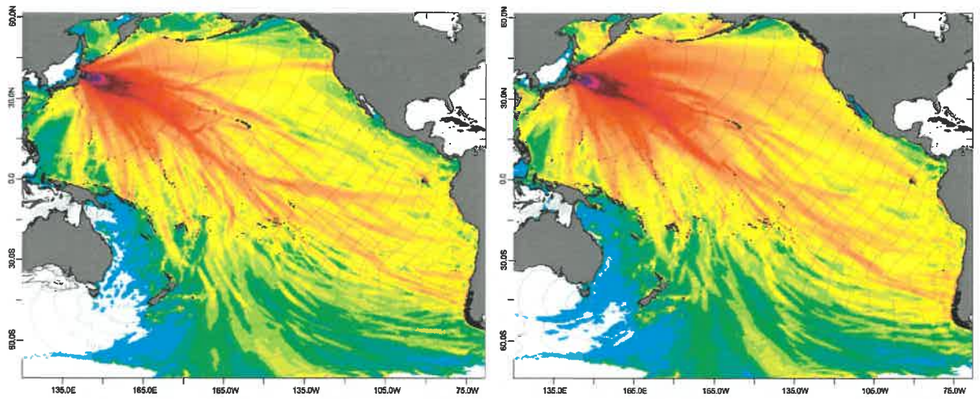

Figure 3.5 Far field propagation patterns for the two tsunami source models shown in Figure 3.4.

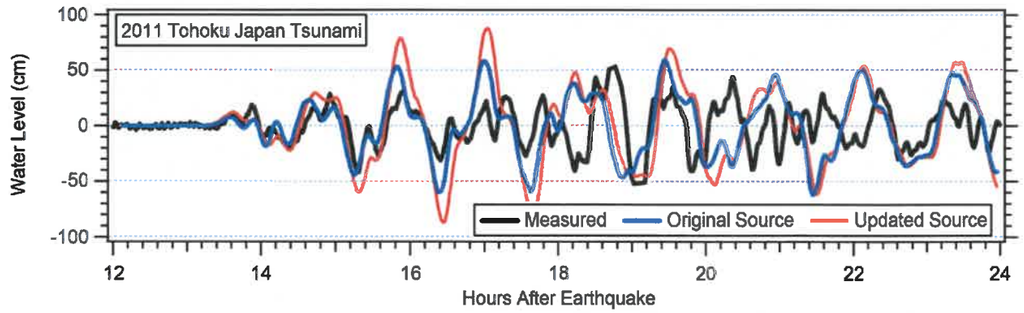

Figure 3.6 Modelled water level time series compared to measured data at the Port Gisborne tide gauge for the 2011 Tohoku, Japan tsunami.

3.2.1 Inundation along the Sendai Plain During the 2011 Tohoku Tsunami

The 2011 Tohoku tsunami caused extensive overland inundation along the east coast of Japan. The largest inundation distances of up to 5 km were seen in on the plains south of Sendai City in the Miyagi Prefecture. The MOST/ComMIT tsunami model – the same model used in this study - was used by Wei et al. (2013) to accurately model the inundation extents. We present the images below for two purposes: 1) to show that the numerical model used in this study is capable of accurately reproducing extreme tsunami inundation extents and 2) to prepare the reader for the results of the modelling study that will be presented in Sections 4 and 6 below.

Figure 3.7 (left) Purple shading denotes inland inundation extents in the vicinity of Sendai, Japan (right) the Poverty Bay and Hawke's Bay region shown at the same scale as the Sendai Map.

Figure 3.8 Images of the overland inundation extents over the Sendai Plain.

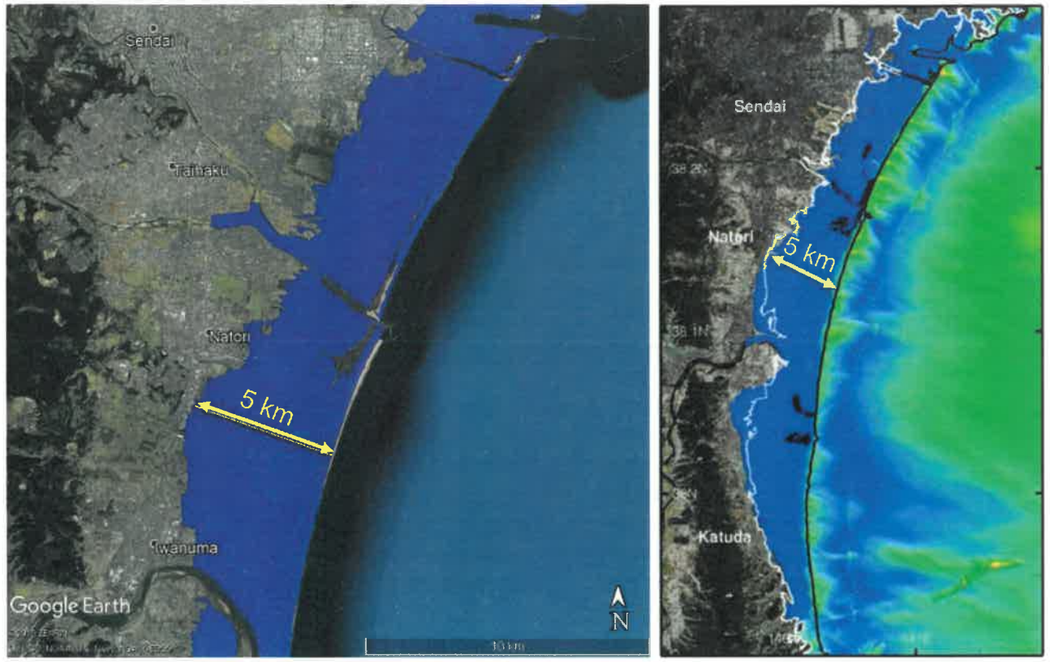

Figure 3.9 (left) close of up the inundation extents over the Sendai Plain. The yellow line across the inundation zone measures 5.2 km. (right) The MOST/ComMIT model results of Wei et al., (2013) compared to the measured inundation extents (white line).

3.3 Case 3: The September 2, 2016 East Cape Earthquake and Tsunami

On 2 September 2016 at 4:37 am NZST (1 September 16:37 UTC), a Magnitude 7.1 (GeoNet) earthquake struck just north-east of the East Cape of New Zealand. The event was felt throughout the North Island. More than 4,000 people filed felt earthquake reports with GeoNet with reports coming in from as far away as Chatham Island and Christchurch (GeoNet, 2017). The event created a small tsunami that was recorded on tide gauges in Gisborne and across the Bay of Plenty.

This event is important in that it was relatively strong and occurred along the Tonga-Kermadec subduction zone and in an area considered as the 'worst-case' source region for generating tsunamis affecting the East Cape, Bay of Plenty, Coromandel and Northland coasts – this due to its proximity and associated short travel times to these regions.

The source mechanism for this event however, was not a straightforward subduction zone event. The strike of the fault plane was oblique to and the source region was displaced west of the trench axis, suggesting a seismic rupture within the overriding Australian plate (Figure 3.11, top panel). Additionally, the sense of the rupture was that of a 'normal' fault - rather than a thrust or 'reverse' fault commonly associated with ruptures on a subduction zone interface. This means that the seafloor displacement above the source area was downward (i.e. negative) rather than upward (uplift). This is indicated by the direction of the slip vector arrows in the bottom panel of Figure 3.11.

To model this event using the pre-computed sources in the ComMIT database, some assumptions and approximations were necessary. Firstly, it was necessary to use a fault segment located to the east of the actual source region. Next, a negative average displacement was applied to the fault plane to produce a negative initial seafloor displacement. Two slip amounts were trialled, -0.4 m and -0.6 m.

The model results are compared to measured tide gauge data at Lottin Point and Tauranga Harbour in Figure 3.12. The comparison of the waveform at Lottin Point is remarkably good - given the approximations - with the results from the two source models neatly bracketing the measured data. Note that the modelled time series had to be shifted 7 minutes earlier to match the timing of the measured data. This accounts for the fact that the source region used in the model is located further away to the west of the actual source region, thus requiring more time for the wave to reach the tide gauge.

The results for Tauranga are not as good with the model over predicting the measured wave heights and requiring a 14-minute time shift to match the timing of the peaks and troughs. However, this is understandable given the very small size of the tsunami and the degree of attenuation that likely occurred as this small signal passed through the narrow entrance of Tauranga Harbour.

Given the limitations of the ComMIT model, the results are good and show that it can be used to accurately predict tsunami heights along the New Zealand coast from near-field tsunami sources

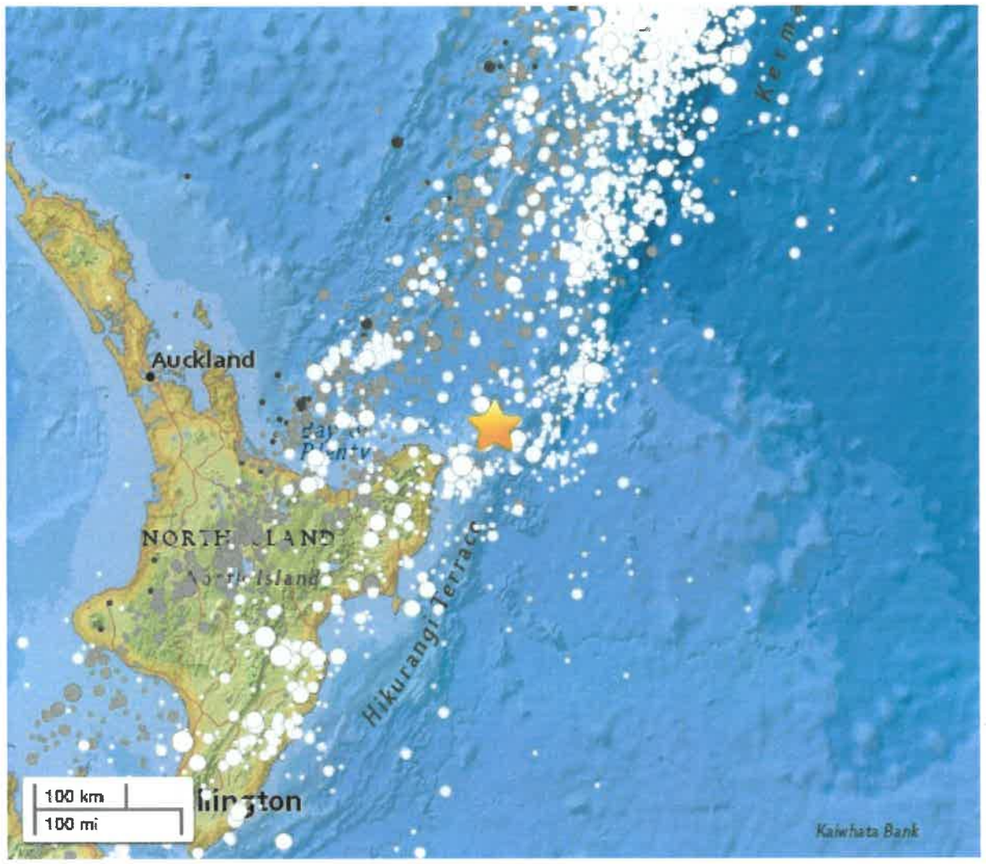

Figure 3.10 Source location of the September 2nd East Cape Earthquake (USGS, 2017).

Figure 3.11 (following page) Top panel: Earthquake source model for the September 2, 2017 East Cape earthquake (reproduced from USGS, 2017). The top panel shows the location of the fault plane (white region). Epicentre of the mains shock is indicated by a star with aftershocks indicated by black circles. Coloured patches indicate coseismic slip amounts according to the colour scale. The thin red line is the top of the fault plane. The white line is the axis of the Tonga-Kermadec Trench. The purple rectangle shows the location of a 100x50 km fault plane source available in the ComMIT tsunami modelling database. Bottom panel: A detail of the slip distribution along the fault plane with the amount of slip indicated by the colour scale. The location of the earthquake hypocentre is indicated by the star with the arrows indicating the direction of the rupture displacement. The contour lines are the timing (in seconds) of the rupture. The red arrow at the top of the fault plane corresponds to the red arrow in the upper panel. The purple box shows the dimensions of a 100x50 km fault plane.

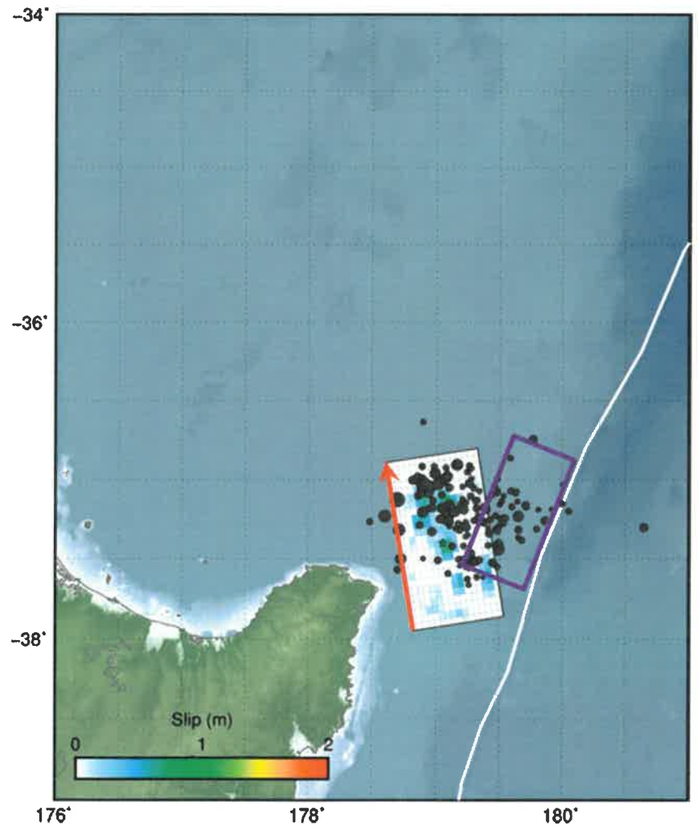
-34°
-36°
-38°
176°
178°
180°
Slip (m)
0
1
2

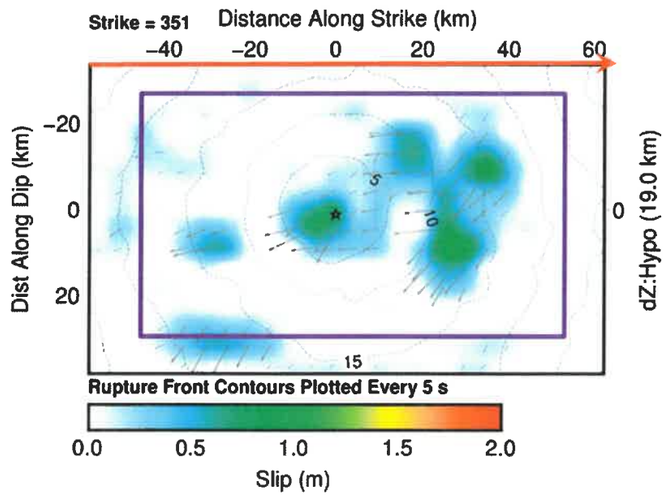
Strike = 351
Distance Along Strike (km)
-40
-20
0
20
40
60
Dist Along Dip (km)
-20
0
20
dZ:Hypo (19.0 km)
0
5
10
15
Rupture Front Contours Plotted Every 5 s
0.0
0.5
1.0
1.5
2.0
Slip (m)

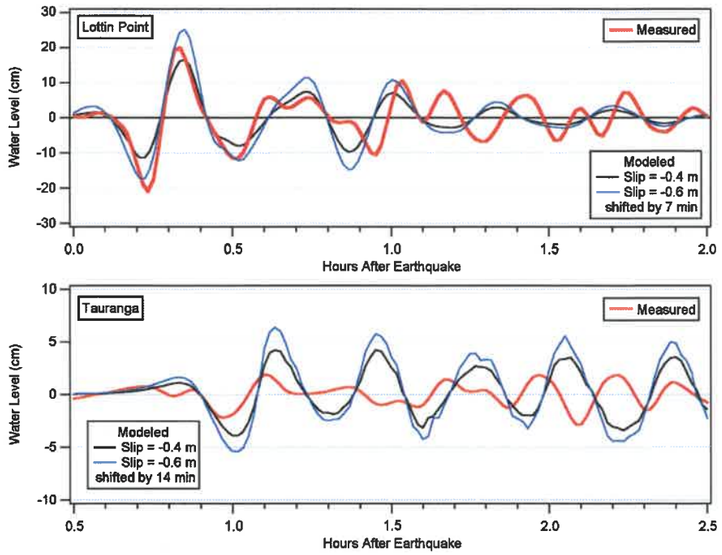

Figure 3.12 Modelled (blue and black traces) versus measured (red trace) water levels at Lottin Point (top) and Tauranga (bottom) for the 1 September tsunami.

4 TSUNAMI SOURCE CHARACTERIZATION

As noted above, the guidelines for the determination of the tsunami evacuation zone extents are based on the severity of the tsunami with the Yellow Zone corresponding to a 'Maximum Credible Event' type source, the Orange Zone corresponding to a severe tsunami event for which there is ample time for warning and evacuation and the Red Zone corresponding to the most commonly occurring scenario resulting in a 'marine and beach' threat level.

Thus, we conducted a series of simulations considering the effects of tsunami sources over a range of magnitudes. The objective of these tests was to determine the best source or set of sources to use for each of these evacuation levels.

4.1 Recurrence Interval Analysis

The GNS (Power 2013, 2014) probabilistic model was run on a numerical grid of approximately 200 m resolution. From this grid, polygons were defined for different coastal areas (Figure 4.1 and Figure 4.2). The maximum computed tsunami amplitudes from within each polygon for each model run in the probabilistic analysis were then used to produce the hazard curves. The hazard curves from the Power (2013, 2014) report are reproduced in Figure 4.3 below. By selecting a recurrence interval (RI) of interest, one can draw a vertical line to determine the corresponding 16th, 50th and 84th percentile tsunami amplitudes for that hazard level. The Maximum Credible Event (MCE) is taken to be a source capable of generating the 84th percentile tsunami heights for the 2500-year RI.

The probabilistic national tsunami model produced by GNS (Power et al., 2013) was used as the basis for this inundation mapping exercise. This model defined nine regions along the coast that coincide with the geographic extents for this study (Figure 4.1). For each of these regions, separate tsunami hazard curves were produced that give maximum offshore tsunami heights as a function of recurrence interval. These curves are then used to determine the recurrence interval associated with a tsunami height for a particular earthquake source.

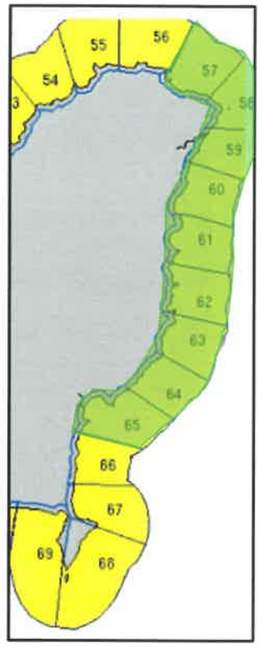

Figure 4.1 Coastal segments considered for this project (57-65) shaded in green.

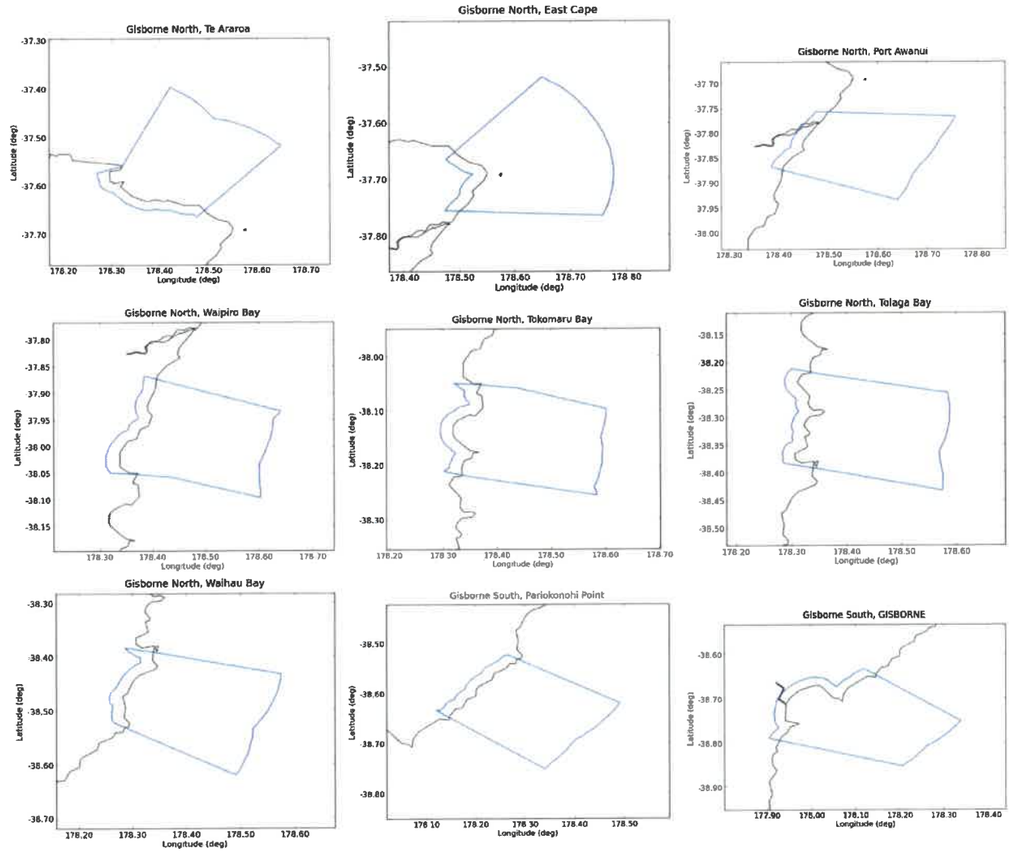

Figure 4.2 The nine target regions from the probabilistic modelling that are applicable to this study.

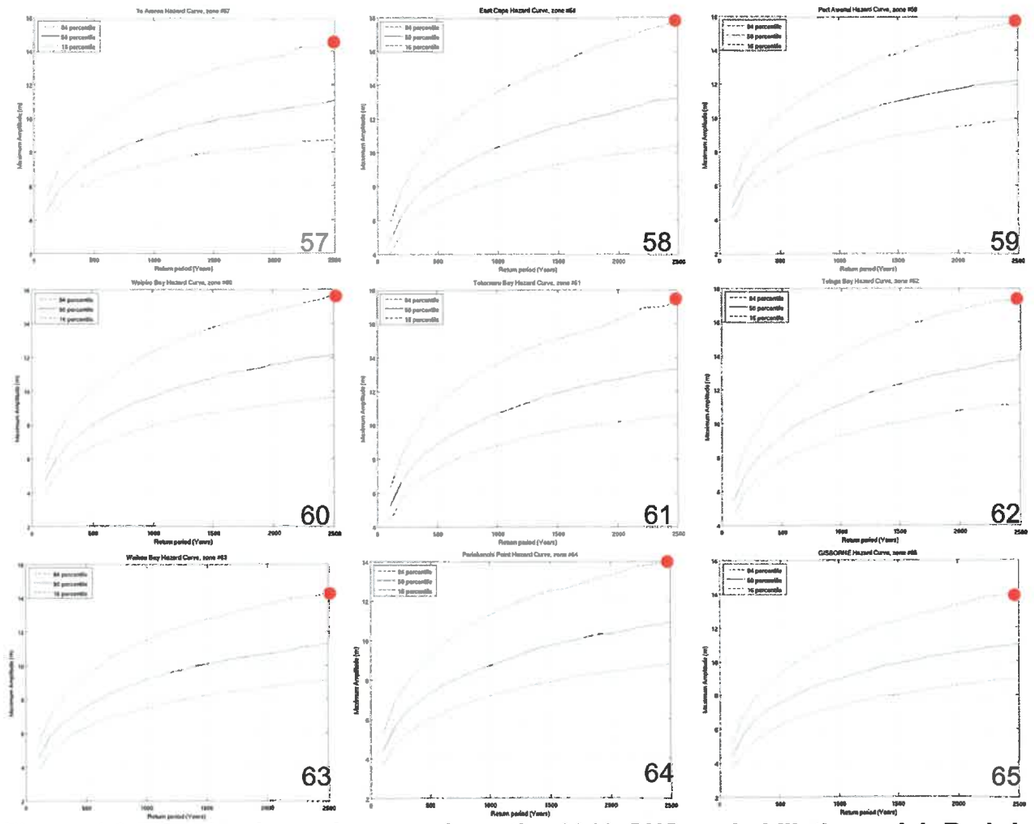

Figure 4.3 The nine hazard curves from the 2013 GNS probabilistic model. Red dot denotes the 84th percentile, 2500-year RI offshore tsunami height. Height values for the maximum credible event (MCE) are listed in Table 4.1 below.

Table 4.1 Offshore tsunami heights associated with the maximum credible event (MCE) for each of the nine coastal regions.

Name	Region Number	MCE H (m)
Te Araroa	57	14.5
East Cape	58	17.8
Port Awanui	59	15.8
Waipiro Bay	60	15.8
Tokomaru Bay	61	17.5
Tolaga Bay	62	17.5
Waihau Bay	63	14.2
Pariokonohi Point	64	14.0
Gisborne/Poverty Bay	65	14.0

4.2 Sensitivity Analysis for Near Field Tsunami Sources

To begin the assessment, we first considered an extreme near-field event as the source for an MCE type tsunami event. We trialled several different source configurations to match the maximum tsunami amplitudes in the hazard curves described above. In our modelling we are focussing on the tsunami amplitudes in the intermediate B-level grid, as this matches the model grid resolution of 200 m used in the determination of the hazard curves. For this initial sensitivity assessment, we will focus on the Poverty Bay region, Zone 65 from the GNS probabilistic assessment. The target geographic region and the associated hazard curve are presented in Figure 4.4.

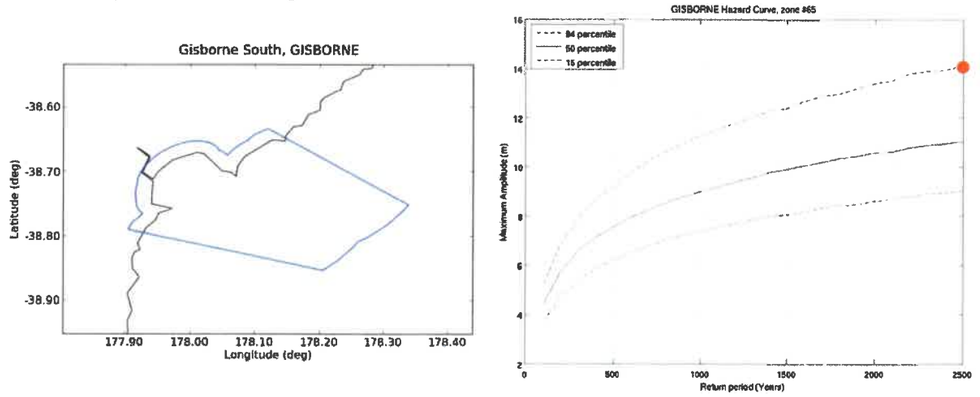

Figure 4.4 The Gisborne target region and associated hazard curve. The target tsunami height is ~14 m

We start first by looking at the relative inundation extents for events with slip concentrated on one segment of the shallow portion of the subduction zone interface. This type of rupture would be analogous to a 1947 type tsunami source. In Figure 4.5 we compare inundation extents for ruptures with 5 m and 15 m of co-seismic slip corresponding to earthquake magnitudes (M_W) of 8.0 and 8.3 respectively. The maximum tsunami amplitude produced in the offshore B level grid for these cases is 5.7 and 14.4 m respectively, roughly corresponding to the slip amount on the fault segment.

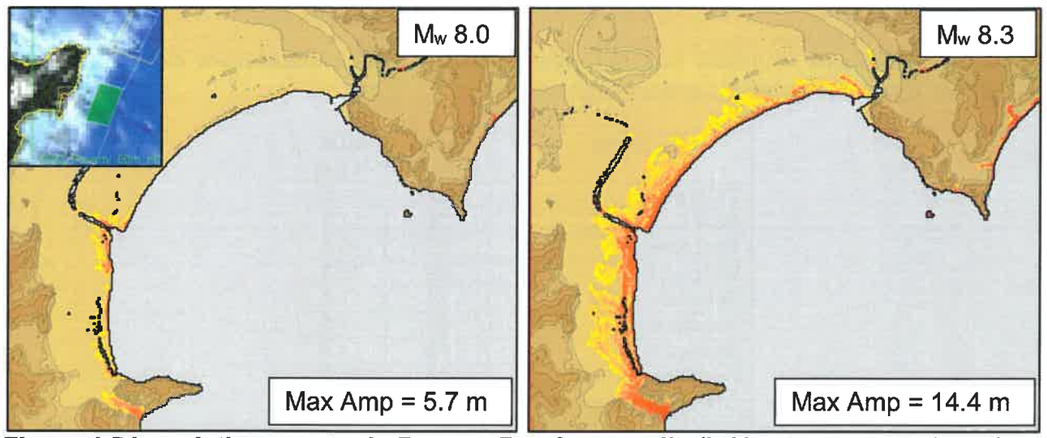

Figure 4.5 Inundation extents in Poverty Bay for 5 m slip (left) and 15 m slip (right) on the shallow fault segment (Source nt7b highlighted in green in the inset figure). Maximum amplitude vales are for the 200 m resolution B-level model grid.

We next consider cases where we maintain the slip amount of 15 m on the shallow fault segment, but we extend the rupture length by 100 km north, 100 km south and 100 km north and south (Figure 4.6).

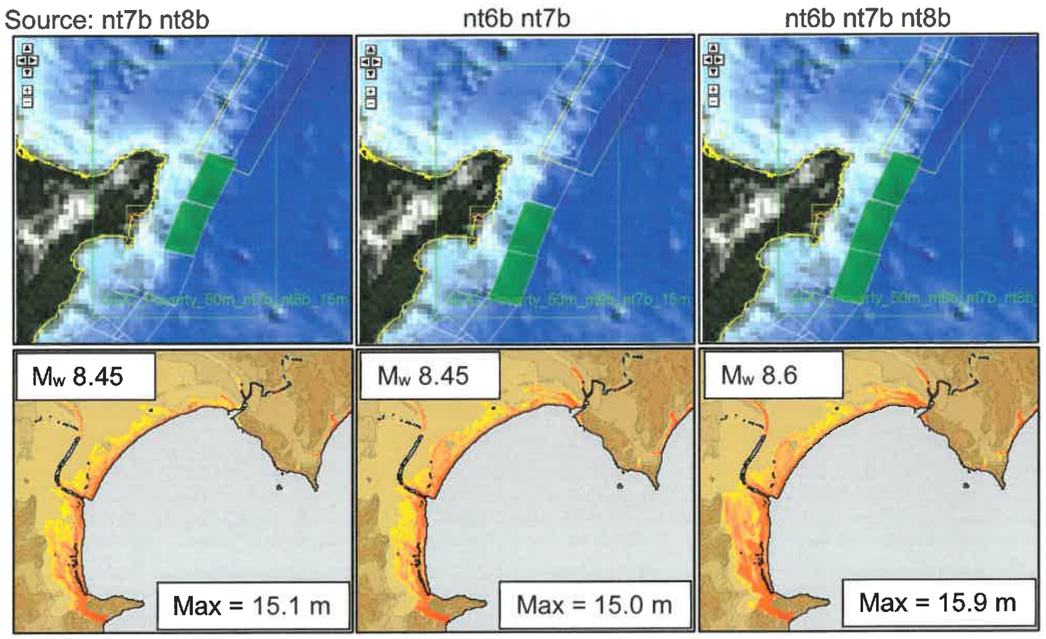

Figure 4.6 Modelled inundation in Poverty Bay from 15 m slip on the shallow fault segments for 200 and 300 km fault lengths.

The take away message from these scenarios is that the modelled maximum offshore tsunami amplitude is roughly equivalent to the slip placed on the fault segments and that extending the rupture length to the north or south has relatively little effect on that maximum tsunami amplitude or the inundation extents.

However, the story changes drastically when significant slip is applied to the deeper fault segments as shown in Figure 4.10 below. In this case we apply 15 m slip to the deep fault segments located directly offshore of Poverty Bay. The model predicts much greater inundation along the shores of Poverty Bay despite producing a smaller maximum tsunami amplitude in the B-level grid (Figure 4.7). This presents a paradox when trying to represent inundation extents based solely on an offshore tsunami amplitude value.

The reason for the increased inundation despite the smaller overall offshore tsunami heights can be seen in Figure 4.8 comparing the deformations from a rupture on the deep fault segments versus the shallow fault segment. Firstly, the deeper rupture results in approximately 1.0 m of subsidence along the Poverty Bay coastline (see Figure 4.9) and secondly, the waves length of the deeper rupture is longer than that of the shallower rupture contributing to greater inundation potential.

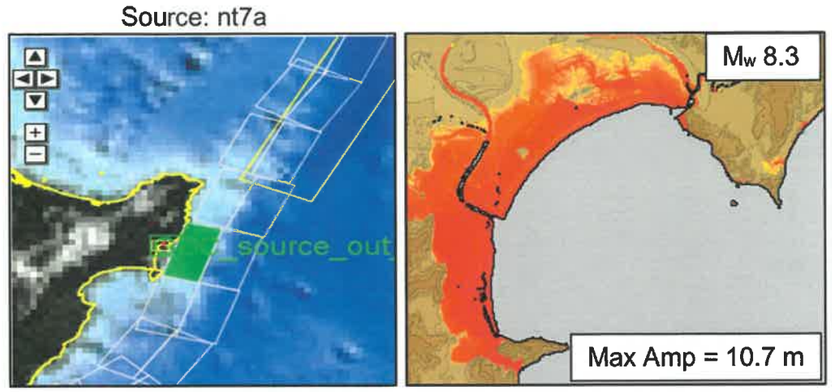

Figure 4.7 Inundation extents from 15 m slip on a single deep fault segment, source nt7a.

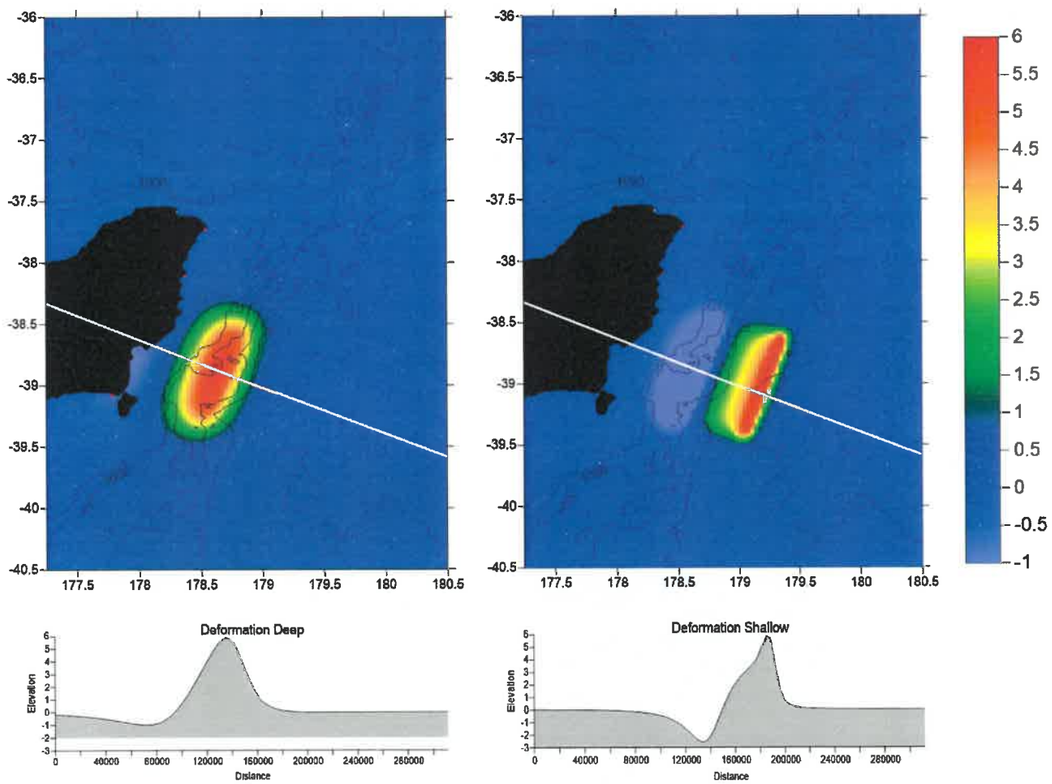

Figure 4.8 Comparison between the seafloor deformation pattern for the deep segment (source nt7a, left) and shallow segment (source nt7b, right).

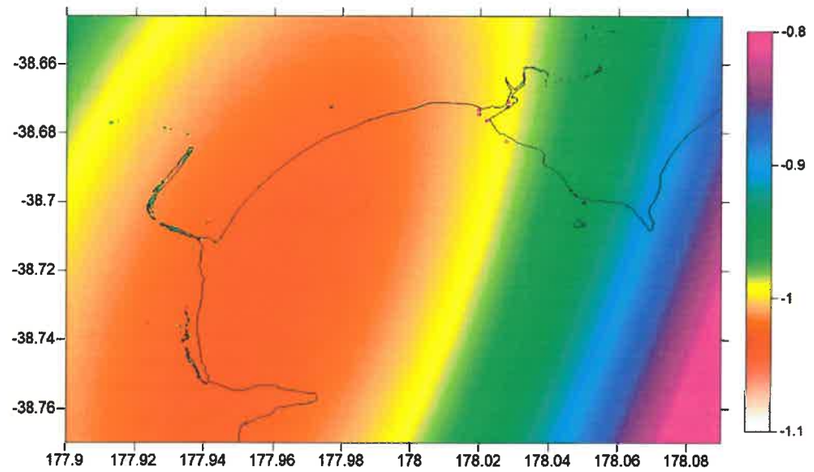

Figure 4.9 Predicted deformation (in meters) along the shoreline of Poverty Bay resulting from the rupture of the deeper fault segment.

We then tested the case for a uniform 15 m rupture on both the deep and shallow segments. This corresponds to a moment magnitude of 8.45 (equivalent to two of the cases in Figure 4.6 above). The model predicts significantly more inundation than and of the shallow segments cases and roughly equivalent inundation extents to the deep segment alone. However, the maximum tsunami amplitude in the B level grid is reduced to 8.6 m.

We then tested the sensitivity of the deep rupture scenario to rupture length by extending the fault length to 300 km (100 km north and south) and maintaining the 15 m slip amount. The results (Figure 4.11) show an increase in inundation and maximum B grid tsunami amplitude, but that the maximum amplitude is still well below the 14 m target for a Maximum Credible Event based on the GNS hazard curves.

Source: nt7ab

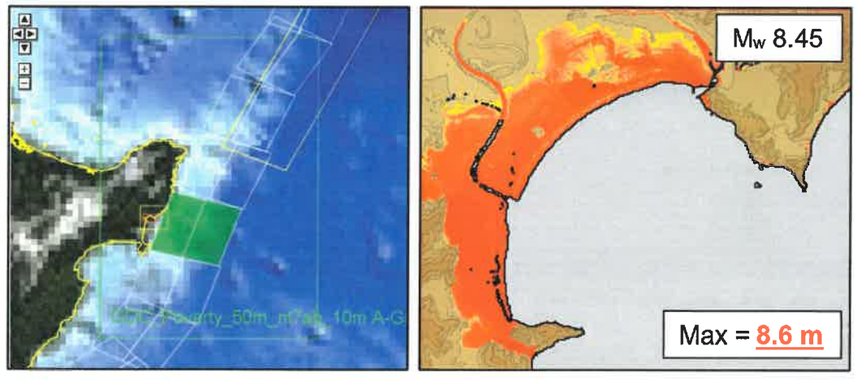

Figure 4.10 Inundation extents from 15 m slip on the deep and shallow fault segments (source nt7a nt7b).

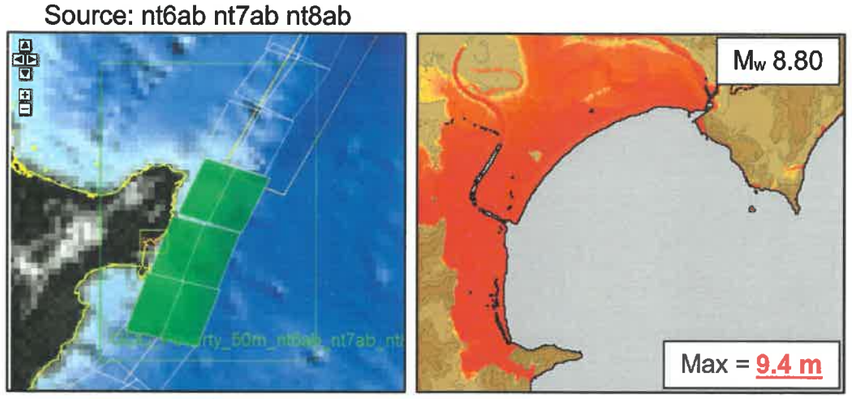

Figure 4.11 Projected inundation extents in Poverty Bay for a 300x100 km fault plane with 15 m uniform slip (source: nt6ab nt7ab nt8ab).

While the inundation projections are by any account 'extreme', it is important to compare these results to a real-world example. For this we use the tsunami source model of the 2011 Tohoku Japan tsunami used by Wei et al., (2012, 2014) to accurately model the near source tsunami propagation and inundation during that event. Results are presented in Figure 4.12.

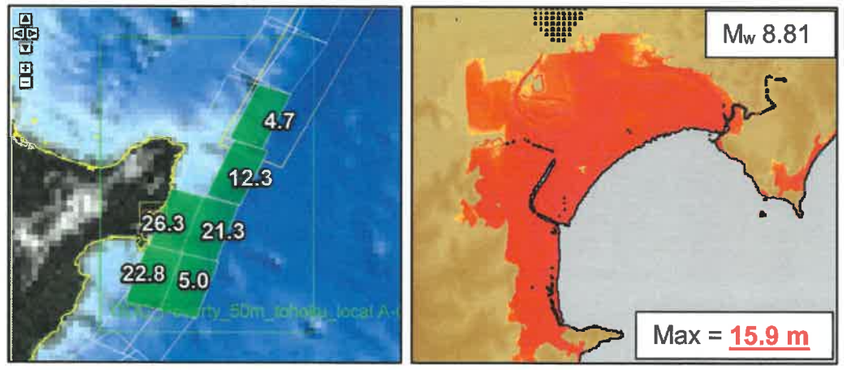

Figure 4.12 Slip distribution (left) and projected inundation extents (right) in Poverty Bay using a source identical to that used to accurately model near source inundation caused by the 2011 Tohoku, Japan tsunami.

The source area for this version of the Japan tsunami source is equivalent to that of the uniform slip case presented previously (i.e. 300x100 km). While the slip amounts on individual fault segments for this source are much greater (up to 26.3 m) the average slip amount is 15.4 m, just slightly more than the 15 m used in the previous scenario. However, the maximum computed tsunami amplitude in the B grid is 15.9 m, much greater than the 9.4 m from the uniform slip case. This value of 15.9 m now exceeds the target maximum amplitude of 14 m from the probabilistic hazard curves.

In order to more closely match the target offshore tsunami amplitude of 14.0 m for the Maximum Credible Event, we reduced the slip amounts of the 2011 Japan source by 15%. This resulted in a maximum modelled amplitude of 13.7 m in the model B grid with inundation

extents as shown in Figure 4.13. The inundation extents from the reduced Tohoku source and the 15 m uniform slip source are compared side by side in Figure 4.14.

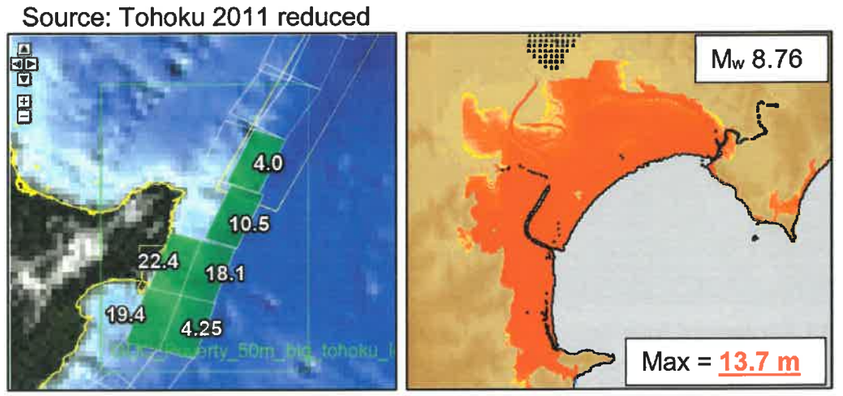

Figure 4.13 Slip distribution (left) and projected inundation extents (right) in Poverty Bay using the 2011 Japan source scaled down by 15%.

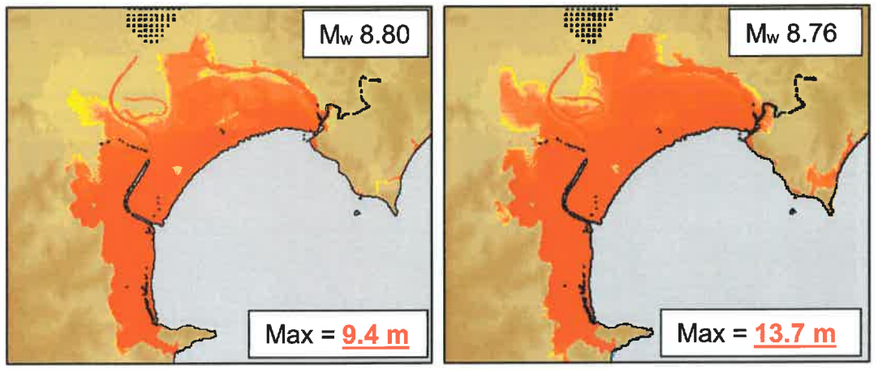

Figure 4.14 Side by side comparison of the 300x100 km source with 15 m uniform slip (left) and the variable slip, reduced Tohoku 2011 tsunami source (right).

4.2.1 Near Field Source Sensitivity Summary

The objective of the near field source sensitivity modelling was to determine the appropriate tsunami source for defining the yellow evacuation zone. According to the MCDEM guidelines, the yellow zone should "cover all maximum credible tsunami, including the highest impact events. The intention is that the yellow zone provides for local-source maximum credible events, based on locally determined risk." Hence, we have focussed on extreme near field source mechanisms which present the greatest potential for producing an extreme tsunami event.

To select the appropriate tsunami source, we modelled the tsunami from a range of earthquake magnitudes and matched the modelled tsunami amplitudes in the intermediate 'B-level' modelling grid to the heights predicted in the GNS probabilistic tsunami study. For the case of Poverty Bay, 14.0 m is the target tsunami amplitude for the maximum credible event (84th percentile amplitude at 2500-year return period, see Figure 4.3 and Figure 4.4).

Based on the historical precedent of tsunami events along the north east coast of New Zealand, specifically the 1947 events, we initially investigated the potential inundation from sources with the co-seismic slip concentrated on the shallower segment of the subduction zone interface. Based on the model results, it was apparent that the modelled tsunami amplitudes closely matched the co-seismic slip forced on to the fault segment. Thus, slip amounts of 14-15 m were necessary to produce the target tsunami amplitudes. It was then shown that this tsunami amplitude was relatedly insensitive to the length of the tsunami source with 200 and 300 km long ruptures producing similar amplitude and inundation extents to 100 km long ruptures.

We then investigated the effect of placing the slip on the deeper fault segments. It was seen that adding slip to the deeper segments of the fault produces greater inundation along the coastline than an equivalent shallow rupture. However, paradoxically, despite the increased inundation, the maximum tsunami amplitude in the B level grid is considerably smaller than in the equivalent magnitude shallow rupture scenario.

We then compared the inundation extents from a 300 x100 km fault plane rupture with 15 m of uniform slip to the inundation caused by a tsunami source representative of the 2011 Tohoku, Japan event. While the Tohoku source has larger slip on individual fault segments, the average slip is 15.4 m, comparable to the 15 m used in the uniform slip case.

The Tohoku source was shown to produce much greater inundation as well as a maximum B-grid tsunami amplitude of ~16 m, much greater than the target of 14.0 m. We then reduced the slip amounts of the Tohoku source by 15% to bring the maximum B-Grid amplitudes in line with the target. This source was shown to have similar inundation extents to the 15 m uniform slip case.

Thus, for the purposes of this project, which is to define worst case inundation extents, we opted to use the 300x100 km fault plane with 15 m of uniform slip as the 'Maximum Credible Event' source for a near field tsunami. While this source does not match the target offshore tsunami amplitudes, the inundation extent caused by this source is comparable to a known, real world tsunami source.

4.3 Sensitivity Analysis for Far Field Tsunami Sources

To determine the appropriate far-field tsunami sources for use in the inundation zone study we conducted two types of sensitivity study. We first looked at identical, idealised tsunami sources positioned along the South American Subduction Zone to determine the relative tsunami effect in Poverty Bay as a function of source location. We then conducted a deterministic sensitivity study whereby we compared the tsunami inundation extents caused by a range of large to very large earthquakes based on historical tsunami events. These sources are positioned in different regions along the South American Coast. Far-field or Regional sources are used to define Orange Zone since it is the area that could be evacuated in the case where an official warning is possible. This would preclude near field events where official warning are impossible due to the short arrival times.

4.3.1 Normalised Source Sensitivity Analysis

The first sensitivity analysis considered 20 identical tsunami sources placed along the coastline of South America from northern Peru to southern Chile (Figure 4.15). Each source was 100 km wide by 300 km long with 6 m of uniform slip, equivalent to a M 8.0 earthquake. The maximum positive and negative amplitudes were recorded at the Gisborne tide gauge location and normalised by the overall maximum values. The results show which section of the South American Subduction Zone produces the strongest response along the Gisborne coast. Plotted in Figure 4.15 we see that the Sources 5-7, 10 and 14-16 give the strongest response along the Gisborne coast.

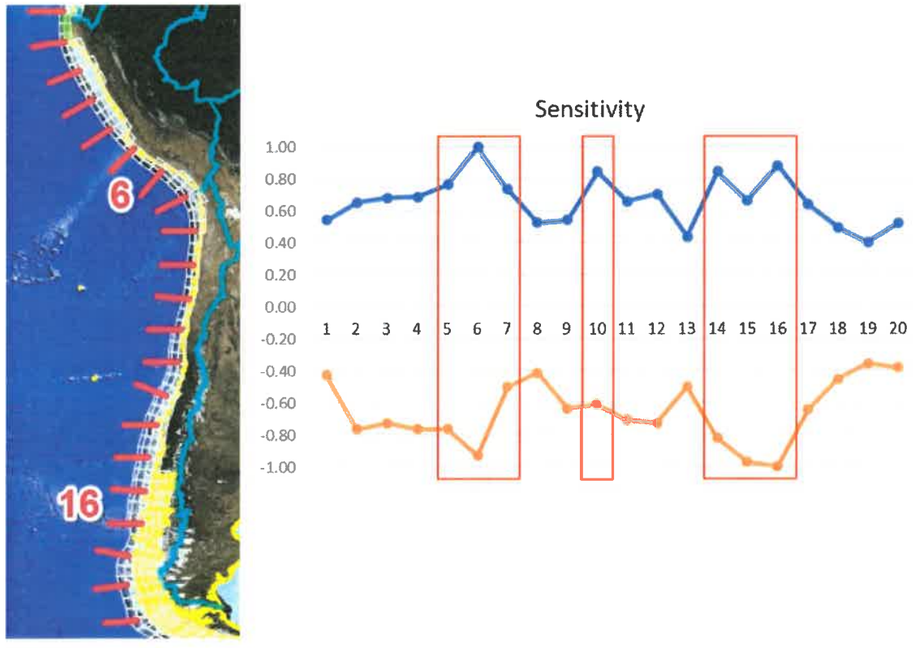

Figure 4.15 (left) Source zones numbered from 1-20 (north to south) Each source was 300 km long x 100 km wide with 5 m of co-seismic slip. (right) normalised maximum positive and negative tsunami amplitude at the Gisborne tide gauge for each source. The strongest response is seen for source regions 6 and 16. Sources 10 and 14 also produce a relatively strong response.

4.4 Deterministic Source Sensitivity Analysis

Knowing which sections of the South American Subduction Zone produce the strongest response at Gisborne guides the selection of the source regions for the deterministic far-filed source sensitivity analysis. For this analysis we trialled 12 different source models with magnitudes ranging from 9.0 to 9.4. Three of the sources were based on the slip distribution of the 1960 Valdivia Chile earthquake while the remainder were idealised rectangular sources with uniform slip. Details of the sources are listed in Table 4.2

Table 4.2 Details of the far field source models.

Case Name	L	W	slip	M_w	Description
1960	800	150	var	9.19	1960 Chile, Fujii & Satake (2013) source
ff_1	500	100/150	20.9	9.10	Source Zone 6 from sensitivity study, 500 x 100 to 150 km
ff_2	800	150	var	9.19	Chile North 2 (1960, version 6) slip concentrated to north
ff_3	800	150	var	9.19	Central Peru (1960, version 5) slip concentrated to south
ff_4	800	150	var	9.19	Chile North 3 (1960, version 6) slip concentrated to south
ff_5	800	150	14.2	9.19	Same as ff_3, but uniform slip, 14.184 m
ff_6	500	100	20.0	9.00	Central America (El Salvador - Nicaragua)
ff_7	800	150	20.8	9.30	Same as ff_3, but uniform slip, 20.83 m
ff_8	800	150	29.4	9.40	Same as ff_3, but uniform slip, 29.43 m
ff_9	800	150	29.4	9.40	Southern Peru, uniform slip, 29.43 m
ff_10	800	150	29.4	9.40	Far Southern Chile, uniform slip, 29.43 m
ff_11	600	150	39.6	9.35	1868 North Chile/Southern Peru (Borrero and Goring, 2014)
ff_12	900	150	26.2	9.40	1960 Chile source region with uniform slip 26.2 m

For case ff_1 we considered a 500 km long source located at Zone 6 from the normalised sensitivity analysis presented above. This source has 20.9 m of uniform slip.

Cases ff_2, 3 and 4 were based on the 1960 Valdivia, Chile earthquake as described by Fujii and Satake (2013). The slip distribution used here in the ComMIT simulation was developed in Borrero (2013) who conducted a detailed analysis of the effects of the 1960 tsunami at Whitianga. In that study the numerical model results from 6 different versions of the 1960 tsunami source were compared to eyewitness accounts and observations of inundation at Whitianga. The results suggested that the earthquake slip distribution proposed by Fujii and Satake (2013) provided the best overall fit to the observed effects. However, it was necessary to increase the slip amounts by 20% to most accurately reproduce the observed inundation. The fault segments, initial seafloor deformation and slip amounts used for that source are shown in Figure 4.16 and Table 4.3.

Using that slip distribution as a starting point, the slip values on individual fault segments were rearranged to concentrate the segments with largest slip together either in the northern or southern ends of the fault plane. This was done to constrain the overall magnitude while generating a stronger tsunami due to the concentration of the high slip areas. The resulting slip distribution is then positioned at the desired location along the South American Subduction Zone. For this study we used both the northern and southern concentrated slip cases straddling the Peru-Chile border (cases ff_2 and 4) and the southern concentrated slip case in central Peru (case ff_3).

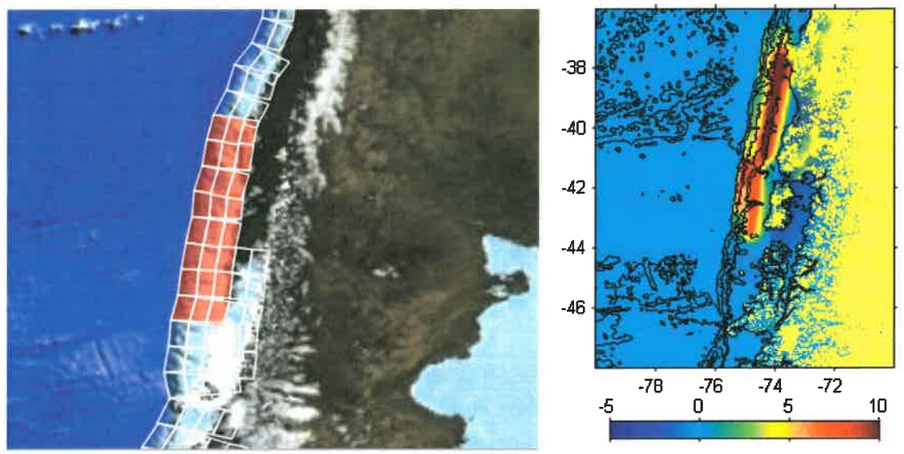

Figure 4.16 (left) Unit source segments used to define the 1960 Chilean Earthquake suite of events. (right) initial sea floor deformation at the source region.

Table 4.3 Faults segment slip amounts for the 1960 Chilean tsunami. Segments with slip >20 m are highlighted in pink.

	Fault Segment Slip Amounts		
North	5.0	12.9	1.2
	6.6	36.1	21.0
	2.8	31.1	11.3
	4.9	29.6	11.5
	7.8	32.9	6.6
	25.7	17.8	6.2
	15.3	21.7	5.5
South	3.7	20.5	2.7
	East ←	→	West
	Shallow ←	→	Deep

Table 4.4 The rearranged slip distribution for the southern concentrated slip (left) and northern concentrated slip cases (right). Segments with slip >20 m are highlighted in pink.

2.8	17.8	1.2	3.7	12.9	2.7
4.9	20.5	5.5	7.8	29.6	11.3
5.0	21.7	6.2	25.7	36.1	21.0
6.6	31.1	6.6	15.3	32.9	11.5
15.3	32.9	11.5	6.6	31.1	6.6
25.7	36.1	21.0	5.0	21.7	6.2
7.8	29.6	11.3	4.9	20.5	5.5
3.7	12.9	2.7	2.8	17.8	1.2

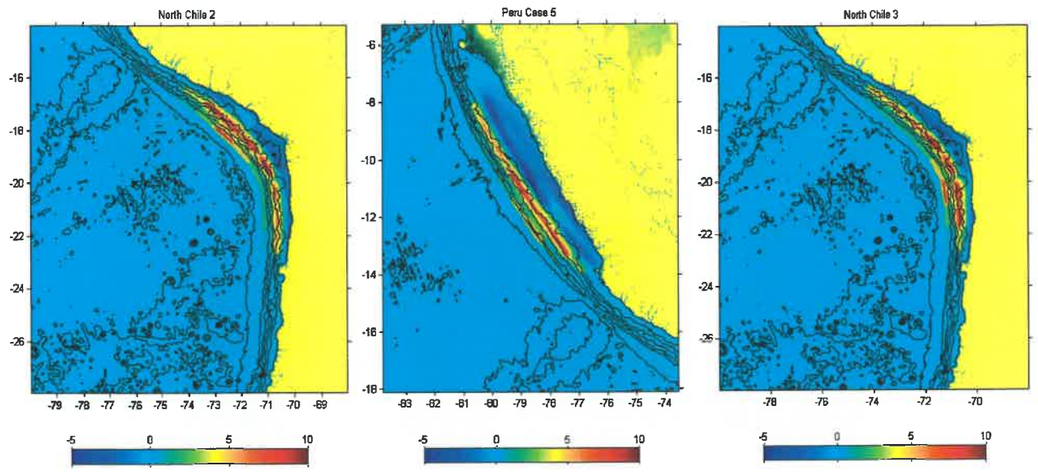

Figure 4.17 (L: to R) Seafloor deformation for cases ff_2, ff_3 and ff_4. ff_3 uses the northern concentrated slip distribution while ff_3 and ff_4 use the southern concentrated slip distribution.

For cases ff_5, ff_7 and ff_8 we used the same fault segments as ff_3, but instead of the variable slip, we used uniform slip of 14.8, 20.2 and 29.4 m respectively.

Case ff_6 was used to assess the sensitivity to sources from Central America. This area was chosen since a similar sensitivity study conducted by Borrero et al. (2014) showed that this area produced a relatively strong response at several New Zealand sites.

Case ff_9 expanded on case ff_1 by extending the fault rupture to 800 km and increasing the slip to 29.4 m.

Case ff_10 focussed on the far southern source region (segments 14, 15 and16) highlighted in the Normalised Sensitivity Analysis described above.

For case ff_11, we consider the event of 13 August 1868. While there were no instrumental recordings of this tsunami, there are detailed accounts of the wave effects in New Zealand (de Lange and Healey, 1986). It is interesting to note that the effects on the North Island seem to be less severe than those on the South Island, with reported tsunami heights of 1-2 m at Mount Maunganui, Great Barrier Island and in the Tamaki Estuary. Even at Port Charles, the tsunami was only described as 'a high tide'. This contrasts with the effects a Lyttleton Harbour near Christchurch, where the observations of Gibson (1868) suggested a peak to trough tsunami height of ~7.6 m (25 feet) for the first tsunami wave. To model this event, we based our tsunami source on the rupture length estimate of 600 km presented in Dorbath et al., (1990). Using fault segments extending from Arica northward (Figure 4.18) the model is initialized with a uniform slip amount of 39.6 m. Borrero and Goring (2015) showed that this amount of slip was necessary to replicate the observed 7 m water level change observed in Lyttleton Harbour as described by Gibson (1868).

And finally, case ff_12 used the same source region as the 1960 Valdivia event but used a uniform slip of 26.2 m.

Initially, these cases were run over a relatively coarse 50 m resolution grid for Both Poverty and Tolaga Bays. The objective was to compare the inundation patterns between two different sites and to select the sources that yielded the greatest inundation for more detailed modelling over 10 m grids. The results of this initial test are presented in Figure 4.19 through Figure 4.22. Ultimately, cases ff_3, ff_6, ff_8, ff_10, ff_11 and ff_12 were selected for the detailed modelling over all of the C-Level modelling grids

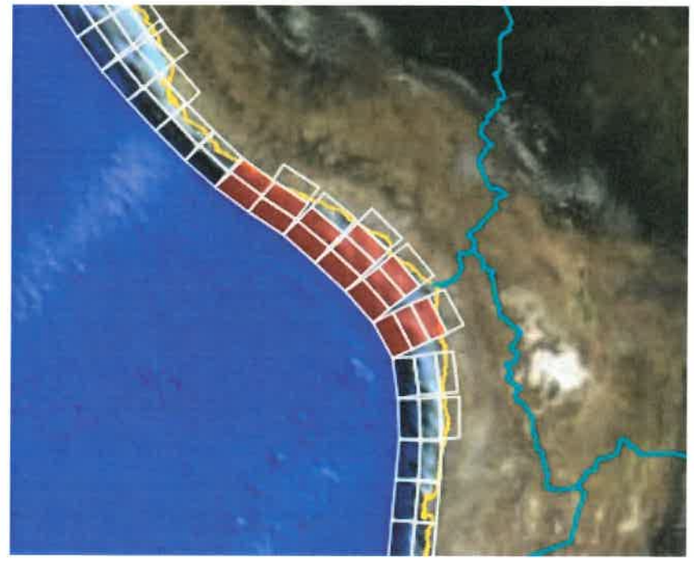

Figure 4.18 Source segments used to model the 1868 Arica tsunami. A uniform slip amount of 39.6 m was applied to each segment.

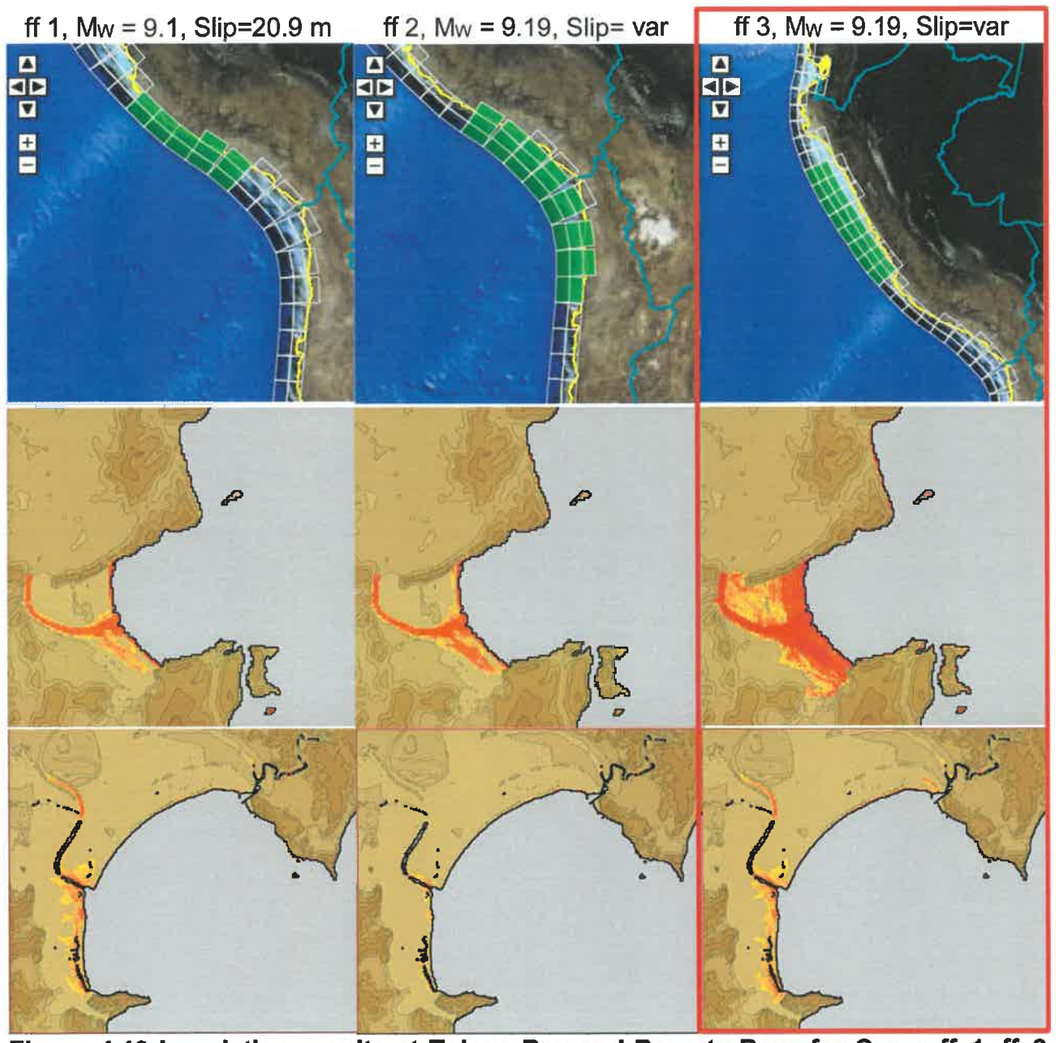

Figure 4.19 Inundation results at Tolaga Bay and Poverty Bays for Cases ff_1, ff_2 and ff_3.

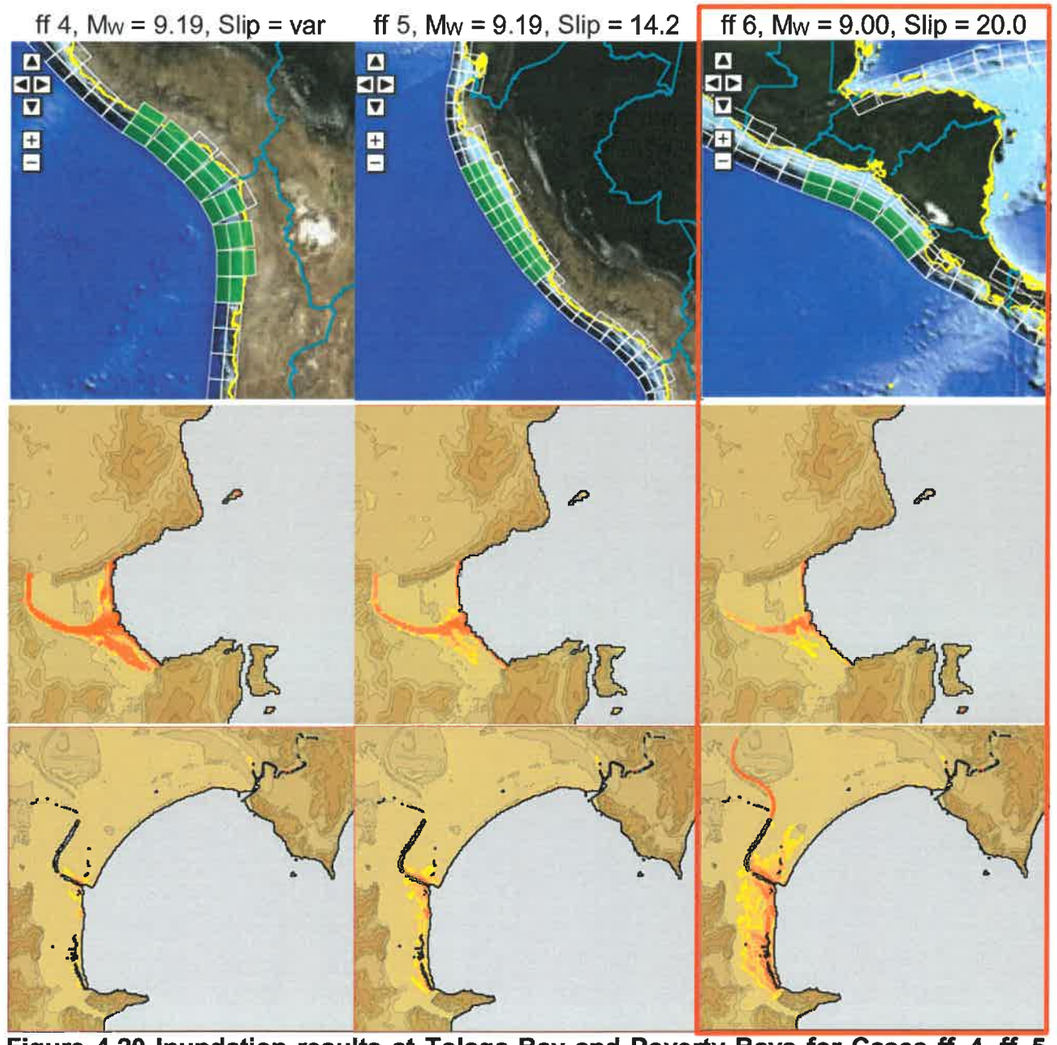

Figure 4.20 Inundation results at Tolaga Bay and Poverty Bays for Cases ff_4, ff_5 and ff_6.

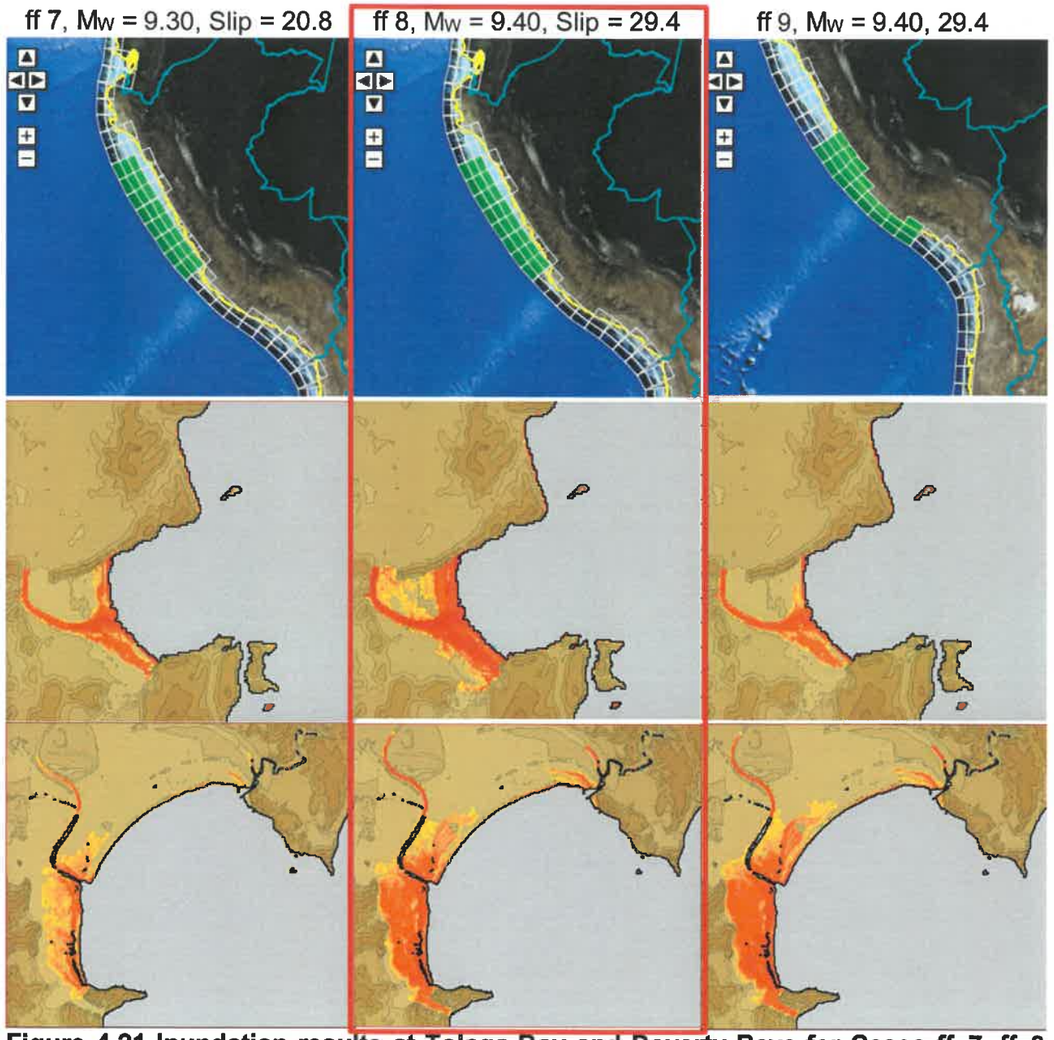

Figure 4.21 Inundation results at Tolaga Bay and Poverty Bays for Cases ff_7, ff_8 and ff_9.

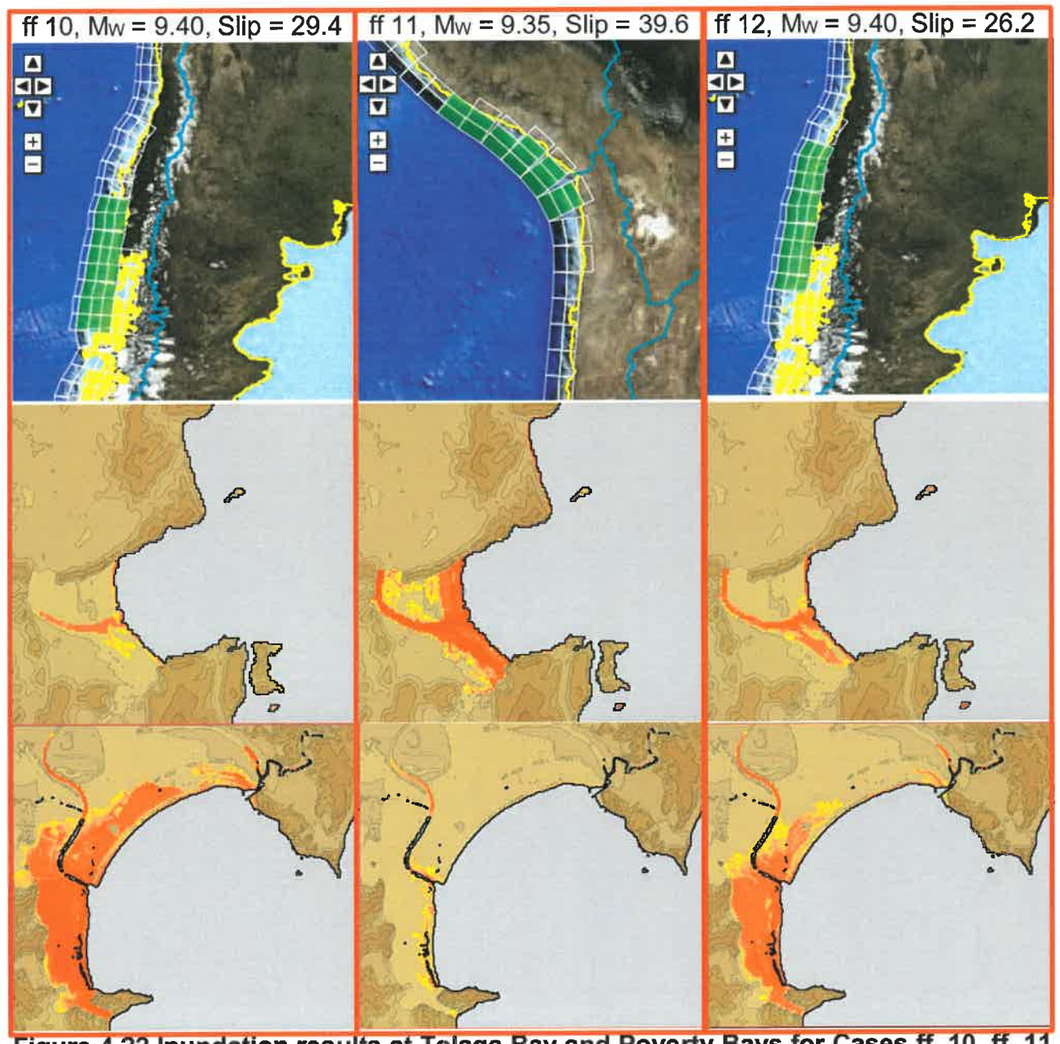

Figure 4.22 Inundation results at Tolaga Bay and Poverty Bays for Cases ff_10, ff_11 ad ff_12.

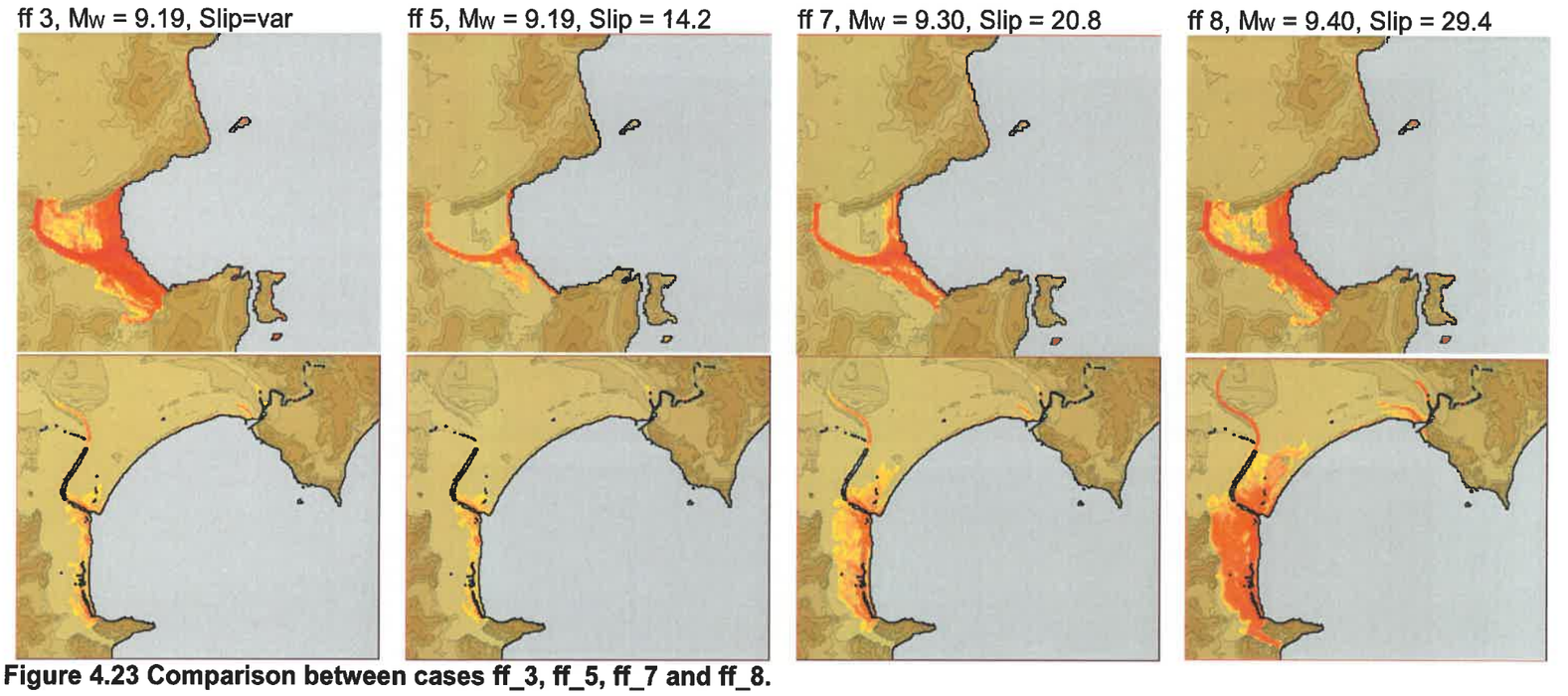

Figure 4.23 Comparison between cases ff_3, ff_5, ff_7 and ff_8.

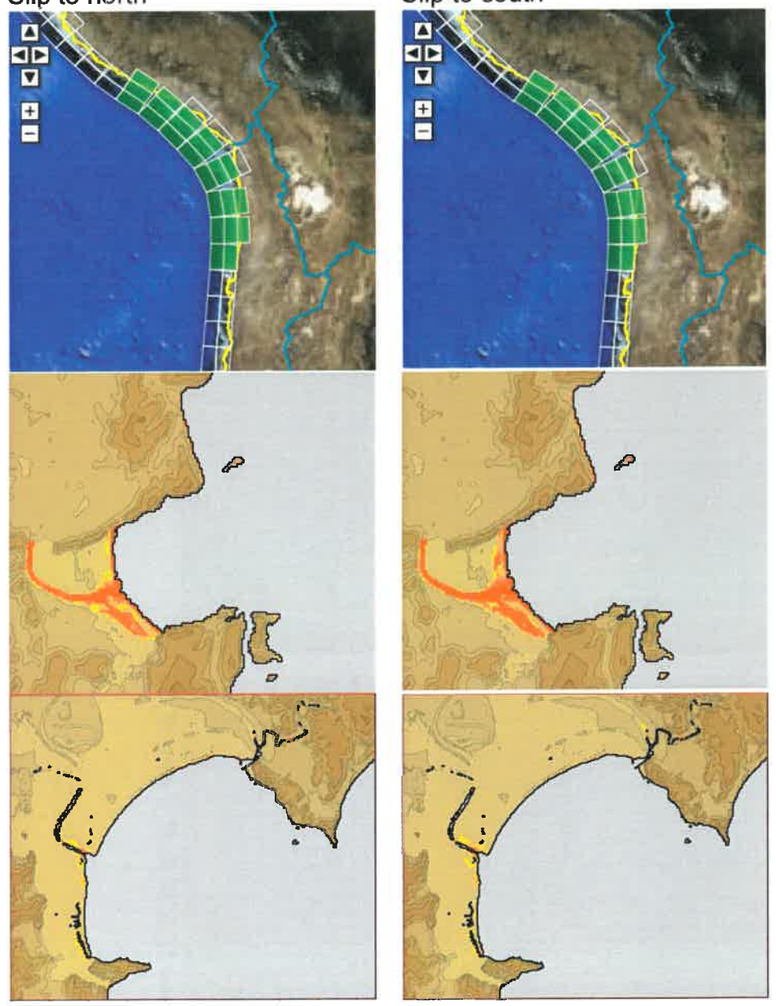

Figure 4.24 Comparison of modelled inundation results from the ff_2 (high slip north) and ff_4 (high slip south) scenarios. These cases produce stronger inundation in Tolaga as opposed to Poverty Bay.

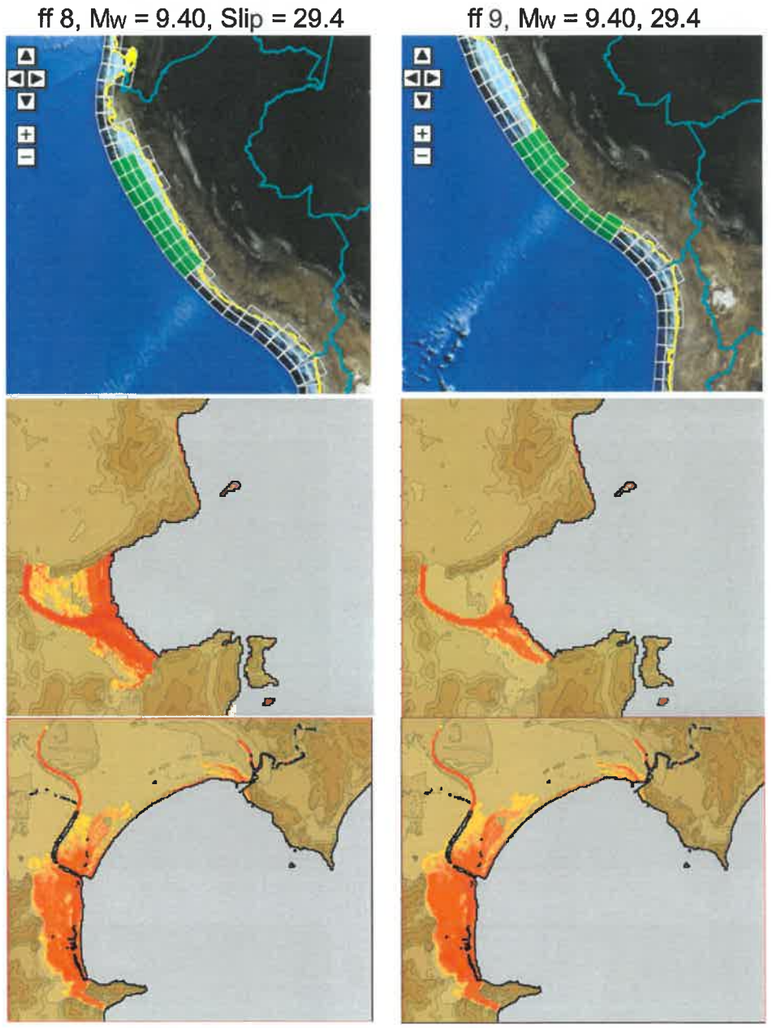

Figure 4.25 Comparison of modelled inundation results from the ff_8 and ff_9 scenarios. These cases both cover Source Region 6 from the Normalised Source Sensitivity Study.

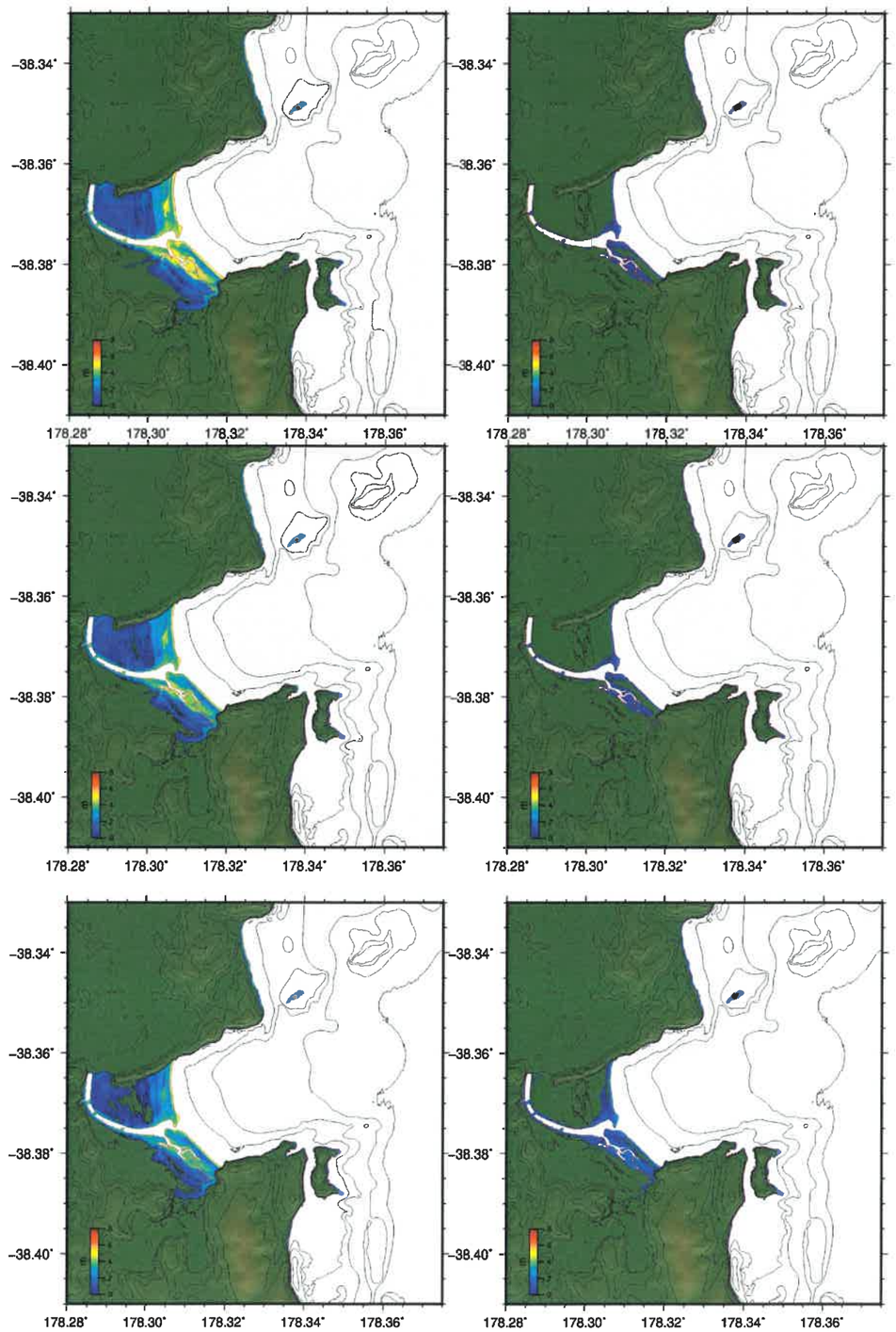

Figure 4.26 Inundation at Tolaga Bay for the 6 cases used int eh final analysis (ff_3, ff_6, ff_8, ff_10, ff_11, ff_12).

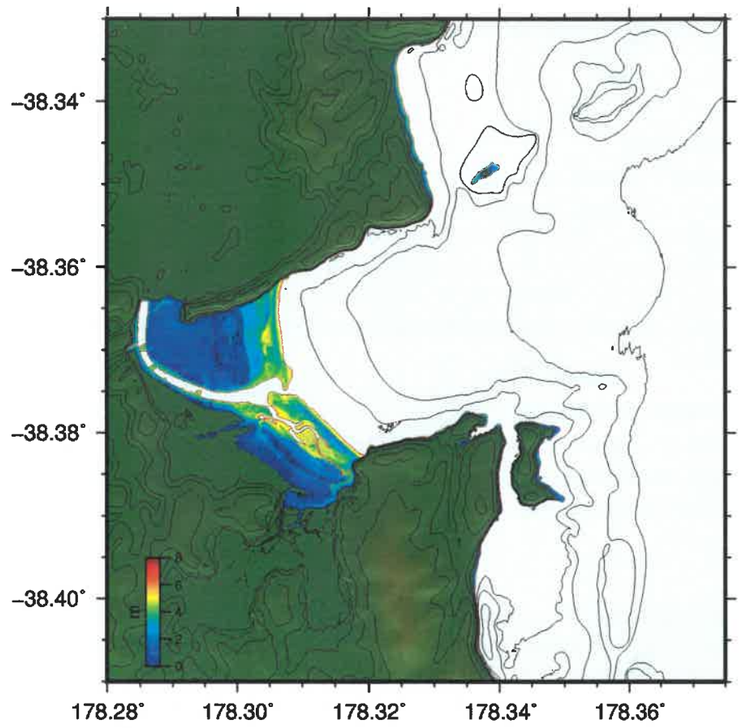

Figure 4.27 Aggregate flow depth and inundation from the six scenarios plotted in Figure 4.26 above.

5 DEBRIS TRANSPORT AND DUNE EROSION MODELLING

5.1 Tsunami Debris

During major tsunami inundation, floating debris can cause severe damages and exacerbate tsunami impact. In addition, clumps of debris can obstruct the flow of water draining from land and back out to sea. The same clumps of debris can also block access to critical areas and slow down the progress of first responders. The numerous logs stored at Gisborne Port awaiting export as well as drift wood on the beach could become such tsunami debris. In order to find the pathways of the Logs and drift wood picked-up by tsunami waves a dispersal model was used.

5.1.1 Debris Dispersion Model

The dispersal model used is a standard Lagrangian formulation (Lal et al.2016, Viikmäe et al. 2013), where particles have no physical representation, but rather track the displacement of neutrally buoyant small objects such as debris. Particle displacement is expressed as:

$$\Delta x = u_p * \Delta t + K$$

x represents particle position (latitude and longitude), Δx is particle displacement during a time step Δt (calculated automatically to satisfy the CFL condition), u_p is the depth averaged current speed at the location of the particle. K is the eddy diffusivity which takes account of the random displacement of the particle, due to turbulent eddies at a scale smaller than the hydrodynamics model resolution. u_p is calculated by interpolating the velocity from the hydrodynamic model, both spatially and temporally. Gridded surface currents are first interpolated to the dispersal step, after which the current velocity at each particle position is calculated using a bi-linear interpolation of the gridded surface currents, where only surface currents are considered, and vertical movements neglected.

The number of particles in each model cells for each time step is retained as well as the actual particle positions. The cumulative number of particles in each cell at the end of the simulation is a tally of the number of particles visiting each model cells (here the same particle is counted as many times as it visits a cell). Since the actual behaviour of the debris (e.g. clumping in a narrow drain on being stuck near bridge pile) cannot be accounted for, the cumulative number of particle visits is regarded as a proxy for the probability for debris the reach the cell.

Although the model does not simulate the dispersal of logs or account for how their shape may interact with the flow, Lagrangian particles are an appropriate proxy for general debris. A limit on the flow depth was imposed only allowing particles to move if the water depth is equal or larger than 0.1 m to represent larger debris (with a diameter of 0.2m).

5.1.2 Initial Debris Source Locations

In this study 2 sources of tsunami debris are considered as shown in Figure 5.1:

1) Logs and floating debris from the Port. Here the debris are spread evenly throughout the port prior to the tsunami.

2) Drift wood accumulated on the beaches.

Figure 5.1 Initial location of debris from the Port (left) and beach (right).

5.1.3 Tsunami Scenario

The dispersal of debris was simulated for 3 far field scenarios and 2 near field scenarios occurring at MHWS. For each scenario the cumulative number of particles visits was recorded as a proxy for probability of debris damages.

5.1.4 Port Debris

For debris originating in the Port, the dispersal is highly dependent on the origin of the tsunami which then controls the period of the inundation and the direction of the currents. Naturally tsunami that produces the most severe inundation will be able to carry debris further inland. In general, the breakwater can hold a large number of particles. A large amount of debris is carried in the Waikanae Creek and could restrict the return flow of the tsunami if they clumped at the foot of the SH35 bridge. The far field scenarios appear to disperse debris from the Port toward the beach in the west but the debris do not appear to reach beyond the dunes.

5.1.5 Beach Debris

Debris from the beach can reach inland either by flowing over the dunes or through access ways between the dunes (Grey street in scenario ff_8 and nt6b_nt7b_15m). In the severe inundation (scenario nt6ab_nt7ab_nt8ab_15m_f2) the debris from the beach has a proportionally larger number reaching the edge of the town.

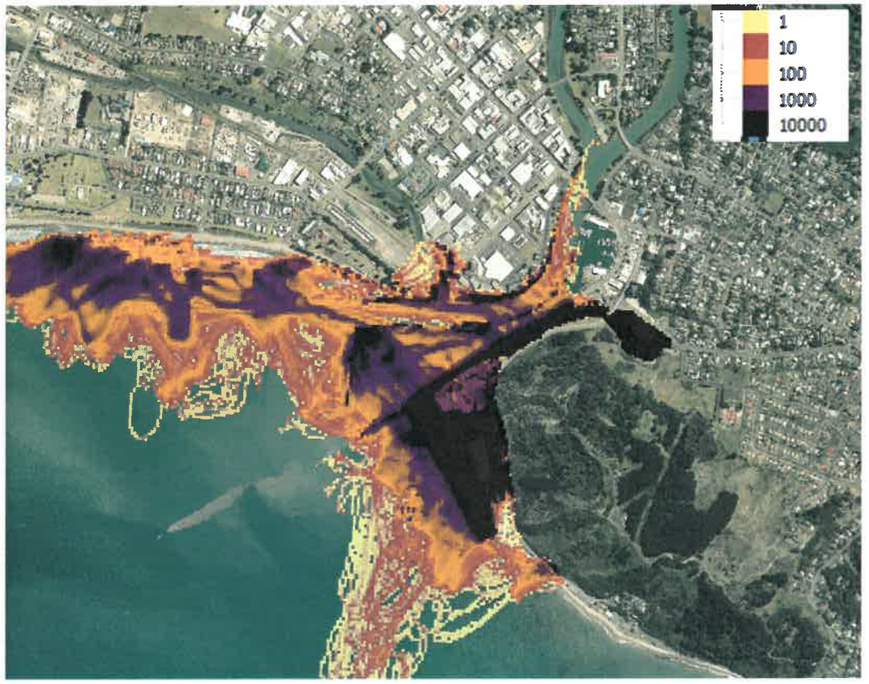

Figure 5.2 Cumulative particle visits for scenario ff_8

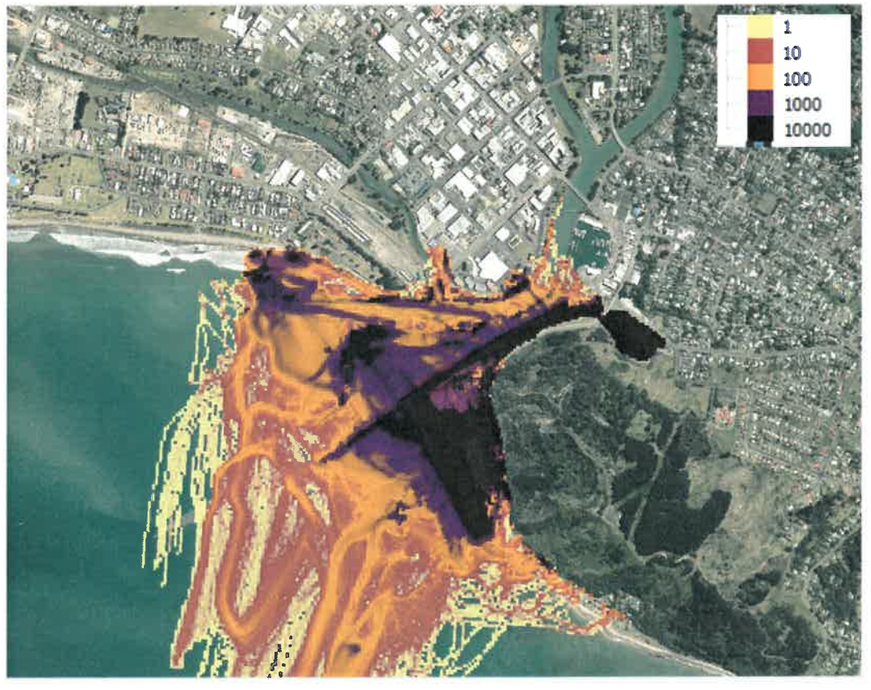

Figure 5.3 Cumulative particle visits for scenario ff_10

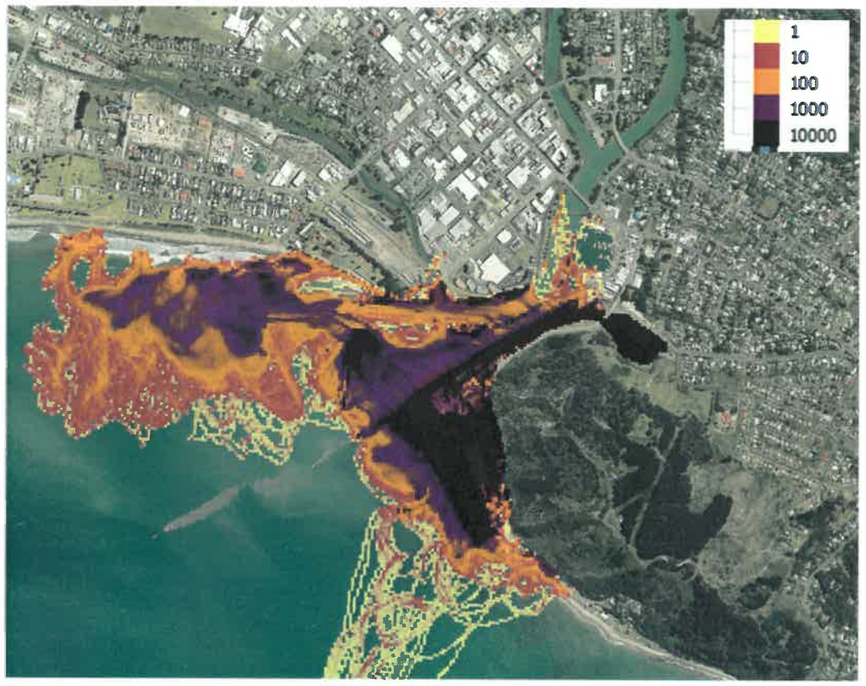

Figure 5.4 Cumulative particle visits for scenario ff_12

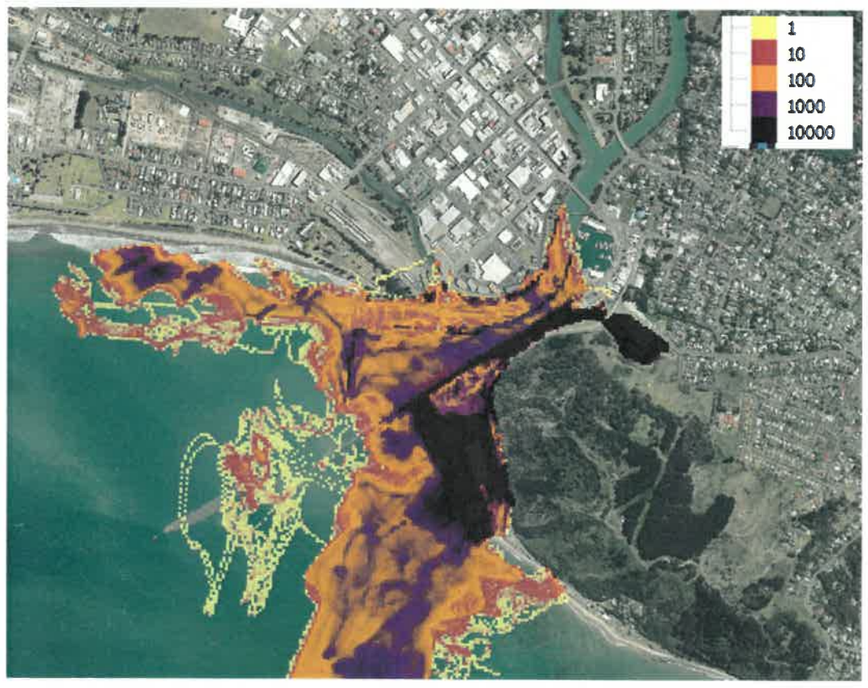

Figure 5.5 Cumulative particle visits for scenario MWHS_nt6b_nt7b_15m

Figure 5.6 Cumulative particle visits for scenario nt6ab_nt7ab_nt8ab_15m_f2

Figure 5.7 Cumulative particle visits for scenario Ff_8

Figure 5.8 Cumulative particle visits for scenario Ff_10

Figure 5.9 Cumulative particle visits for scenario Ff_12

Figure 5.10 Cumulative particle visits for scenario nt6b_nt7b_15m

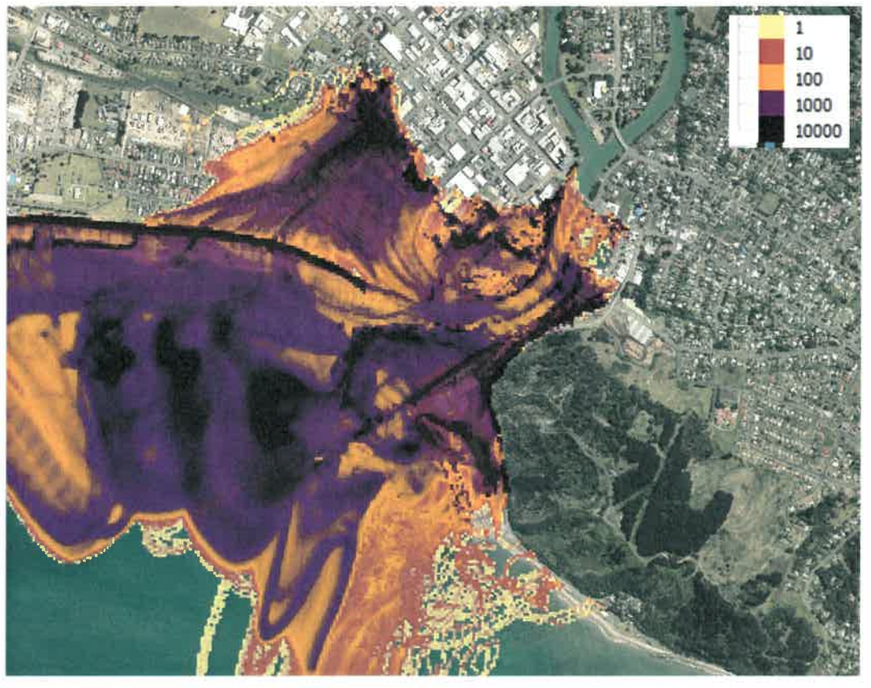

Figure 5.11 Cumulative particle visits for scenario nt6ab_nt7ab_nt8ab_15m_f2

5.2 Beach and Dune Erosion Modelling

Tsunami runup and overland flow is known to cause severe erosion of beaches and dune systems. At the same time dunes are often regarded as a natural protection against tsunami. In order to evaluate how the dunes in Gisborne and Wainui may help dampen the tsunami inundation, a morphodynamic model was used to simulate the beach and dune response to a variety of tsunami scenarios.

Dune breach is a common problem for evaluation of inundation during extreme storms but is also known to occur with large tsunami waves. Strom driven dune breach typically occurs during strong tropical cyclones where waves attack, erodes the dune front while long waves overtop the dune, ultimately breaching the dune system allowing the flooding of the backshore.

The simulation of the dune breaching process has been a core goal for the development of the XBeach model (Roelvink et al. 2009) and the dune breach processes are part of the testbed of the model ensuring that the model is skilled at simulating the dune breaching capability of the model. Tsunami waves have a similar effect on the dune breach as storm surge and long waves, suggesting that XBeach is appropriate for use in tsunami dune breaching simulation.

Tsunami dune breach using XBeach as previously been tested and used by Li et al. 2012, Li and Huang 2013, and Costa et al. 2016.

5.2.1 XBeach_GPU

The XBeach model is computationally demanding because it incorporates a robust flow model that can handle shock waves, a wave model (although this is not used in tsunami simulation), a sediment transport model and a morphological model. A lightweight version of XBeach that can run on Graphics Processing Units (GPU) allows computation to be completed much faster. XBeach_GPU has the core features if the regular version of XBeach and has been used for beach and dune erosion (Bosserelle, 2013) and for coastal inundation (Bosserelle et al. 2015).

Although the model is skilled for simulating dune breach, the processes are dependent on local sediment characteristics and dune morphology. The model requires sand density, median size (D50), 90th percentile grain size (D90), the dry slope of dune, the wet slope of the dune and a limiter for dune slumping.

5.2.2 Bathymetry

Model simulations were completed in a projected coordinate system (NZTM2000) rotated so that the offshore boundary of the model would be located on the left-hand side of the rectangular grid.

For Waikanae the model grid covered an area along 3km of coastline at 5m resolution starting at the Waikanae creek in the east, the grid was rotated 90° clockwise to fit the model requirements (Figure 5.12). For ease of interpretation, the model results were converted back to the NZTM coordinate system.

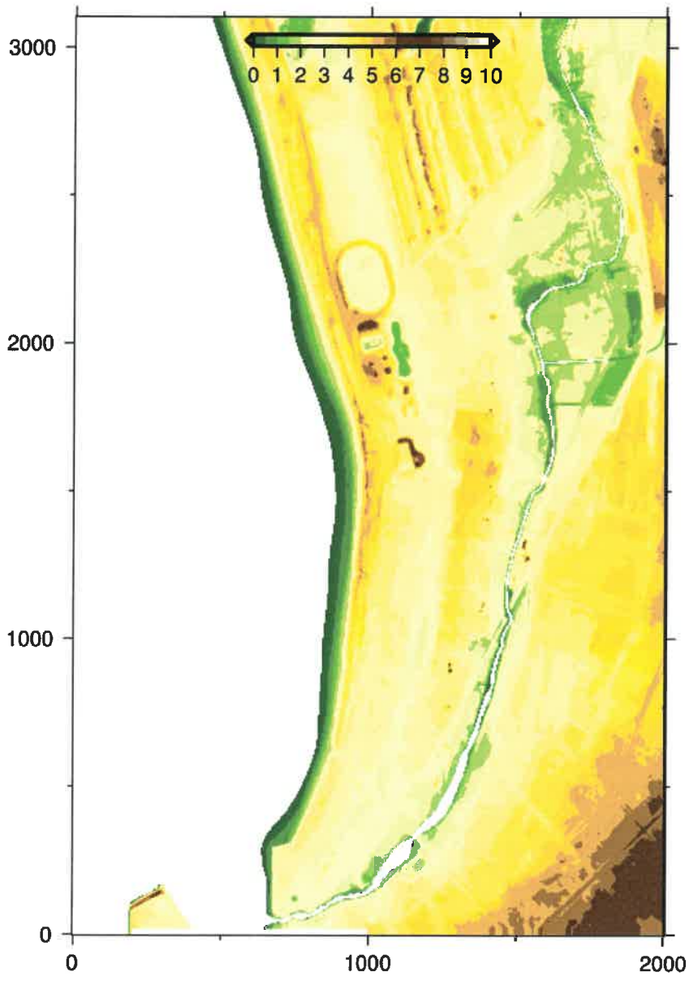

Figure 5.12 The Waikanae rotated model grid.

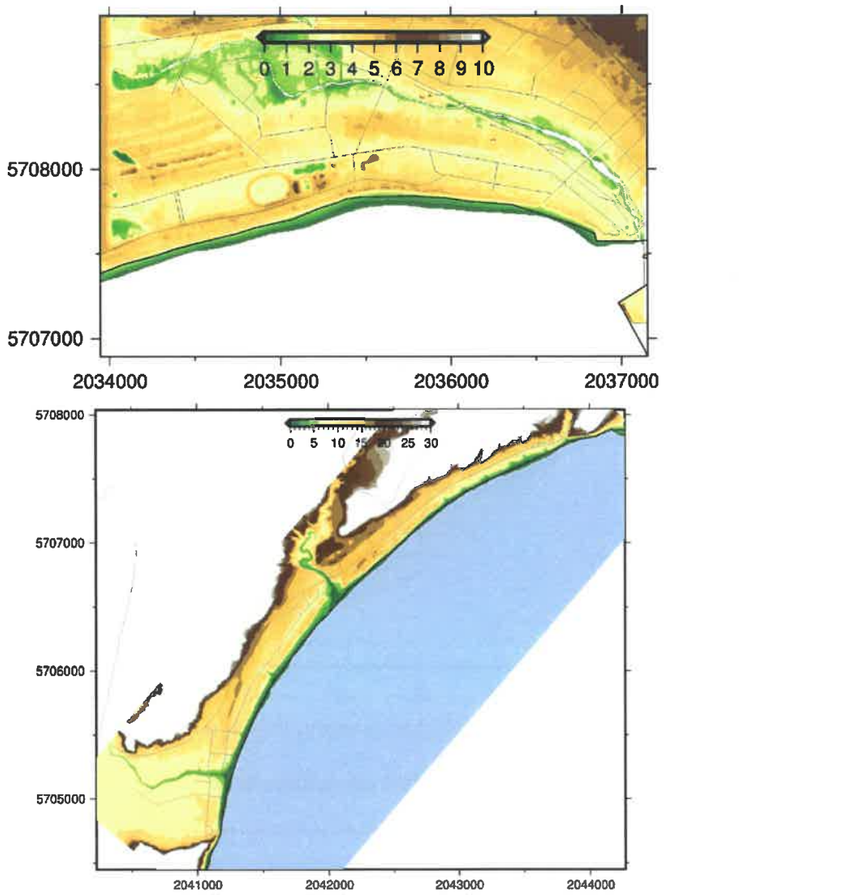

Figure 5.13 Initial bathymetry grids for Waikanae (top) and Wainui (bottom) in NZTM 2000 coordinates.

5.2.3 Sediment Model Parametrisation

The sediment transport model was set up to simulate beach sediment and therefore, no erosion is allowed in the model landward of the coastal strip. The sediment in the coastal strip was approximated to a single sediment fraction characterised by a density, median size (D50), 90th percentile grain size (D90), a critical dry slope of sediment, the critical wet slope of the sediment. Several sediment transport formulation are present in XBeach_GPU, in this study we used the Soulsby-Van Rijn equations. The effect of dilatancy, where the high flow and rapid erosion hinder further erosion were not taken into account. This suggest that the model results may be conservative. The sediment characteristics used in this study are listed in Table 5.1. Note that to avoid unrealistic collapse of the dunes, the dune slopes were not allowed to change by more than 0.01 per model timestep (approx. 0.06s).

Table 5.1 Sediment parameters used in the XBeach modelling.

(D50) mm	(D90) mm	Density (kg/m3)	Slope dry (m/m)	Slope wet (m/m)
0.20	0.28	2650.0	1.0	0.3

5.2.4 Historical Beach Profiles and Critical Slopes

The critical sediment slope presented in Table 5.1 were obtained from beach profile data. In Poverty Bay, Beach Profile 7 is the only profile located within the model domain (Figure 5.14). Using this historical data, the slope of each beach section was calculated (Figure 5.15). The beach profile shows a slope that is both driven by wave dissipation and slope stability of the beach. Based on this data a critical slope of 1.0 for dry sand and 0.3 for wet sand appear reasonable.

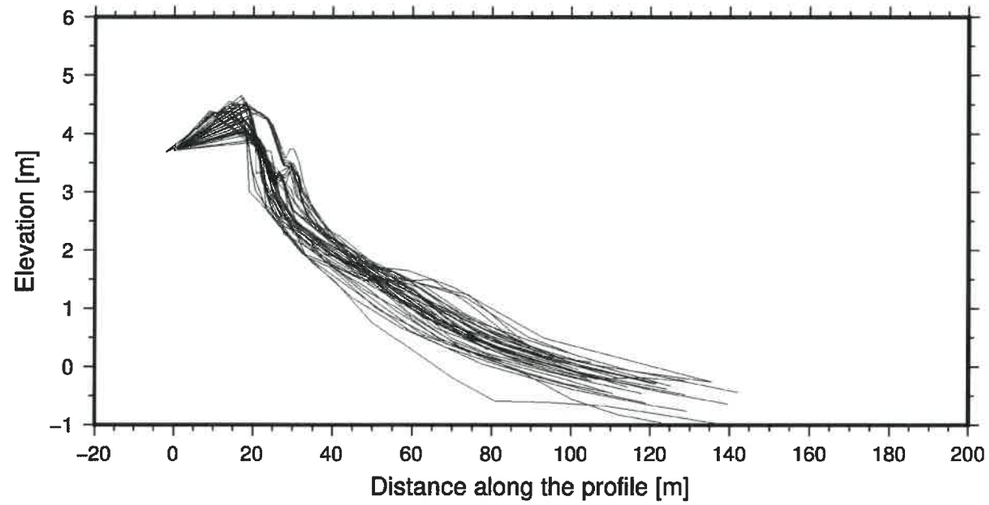

Figure 5.14 Beach profiles collected at benchmark 7

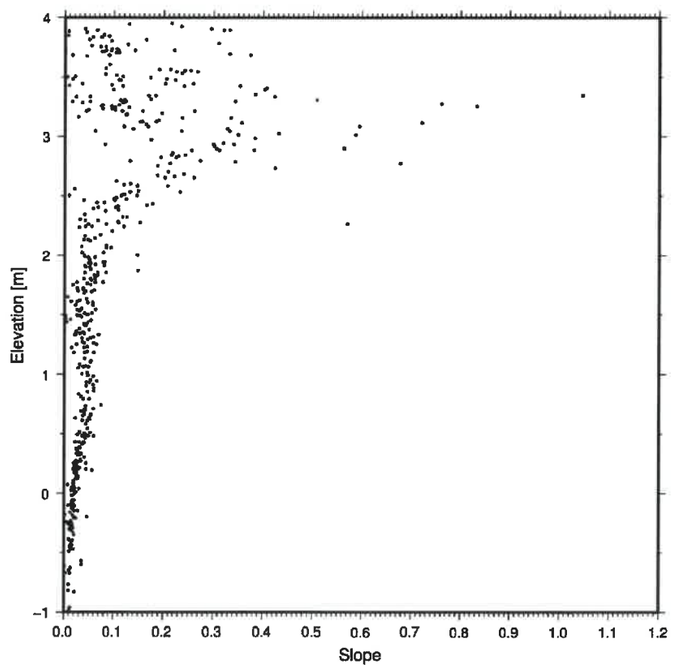

Figure 5.15 Beach profile slopes for all the beach profile collected at benchmark 7

5.2.5 Sensitivity Test

In order to test whether the uncertainties about the beach slope parameter for the model a sensitivity analysis was undertaken using the largest tsunami wave scenario (nt6ab, nt7ab and nt8ab). The sensitivity was completed by running 9 simulations, each time varying the critical slope for dry beach (0.7, 1.0, 1.3) and the critical slope for wet beach (0.1, 0.3, 0.5). The dune erosion is presented for all the scenarios along a cross-shore profile in Waikanae just west of Roberts Rd. The result of the between each of the nine simulations is almost undistinguishable showing that, in this case, the model is unsensitive to the critical slopes parameter. This is because most of the sand transport is associated with the high flow rates of the dune overtopping, dune slumping is only a minor contribution to the change in the morphology.

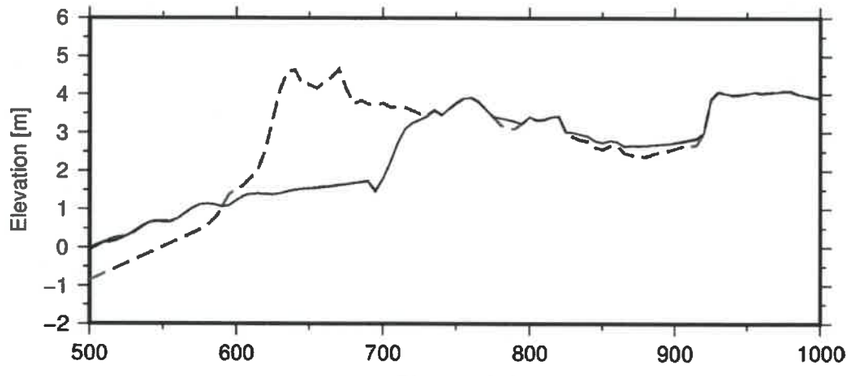

Figure 5.16 Result of sensitivity analysis. The dashed grey line is the initial topography. The black lines show the topography of the dune after 3hrs. Note, where only one black line is visible the model 9 outputs are identical.

5.2.6 Waikanae Results

In Waikanae the inundation was tested using 6 tsunami scenarios, 3 far field events (ff_8, ff_10 and ff_12) and 3 near field events:

- Yellow Zone: MHWS_nt6ab_nt7ab_nt8ab_15m
- nt6b_nt7b_15m
- nt6b_nt7b_15m at MHWS

For the far-field scenario, the inundation occurs along the Waikanae Creek and the tsunami surge, although large enough to overtop the dunes, causes only localised scouring and beach erosion. Because the inundation flows preferentially along the Waikanae creek, the banks of the creek are scoured widening the creek. The model however overestimated the depth of the creek and the bank erosion is amplified (Figure 5.18 to Figure 5.20).

For the local tsunami event the inundation is much more severe, the consistent overtopping rapidely erodes the dunes and large channels form to drain the in-lan inundation between waves. For the most severe scenario (nt6ab_nt7ab_nt8ab_15m_f2) the coastal landscape is completelly modified (Figure 5.21).

For scenario nt6b_nt7b_15m, the dunes are affected with a reduction in elevation of nearly 1 m along most of Waikanae. Small channels form in the low lying part of the dunes as the water receeds. The eroded sediment is deposited immediately landward of the dunes and in the nearshore. The landscape is not as severely modiyied as in the nt6ab_nt7ab_nt8ab_15m scenario and could recover quickly.

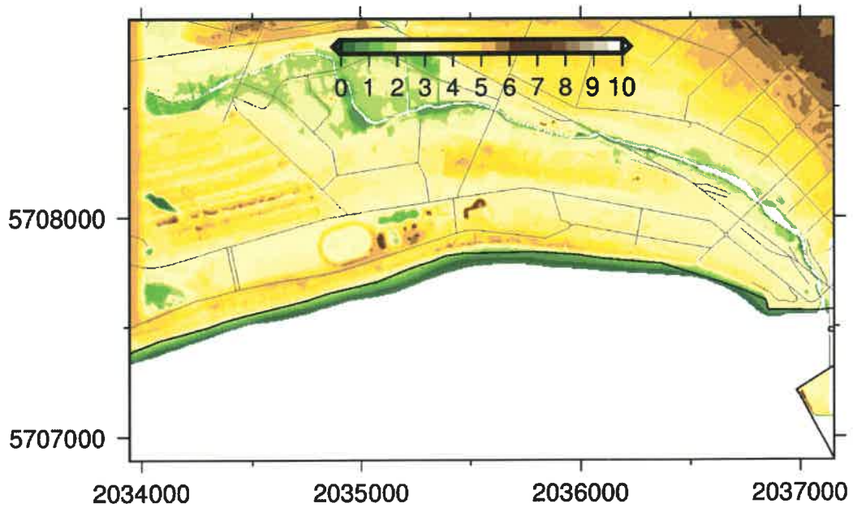

Figure 5.17 Topography at the start of the simulations

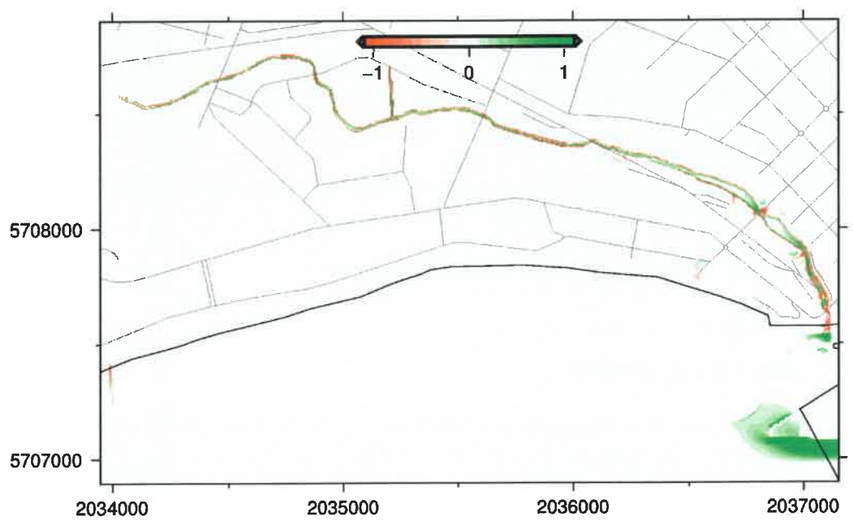

Figure 5.18 Simulated accretion (green) and erosion (red) for scenario ff_8

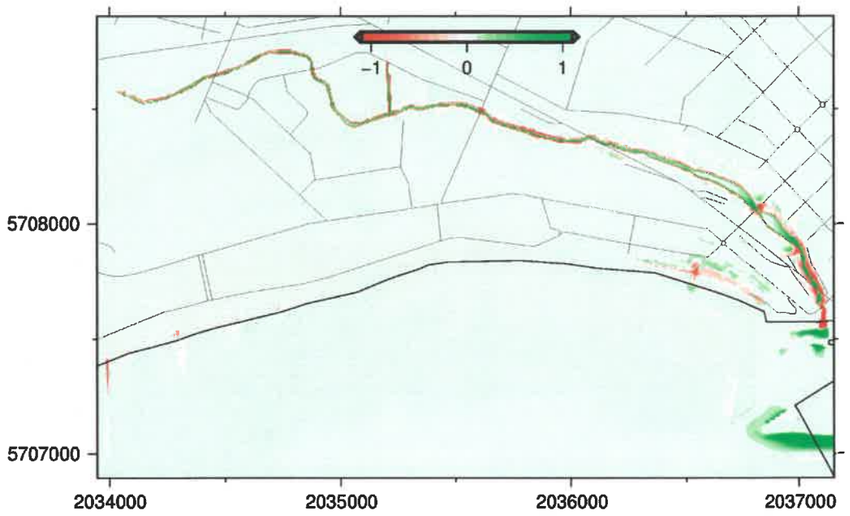

Figure 5.19 Simulated accretion (green) and erosion (red) for scenario ff_10

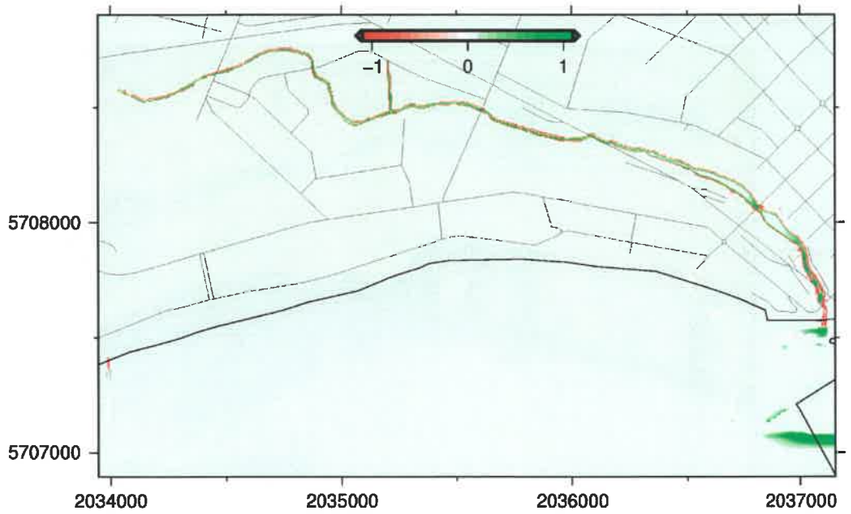

Figure 5.20 Simulated accretion (green) and erosion (red) for scenario ff_12

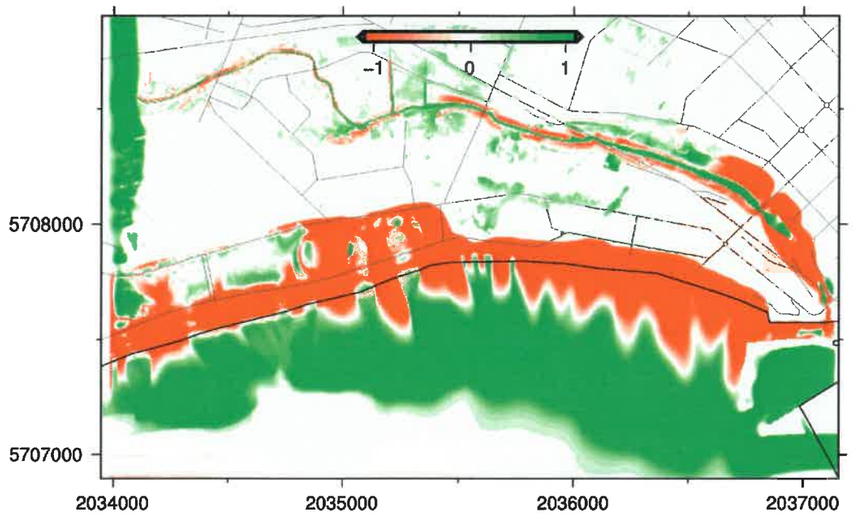

Figure 5.21 Simulated accretion (green) and erosion (red) for scenario nt6ab_nt7ab_nt8ab_15m

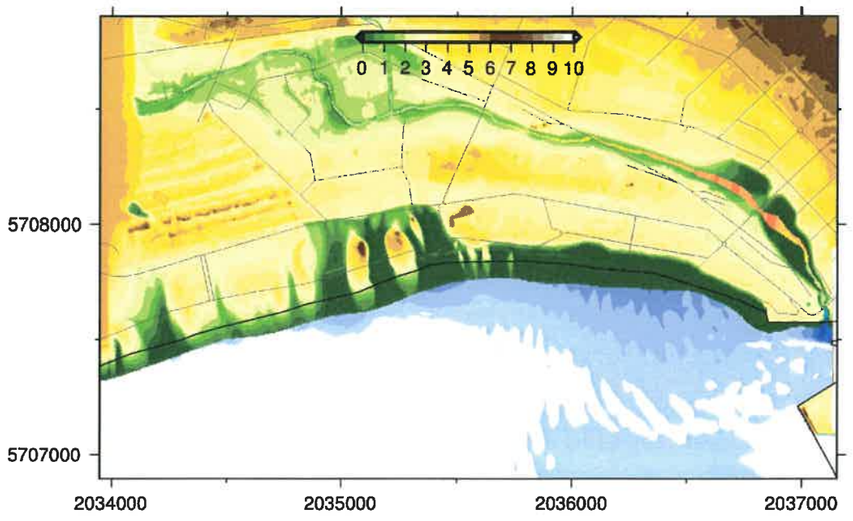

Figure 5.22 Topography at the of the simulation for scenario nt6ab_nt7ab_nt8ab_15m.

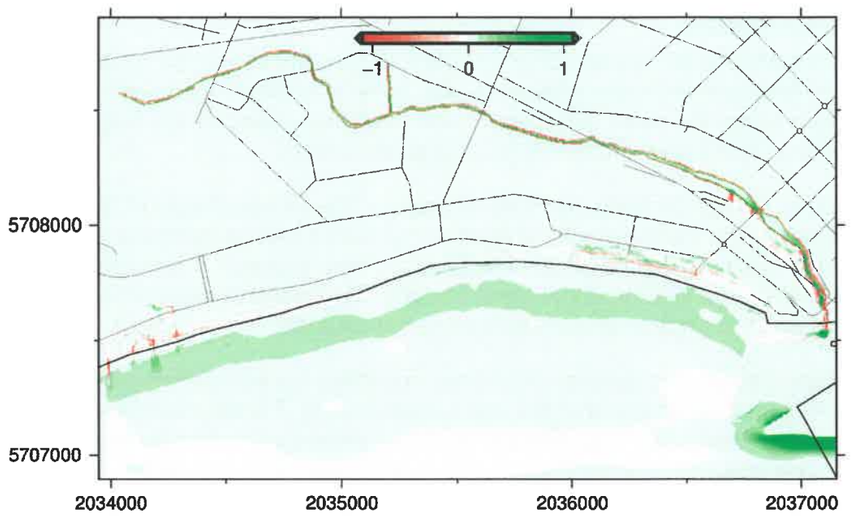

Figure 5.23 Simulated accretion (green) and erosion (red) for scenario nt6b_nt7b_15m

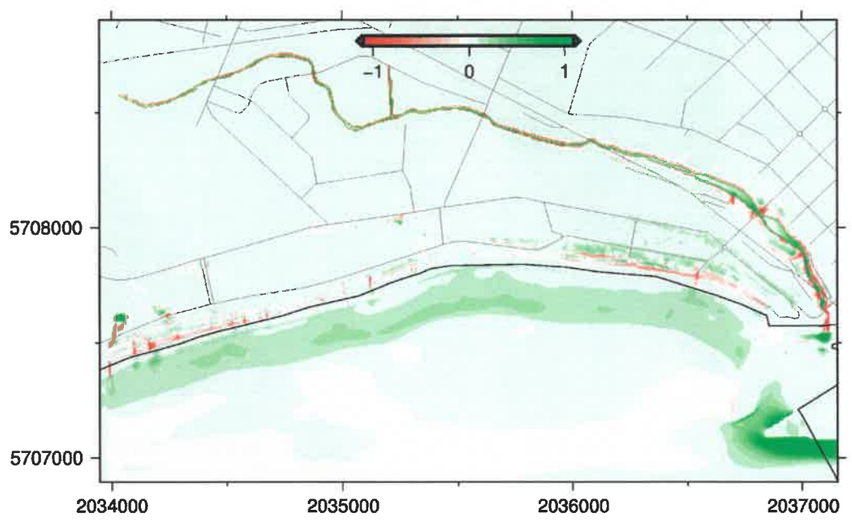

Figure 5.24 Simulated accretion (green) and erosion (red) for scenario nt6b_nt7b_15m at MHWS

5.2.7 Wainui Results

Tsunami erosion was simulated using the same 6 tsunami scenarios as for Waikanae. For all three far-field scenarios the erosion to the dune is small (<0.2m) with the mouth of Te Rimu Stream being the most affected. These predicted changes are negligible compared with the seasonal changes on the beach and storm impact.

The erosion is similar for both nearfield scenario. The seaward side of the dunes are the most affected. In the Northern part of Wainui the dunes are lower and are affected further inland with a pattern of erosion and accession that suggest a smoothing of the dune (flattening of the dune crest and infilling of trough). The extent of the morphological changes is not to the scale of erosion of dunes simulated Waikanae.

For the Wainui model, the dune erosion does not affect the inundation extent and therefore does not warrant an adjustment of the evacuation zoning. For the near-field scenario tested here, the erosion near Te Rimu Stream may compromise the bridge structure and affect evacuation process.

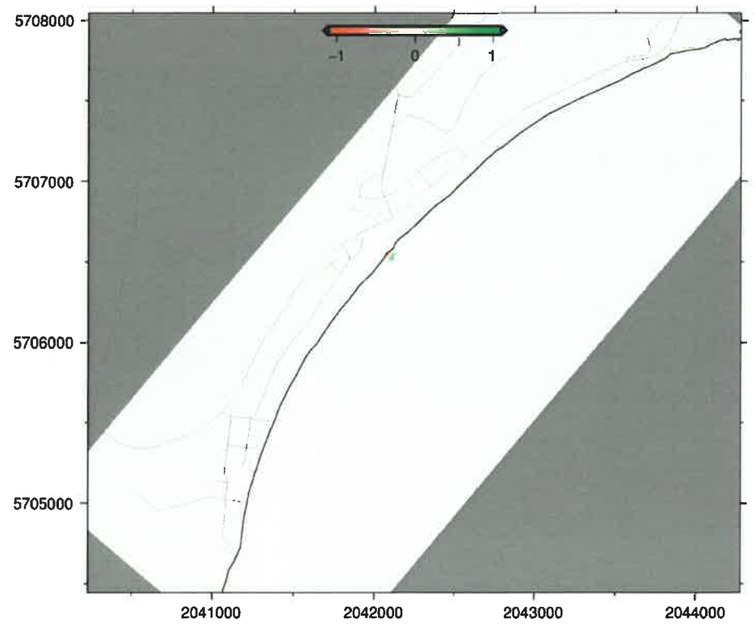

Figure 5.25 Simulated accretion (green) and erosion (red)in Wainui for scenario ff_8. Shaded grey area is outside of the model domain.

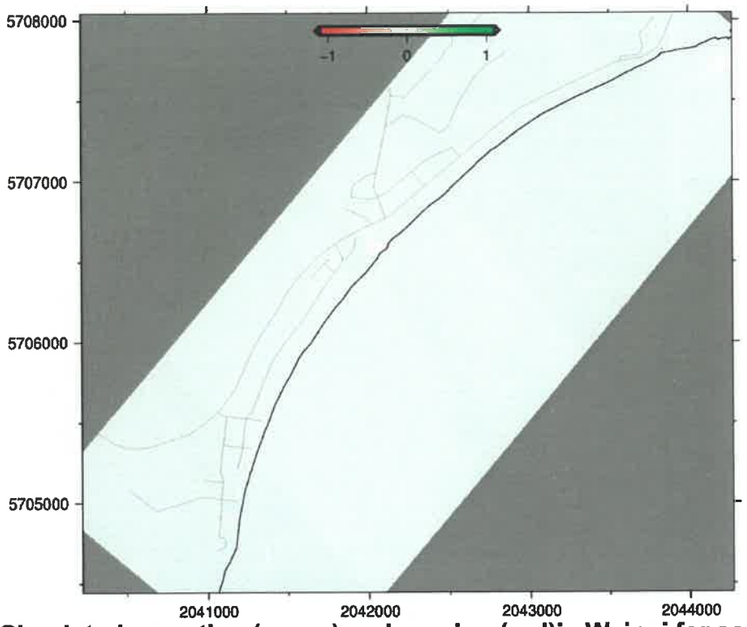

Figure 5.26 Simulated accretion (green) and erosion (red)in Wainui for scenario ff_10. Shaded grey area is outside of the model domain.

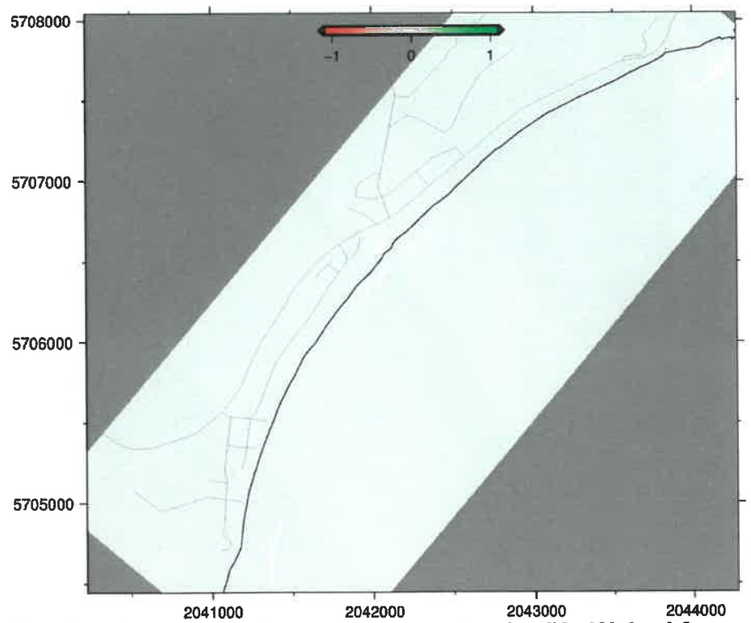

Figure 5.27 Simulated accretion (green) and erosion (red)in Wainui for scenario ff_12. Shaded grey area is outside of the model domain.

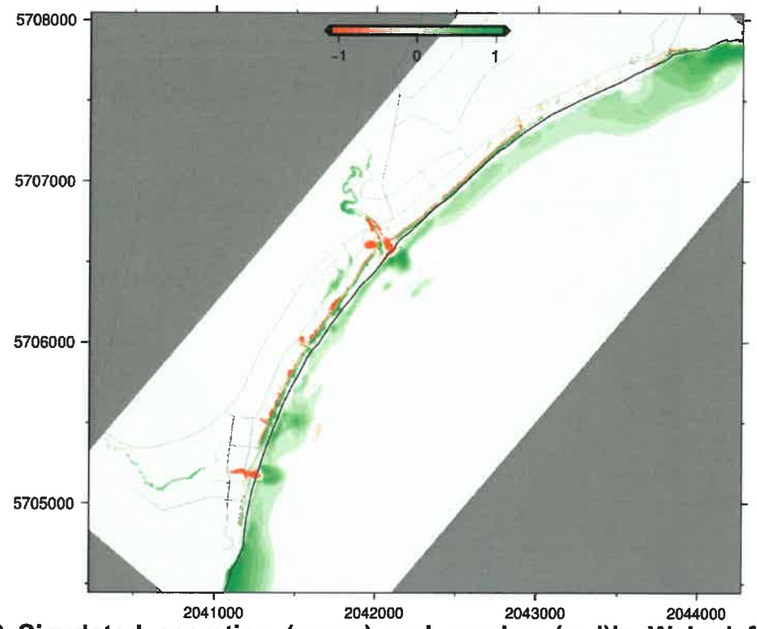

Figure 5.28 Simulated accretion (green) and erosion (red)in Wainui for scenario nt6ab_nt7ab_nt8ab_15m at MHWS. Shaded grey area is outside of the model domain.

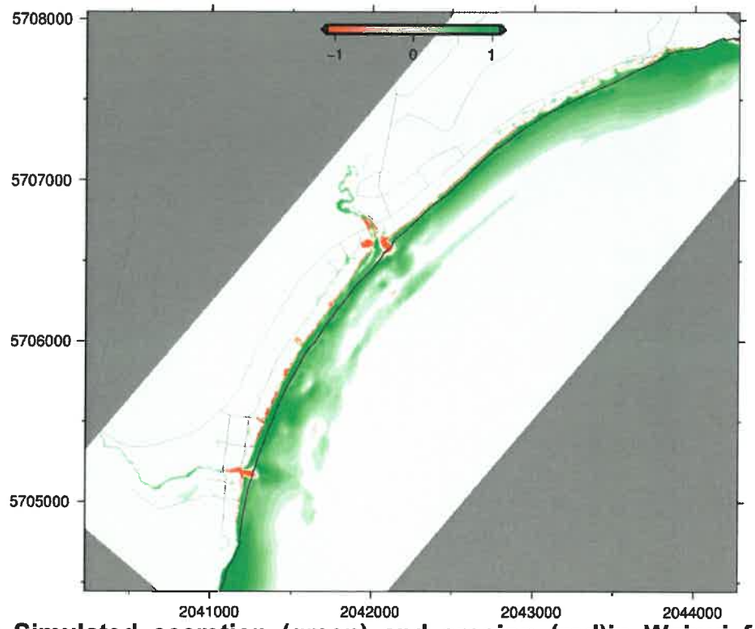

Figure 5.29 Simulated accretion (green) and erosion (red)in Wainui for scenario nt6b_nt7b_15m at MHWS. Shaded grey area is outside of the model domain.

6 DETERMINING THE EVACUATION ZONES

6.1 Evacuation Zones

In this study, the Yellow and Orange Zones were defined using the maximum inundation extent predicted by the numerical modelling of selected tsunami scenarios. The Red Zones are based on the location of the topographical contour showing 2.0m above MHWS (2.63m above NZVD2016 in Gisborne).

Using the simulated inundation extent or contour lines directly from the model output for defining the evacuation zoning is unpractical and can create confusion especially where the inundation line crosses buildings or land parcels. Therefore, a manual process is used to convert the modelled inundation in to the Yellow and Orange Zones and the topographical contour into the Red Zone manually using the following guidance:

Therefore, the final inundation zone was extended using the following guidelines:

- No buildings were crossed by the zone boundary;
- The boundary followed topographical features clearly visible in the LiDAR data;
- The boundary followed a roadway or other obvious physical landmark or feature (i.e. foothills, river bank) and not dramatically increase the number of buildings inside the zone;
- The boundary would not reduce the modelled inundation extent.

An example where the inundation extent was extended outward to the nearest road/passageway to construct the Orange Zone is shown in Figure 6.1 and Figure 6.2.

6.1.1 Important Limitations

The zones provided in this study have been created with great care, however they rely on the output of a numerical models and LiDAR data. Where the zones were extended to more "practical boundaries" this was done using satellite imagery with limited local information. Additionally, the zoning did not consider the location of high risk buildings or buildings that may be occupied by large numbers of people or by highly vulnerable people, such as schools, hospital and rest homes. Also, the zones presented here were designed without knowledge of planning arrangements or consideration about how communities may change in the future. Therefore, the zones require thorough review and consultation with local authority before they can be incorporated in evacuation maps. The proposed zonings have been provided to GDC as sperate GIS files and are presented below at 1:25000 scale from South to North (Figure 6.3 through Figure 6.16)

Figure 6.1 Example of zone adjustment. The darker shading represents the simulated inundation extent for the orange zone scenarios. The Orange shading shows the adjusted Orange zone.

Figure 6.2 Example of zone adjustment. The black shading represents the simulated inundation extent for the orange zone scenarios. The Orange shading shows the adjusted Orange zone.

6.2 Plots of the Individual Evacuation Zones

Below we present plots of each evacuation zone.

6.2.1 Poverty Bay

In Poverty Bay the yellow zone covers an area of 75km^2 covering a large part of Gisborne city (Figure 6.3). The model inundation extended beyond the area covered by the LiDAR data and there are uncertainties about the model results for these areas. In the city, the Orange zone extends beyond the Waikanae Creek and in the low-lying part of the city. At the foot of the hills near the Waimata River the Orange and Yellow Zones are identical (Figure 6.4).

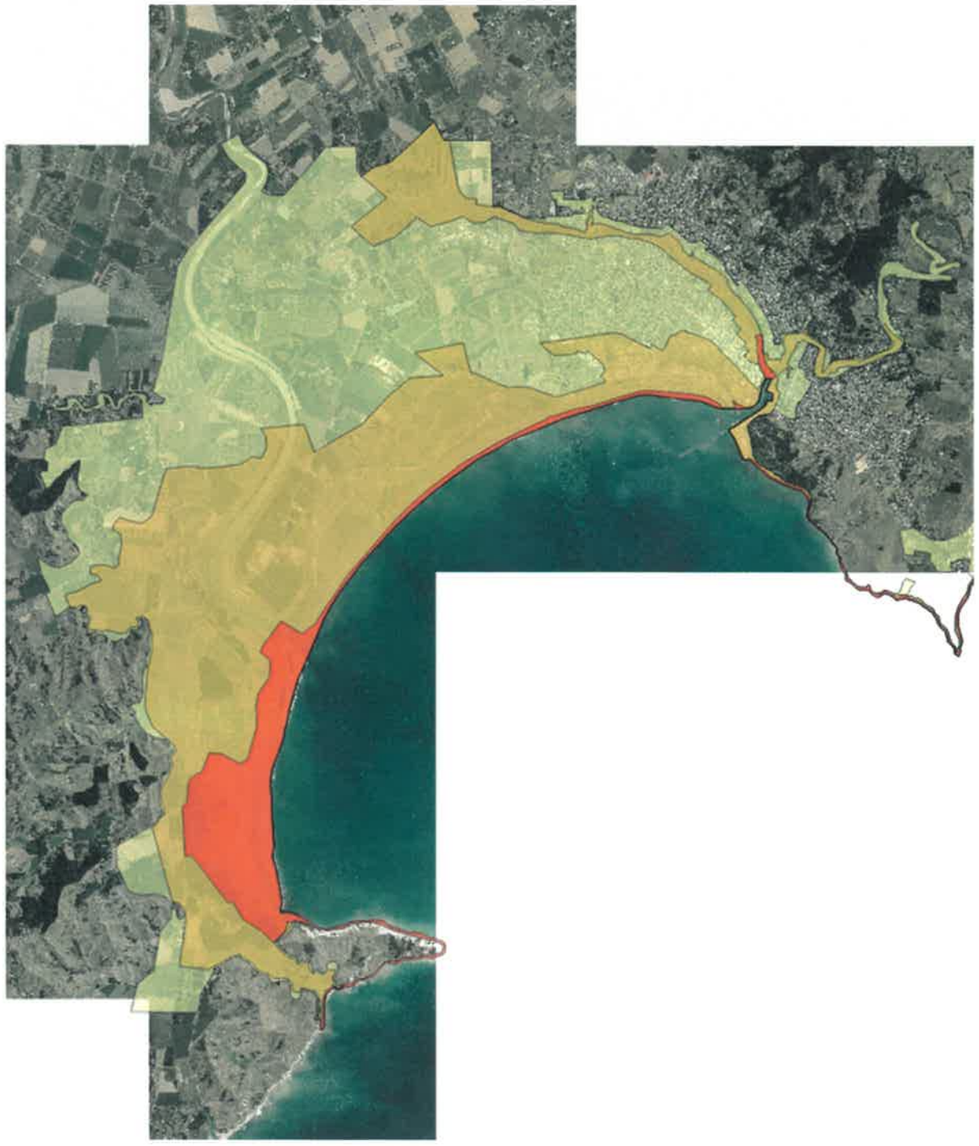

Figure 6.3 Poverty Bay Proposed Yellow and Orange zoning

Figure 6.4 Gisborne city Proposed Yellow and Orange zoning

6.2.2 Wainui

In Wainui, the Yellow Zone extends all the way to Wainui road and further inland near Te Rimu stream. The Orange Zone in Wainui only includes one building, the Wainui Surf Lifesaving Club.

Figure 6.5 Wainui proposed Yellow and Orange zoning

6.2.3 Makarori, Tatapouri

At Makarori the Yellow Zone extends to the Moana Rd and includes a large portion of the buildings in the Makarori settlement.

In Tatapouri, the Yellow zone covers a substantial portion of the camping site and extends nearly 100m inland from the main road.

Figure 6.6 Makarori and Tatapouri proposed Yellow and Orange zoning

6.2.4 Whangara

In Whangara both zones extend beyond Pa Road and the low lying land near the Waiomoko River.

Figure 6.7 Pouawa and Whangara proposed Yellow and Orange zoning

6.2.5 Waihau

In Waihau, the zones do not include any buildings. No reliable LiDAR coverage exist for the North part of the creek.

Figure 6.8 Waihau proposed Yellow and Orange zoning.

6.2.6 Tolaga Bay

In Tolaga Bay the Yellow Zone covers an area of 14 km^2 covering most of the building in the settlement. The Orange Zone although smaller (5km^2) also covers most of the settlement.

Figure 6.9 Tolaga Bay proposed Yellow and Orange zoning

6.2.7 Anaura Bay

In Anaura Bay the Orange Zone extends roughly 400 m inland and as far as 900 m for the Yellow Zone.

Figure 6.10 Anaura Bay proposed Yellow and Orange zoning

6.2.8 Tokomaru Bay

In Tokomaru, both zones cover most of the settlement with the Yellow zone extending further in the Mangahauini River and the Waiotu Stream.

Figure 6.11 Tokomaru Bay proposed Yellow and Orange zoning

6.2.9 Waipiro Bay

The Orange Zone in Waipiro extends roughly 75 m inland and along the main creek. Note that no LiDAR is available for the South and North of the Bay.

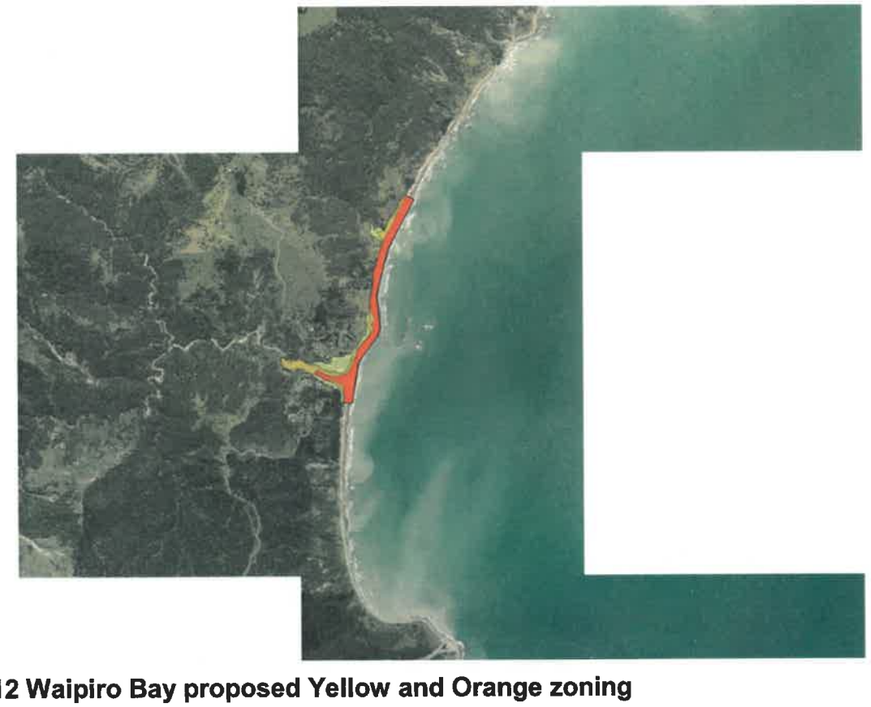

Figure 6.12 Waipiro Bay proposed Yellow and Orange zoning

6.2.10 Whareponga

In Whareponga both zone extents are similar, extending 75m inland.

Figure 6.13 Whareponga proposed Yellow and Orange zoning

6.2.11 Waiapu

In Waiapu the Lidar coverages is not homogenous resulting in strong uncertainties in the simulated inundation extents. Here the Orange zone extends 2km in the Waiapu river.

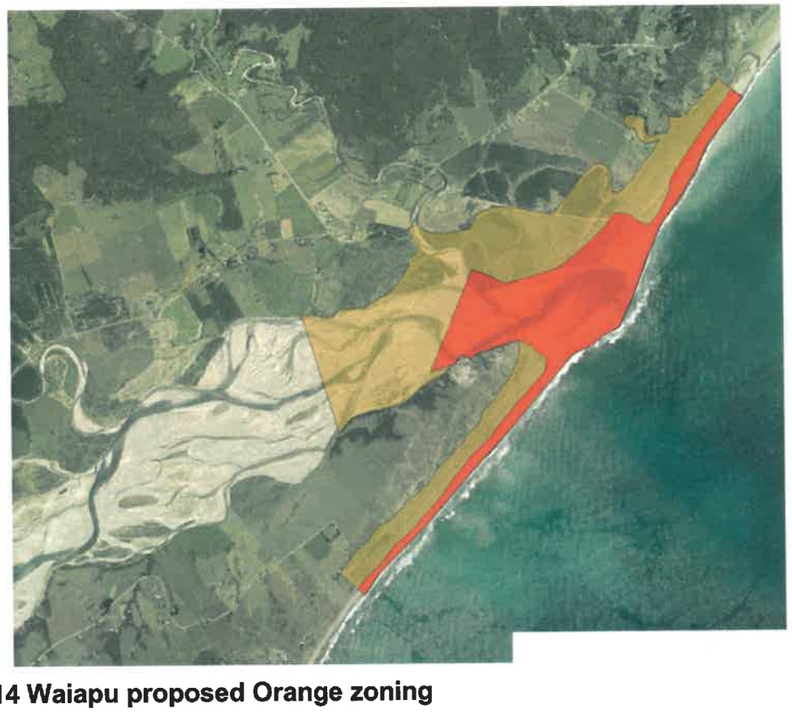

Figure 6.14 Waiapu proposed Orange zoning

6.2.12 Te Araroa

In Te Araroa, the Orange Zone extends 500 m inland and the Yellow Zone 1.5 km inland. The Yellow Zone extends inland beyond SH 35.

Figure 6.15 Te Araroa proposed Yellow and Orange zoning

6.2.13 Hicks Bay

In Hicks Bay, the Orange Zone extend to the SH35 and beyond in the North of the Bay. The Yellow zone extends around 1 km inland.

Figure 6.16 Hicks Bay proposed Yellow and Orange zoning.

6.3 Comparison Between Previous and Updated Evacuation Zones

Previously, the Gisborne District Council used a single zone for their tsunami evacuation protocol which was not in line with the procedure set forth in the most recent MCDEM guidelines. This project undertook the necessary modelling to devise three separate evacuation zones for different threat levels. A comparison between the extent of the original and updated zones in the Poverty Bay area is presented in Figure 6.17 below. In this figure we see that the Yellow Zone has significantly expanded the area considered susceptible to an extreme tsunami event. This however should not be surprising given the discussion of presented above of the inundation extents in Japan following the 2011 event. The updated Orange Zone is largely in line with the previous evacuation zone in the southern and northern parts of Poverty Bay but is extended through the central region while it is reduced immediately west of Gisborne City. The Orange Zone also extends up the Waimata and Taruheru Rivers.

Figure 6.17 Extents of the updated Red, Orange and Yellow Zones compared to the previous evacuation zone (white line).

7 REFERENCES

Bell, R., Holden, C., Power, W., Wang, X., and Downes, G. (2014) Hikurangi margin tsunami earthquake generated by slow seismic rupture over a subducted seamount, Earth and Planetary Science Letters, 397 (2014) 1–9.

Borrero, J., Bell, R., Csato, C., DeLange, W., Greer, D., Goring, D., Pickett, V. and Power, W. (2012). Observations, Effects and Real Time Assessment of the March 11, 2011 Tohoku-oki Tsunami in New Zealand, Pure and Applied Geophys., 170, 1229-1248, DOI 10.1007/s00024-012-0492-6

Borrero, J.C. and Greer, S.D. (2013) Comparison of the 2010 Chile and 2010 Japan tsunamis in the Far-field, *Pure and Applied Geophysics*, 170, 1249-1274, DOI 10.1007/s00024-012-0559-4.

Borrero, J.C., Goring, D.G. (2015) South American Tsunamis in Lyttelton Harbor, New Zealand, Pure and Applied Geophysics, 10.1007/s00024-014-1026-1

Borrero, J.C. (2012) TSUNAMI INUNDATION MODELLING: WHITIANGA, TAIRUA AND PAUANUI, Prepared for Waikato Regional Council, Hamilton, New Zealand, ISSN 2230-4363..

Borrero, J.C., Goring, D.G., Greer, S.D. and Power, W.L. (2014) Tsunami Hazards in New Zealand Ports, Pure and Applied Geophysics, 10.1007/s00024-014-0987-4Borrero and Goring (2015)

Bosserelle, C., (2013) Hydrodynamics and Sand Transport on Perched Beaches in Western Australia. PhD thesis, University of Western Australia, Crawley, Western Australia.

Bosserelle, C., Kruger, J., Movono, M., & Reddy, S. (2015). Wave inundation on the Coral Coast of Fiji. Australasian Coasts & Ports Conference 2015, (September), 96–101.

Costa, P. J. M., Costas, S., González-Villanueva, R., Oliveira, M. A., Roelvink, D., Andrade, C., Murray, A. (2016). How did the AD 1755 tsunami impact on sand barriers across the southern coast of Portugal? Geomorphology, 268, 296–311. http://doi.org/10.1016/j.geomorph.2016.06.019

Dorbath, L., Cisternas, A. , and Dorbath, C. (1990), Assessment of the size of large and great historical earthquakes in Peru, Bull. Seism. Soc. Am. 80, 551–576.

deLange, W.P. and Healy, T.R. (1986). New Zealand tsunamis 1840–1982. *New Zealand Journal of Geology and Geophysics*, *29*(1), 115–134. doi:10.1080/00288306.1986.10427527

Eiby, G.A. (1982) Two New Zealand Tsunamis, Journal of the Royal Society of New Zealand, 12:4, 338-351, DOI: 10.1080/03036758.1982.10415340

Fujii, Y. & Satake, K. (2013) Slip distribution and seismic moment of the 2010 and 1960 Chilean earthquakes inferred from tsunami waveforms and coastal geodetic data, Pure Appl. Geophys. 170: 1493. https://doi.org/10.1007/s00024-012-0524-2

GeoNet (2017), M 7.1 East Cape Fri, Sep 2 2016
http://www.geonet.org.nz/earthquake/2016p661332 Accessed June 22, 2017.

Gibson, F. (1869), On the Wave Phenomena observed in Lyttelton Harbor, August 15, 1868. Transactions and Proceedings of the New Zealand Institute, 1, 195:196

.Lal M. M., Southgate P. C., Jerry D. R., Bosserelle C., Zenger K. R. (2016) A Parallel Population Genomic and Hydrodynamic Approach to Fishery Management of Highly-Dispersive Marine Invertebrates: The Case of the Fijian Black-Lip Pearl Oyster Pinctada margaritifera. PLoS ONE 11(8):e0161390. doi:10.1371/journal.pone.0161390

Li, L., Huang, Z., 2013.Modeling the change of beach profile under tsunami waves: a comparison of selected sediment transport models. Journal of Earthquake and Tsunami 07 (01).

Li, L., Qiu, Q., Huang, Z., 2012. Numerical modeling of the morphological change in Lhok Nga,west Banda Aceh, during the 2004 Indian Ocean tsunami: understanding tsunami deposits using a forward modeling method. Nat. Hazards 64 (2), 1549–1574.

Lynett, P., Borrero, J., Weiss, R., Son, S., Greer, D., Renteria, W. (2012) Observations and Modeling of Tsunami-Induced Currents in Ports and Harbors, Earth and Planetary Science Letters, 327-328 (68-74).

Morris, B. and Borrero, J. (2014) Inundation of Whitianga town during the 1960 Chilean tsunami, Waikato Regional Council Technical Report 2014/65.

MCDEM (2008) Tsunami Evauation Zones Director's Guideline for Civil Defence Emergency Management Groups December 2008 [DGL 08/08] ISBN 978-0-478-25483-

New Zealand Palaeotsunami Database (2017). https://ptdb.niwa.co.nz, Accessed 2018.

Percival, D, Denbo, D, Eble, M, Gica, E, Mofjeld, H, Spillane, M, Tang, L, and Titov, V (2010). Extraction of tsunami source coefficients via inversion of DART buoy data, Nat. Haz. doi:10.1007/s11069-010-9688-1.

Power, W. L. (2013). Review of Tsunami Hazard in New Zealand (2013 Update) GNS Science Consultancy Report No. 2013/131, 238 pages.

Power, W. L. (2014). Tsunami hazard curves and deaggregation plots for 20km coastal sections, derived from the 2013 National Tsunami Hazard Model GNS Science Consultancy Report No. 2013/59, 558 pages.

Roelvink, D., Reniers, A., Van Dongeren, A., Thiel, Van, de Vries, J., McCall, R., Lescinski, J., 2009. Modelling storm impacts on beaches, dunes and barrier islands. Coastal Engineering 56, 1133–1152.

Titov, V. V., & González, Frank, I. (1997). *Implementation and testing of the Method of Splitting Tsunami (MOST) model* (No. ERL PMEL-112) (p. 14). Retrieved from http://www.pmel.noaa.gov/pubs/PDF/tito1927/tito1927.pdf

Titov, V. V., Moore, C. W., Greenslade, D. J. M., Pattiaratchi, C., Badal, R., Synolakis, C. E., & Kânoğlu, U. (2011). A New Tool for Inundation Modeling: Community Modeling Interface for Tsunamis (ComMIT). *Pure and Applied Geophysics*, *168*(11), 2121–2131. doi:10.1007/s00024-011-0292-4

Titov, V.V., and C.E. Synolakis (1995) Modeling of breaking and nonbreaking long wave evolution and runup using VTCS-2. *J. Waterways, Ports, Coastal and Ocean Engineering*, 121(6), 308–316.

Titov V.V. and Synolakis, C.E. (1997) Extreme inundation flows during the Hokkaido-Nansei-Oki tsunami, Geophysical Research Letters, 24 (11), 1315-1318.

Titov, V.V. and Synolakis, C.E. (1998) Numerical modeling of tidal wave runup, Journal of Waterways, Port, Coastal and Ocean Engineering, ASCE, 124 (4), 157-171.

USGS (2017) M 7.0 – 175 km NE of Gisborne, New Zealand https://earthquake.usgs.gov/earthquakes/eventpage/us10006jb, accessed on June 22, 2017.

Viikmäe, B., Torsvik, T., & Soomere, T. (2013). Impact of horizontal eddy diffusivity on Lagrangian statistics for coastal pollution from a major marine fairway Topical Collection on the 16th biennial workshop of the Joint Numerical Sea Modelling Group (JONSMOD) in Brest, France 21-23 May 2012. Ocean Dynamics, 63, 589–597. https://doi.org/10.1007/s10236-013-0615-3

Wang, X.; Power, W.L.; Bell, R.E.; Downes, G.L.; Holden, C. (2009). Slow rupture of the March 1947 Gisborne earthquake suggested by tsunami modelling. P. 221 In: Barrell, D.J.A.; Tulloch, A.J. (Eds.) Geological Society of New Zealand & New Zealand Geophysical Society Joint Annual Conference, Oamaru, 23-27 November 2009: programme and abstracts. Wellington:Geological Society of New Zealand. Geological Society of New Zealand miscellaneous publication 128A.

Wei, Y., Chamberlin, C., Titov, V. V., Tang, L., & Bernard, E. N. (2013). Modeling of the 2011 Japan Tsunami: Lessons for Near-Field Forecast. *Pure and Applied Geophysics*, *170*(6–8), 1309–1331. http://doi.org/10.1007/s00024-012-0519-z

Wei, Y, Newman, A, Hayes, G, Titov, V, Tang, L (2014). Tsunami Forecast by Joint Inversion of Real-Time Tsunami Waveforms and Seismic or GPS Data: Application to the Tohoku 2011 Tsunami. Pure Appl. Geophys. doi:10.1007/s00024-014-0777-z

8 APPENDIX 1: HISTORICAL TSUNAMI OVERVIEW

The following information is copied directly from the GNS Historical Tsunami database.

8.1 1868 Southern Peru Event

8.1.1 Overall New Zealand Tsunami Impact Summary

The tsunami from the 1868 August 13 Mw 8.8-9.3 Southern Peru earthquake first arrived at the main islands of New Zealand early am on August 15. Observations of the tsunami were reported from nearly 90 locations, mainly on the eastern seaboard from Mangonui, in Northland, to Riverton, in Southland, as well as at Nelson and Motueka and at Westport and Greymouth on the West Coast of the South Island and at Wanganui on the west coast of the North Island. It was also observed throughout the Chatham Islands, arriving just after midnight, the greatest water height above sea level at the time reaching 10 m at Owenga on the east coast, washing away several huts and damaging boats. At Tupuanga (Tupuangi) on the northwest coast of Chatham Island, the dwellings of entire Maori village were washed away, the 60-70 residents escaping after the first of three large waves reached the floor of their dwellings. One death occurred nearby at Waitangi West when a person tried to rescue a boat between waves. A European-style house was completely destroyed at Te Raki Bay, the two occupants barely escaping. Damage occurred at other locations on Chatham Island, and an inundation map, dated September 1868, showing water heights as broad or narrow bands of yellow dependent on height, indicates water heights from 1.8 m to over 6 m generally.

The areas most affected in the North and South islands were around Great Barrier Island, eastern Bay of Plenty, Napier, Canterbury, especially Bank's Peninsula, and Oamaru. Fifteen locations reported water heights above sea level at the time of 2 m or more. The greatest reported heights were at Little Akaloa (4.5-5.0 m), and Le Bons Bay (5.8-7.6 m), although the latter may have been overestimated by observers. At Westport, water levels of 1.2-1.5 m above normal were experienced. Bores were observed in the Waimakariri, Heathcote and Avon Rivers, in Canterbury, the Awatere River in Marlborough, and in eastern Bay of Plenty, the greatest distance from the coast being in the Awatere River (15 km).

The tsunami damaged boats and moved moorings and buoys at many places. Around Bank's Peninsula, many wharves, bridges, and fences were damaged or destroyed, and several houses were inundated. The effects may have been significantly greater, had some of the largest waves occurred at higher tide levels, particularly about Bank's Peninsula. Along much of the South Island and southern half of the North Island east coast the first few hours of waves occurred when the tides were below MSL. This and the arrival of the first waves during the night contributed to the first waves not being well observed and, in many cases, the first observed waves being many hours after the forecast arrival time (calculated using ITDB, 2004). On the West Coast, the tsunami was first noticed about 10 hours after the first observed arrivals on the east coast. The waves were greatest within the first 12-20 hours of arrival, and sea level did not return to normal for at least 2-3 days.

8.1.2 Source Parameters

Time UTC: 21:30 13th August 1868

Source Location lon/lat: -71.60, -17.7

The 1868 August 13 southern Peru earthquake was a very large plate interface earthquake, which was destructive in the towns of Arequipa, Moquegua, Mollendo and Ilo in Southern Peru. It generated a tsunami, which was devastating locally, and which was observed over a large part of the Pacific Rim. (NGDC Tsunami Database) There is much uncertainty about the earthquake's location and magnitude, with locations ranging over two degrees latitude and magnitudes ranging from 8.5 to 9.5, two of the more recent estimates of which are: Mw 9.3, Okal et al. (2006); Mw 8.8, Comte & Pardo (1991). Other magnitude and location estimates are available for example, in the NGDC Tsunami Database and Dorbath et al. (1990). Careful consideration should be given to choosing the most appropriate earthquake parameters for tsunami propagation models and for scenario development by Emergency Management for response in a Tsunami Warning situation.

8.1.3 Gisborne

At 10:00 it was low water with the current running out strong, soon after came in with unusual rapidity and at 12:00 was about the level of œ [xx] tide and running out again very rapidly. About 15:00 the largest waves came in raising the level about 2 ft above normal spring tides. It was then nearly the time for high water; spring tides not due for several days. (Williams, 1868); Tidal disturbances observed. (Hawke's Bay Herald, 22 August 1868, reprinted in Daily Southern Cross, 26 August 1868).

In this era there were few Europeans living in Gisborne, the writer (Williams) living away from the immediate coast. While there is no comment on any obvious inundation effects that might have occurred prior to 10:00, it is likely that some waves were higher earlier on the day when the tide was low.

According to NIWA Tide forecaster (www.niwa.co.nz/services/free/tides), HW was at 01:32 (0.61 m) and 14:10 (0.69 m) NZMT, LW at 07:49 (-0.70 m) and 21:22 (-0.61 m).

From LINZ Website tidal information relative to MSL (www.hydro.linz.govt.nz/tides), MHWS 0.75m, MLWS -0.78 m, MHWN 0.52 m, MLWN -0.51 m at Gisborne.

Estimated run-up for MCDEM: 1

Max height reach at inundation limit (m): ≥1.4

8.1.4 Waipaoa River mouth

A vessel anchored in Big River experienced strong “tidal wave” at 14:00, which carried away all lines. Frequent ebbing and flowing about every 15 min from 14:00 on 15 Aug until 12:00 on 16 Aug. Greatest rise 7 ft. (Hawke's Bay Herald, 22 Aug 1868; quoted in other newspapers).

According to NIWA Tide forecaster (www.niwa.co.nz/services/free/tides), HW was at 01:32 (0.61 m) and 14:10 (0.69 m) NZMT, LW at 07:49 (-0.70 m) and 21:22 (-0.61 m).

From LINZ Website tidal information relative to MSL (www.hydro.linz.govt.nz/tides), MHWS 0.75m, MLWS -0.78 m, MHWN 0.52 m, MLWN -0.51 m at Gisborne.

Estimated run-p for MCDEM: 2

Max height reached at inundation limit (m): ≥2.1

Damage built/marine/environmental: Boat mooring lines carried away

8.2 1877 Northern Chile Event

8.2.1 Tsunami Impact Summary

The tsunami from the 1877 May 10 Mw 8.8 Northern Chile earthquake first arrived on the main islands of New Zealand early on the morning of 1877 May 11 NZMT. The tsunami was reported observed from nearly 50 locations, from Mangonui, in Northland, to Riverton, in Southland, and at Westport on the West Coast. It was also observed at Waitangi (est. 3-3.5 m water height above sea level at time) in the Chatham Islands, where a house and bridge were washed away, and another house inundated, and at Perseverance Harbour, Campbell Island, where it did some damage and reached an estimated 3-4 m above MSL.

The data are probably incomplete for the Chatham Islands. The areas most affected areas in the North and South Islands were Northland, Coromandel, Banks Peninsula, and Oamaru, with water heights above sea level at the time reaching just over 3 m at Little Akaloa, possibly Pigeon Bay, and Akaroa. Heights of 1-1.5 were common, with 8 locations only experiencing heights of 2 m or more. Westport experienced waves with a peak-to-trough of 1.8 m, i.e. the height above sea level at the time of about 0.9-1.0 m.

The tsunami was not observed at Hokitika, nor reported from other west coast North or South Island locations. Bores were observed in the Piako and Waihou Rivers near Thames, in the Waimakariri and Avon Rivers, in Canterbury. Generally, the tsunami was less pronounced than the 1868 tsunami and it not cause as much concern or damage, probably because some of the largest waves about Bank's Peninsula and Oamaru, and along much of the South Island and southern North Island east coast occurred when the tides were below MSL. On the other hand, the Coromandel and Northland were impacted close to high tide. The first waves of the tsunami generally arrived not long after the forecasted arrival time, (calculated using ITDB, 2004), and were greatest within the first 6-12 hours. The tsunami was first observed at Westport about 10 hours after the first arrivals on the east coast.

8.2.2 Source Parameters

Time UTC: 00:59 10th May, 1877

Source Location lon/lat: -70.20, -19.60

The 1877 May 10 Mw 8.8 (Comte & Pardo, 1991) Northern Chile earthquake was most strongly felt between Iquique and Antofagasta. Uplift and subsidence occurred at various points along the coast. Most of the loss of life and damage is attributed to the tsunami, which reached a maximum of 24 m above sea level at the time. (Principally from NGDC Tsunami Database, April 2009) The earthquake followed nine years after the disastrous 1868 Southern Peru earthquake and tsunami, immediately to the north along the plate boundary.

As with many of the historical earthquakes there is much uncertainty about the earthquake's location and magnitude, with locations ranging over three degrees latitude and magnitudes ranging from 8.3 (NGDC Tsunami database) to 8.8 (Comte & Pardo, 1991). Other magnitude and location estimates are available on the NGDC Tsunami Database. The extent of tsunami effects in New Zealand suggests that the magnitude of the earthquake was greater than the Mw 8.3 in the NGDC Tsunami database, and more consistent with Comte & Pardo (1991) Mw 8.8. More recent estimates may be available. Hence, careful consideration should be given to choosing the most appropriate earthquake parameters for tsunami propagation models and for scenario development by Emergency Management for response in a Tsunami Warning situation.

8.2.3 Gisborne Port

First wave hit between 00:01-02:00 on May 11. This was slight. Another wave at 04:00 rose 2 ft, appearing like a slight increase of high tide. At 07:00 a heavy wave, rushing in with terrific force, rising 7 or 8 ft vertically in as many minutes and then receding as quickly, washing away about 50 yds of a sandy point in the harbour. No noise was given of its approach. Similar waves occurred at 09:00, 11:00, 12:40 and 14:30, each rising from 2-3 ft. Disturbances thought to have ceased morning of May 12 but resumed later in the day and continued irregularly to morning of May 14

Waves were somewhat regular at first but not later. (Crisp 1877);

Report at 09:10, May 11: At xxŸ ebb, water rushed in past usual HWM, receded and second smaller rush occurred. Later report at 12:30 May 11: Tidal disturbances throughout night May 10-11. At 03:00 [sic] at 3/4 ebb tide, wave rushed in at 8 ft above top of the hull of SS Go-Ahead, then wave struck the bar that partially broke it, causing only a 3-4 ft rise in the river, overflowing the banks in low-lying places. At 09:30 another wave ran up the river, at 09:45 another, and almost immediately a fourth. Water in the bay was agitated. (Evening Post 11 May 1877);

Report to May 12 09:00: Disturbances ceased. Press Agency Report to 14:45 May 11 [sic, probably should be 12]: The tidal disturbances continue. At 7:00 tide rose 8 ft in 10 min; at 09:00. it rose about 4 ft; and at 11:00. about 3 ft. At 12.40, and again at 15:30, tide rushed in for about 10-15 minutes, rising 3-4 ft. (Evening Post 12 May 1877);

From Gisborne eyewitness: Tide was about xxœ ebb, slowly receding for several hours, when immense roller fully 5ft vertically surged inshore washing high above where men had been at work on the boat Go-Ahead. Almost immediately water receded and was followed by minor surges. First big wave occurred at a few minutes after 07:00. (NZ Herald 15 May 1877);

Eight waves over the bar. [Extract as in other newspapers plus following additional information] eighth wave up river at 12:30 at xxŒ flood tide. River much higher than ordinary high tides. Current upriver estimated at 10 mph. Many boats in river adrift. (NZ Herald 12 May 1877); [As in other newspapers, plus following.]

At Œ flood Turanganui river was higher than ordinary high-water mark. Boats went adrift, punt was carried away, and all operations suspended between the river and the bar. (Bay of Plenty Times 12 May 1877).

Note that arrival time at 00:01 - 02:00 (travel time 11.5-13.5 hrs) is too early and not used. Note also that there are no local newspapers in this era. According to NIWA tide Forecaster (www.niwa.co.nz/services/free/tides), HW occurred at about 03:18 NZMT (0.52 m) and at 15:54 NZMT (0.50), LW at 09:38 NZMT (-0.55). Hence 3/4 ebb would have occurred at about 08:00 not 03:00 as in some extracts. According LINZ website, MHWS is 0.75 m above MSL, highest Astronomical Tide 0.95 m above MSL.

Estimated run-up for MCDEM: 2.4

Max water elevation at shore (m): 2.1-2.4

Max height reached at inundation limit (m): 1-1.3

Max observed height of inundation (m): 0.9-1.2

Damage built/marine/environmental: small punt and several boats set adrift

8.3 March 1947 Event

8.3.1 Tsunami Impact Summary

The 25 March 1947, (2032 UT March 26, 0832 NZST M_L 5.9, M_S 7.2, M_W 7.0 - 7.1) Offshore Poverty Bay, New Zealand, earthquake, identified as a "tsunami earthquake" (Downes et al. 2001. Doser & Webb, 2003), generated one of the largest tsunamis in New Zealand's historical record. The tsunami was observed along 115 km of coastline from Mahia Peninsula to Tokomaru Bay, probably at Waitangi, and possibly at Tuapeka, in the Chatham Islands. A large part of the affected coastline was sparsely populated. The tsunami occurred less than half an hour before high tide (at Gisborne), which was about the level of mean high-water spring (MHWS) tide, and hence its effects were at their maximum.

Several beachside cottages and buildings, as well as bridges, fences and roads were damaged at several locations from Waihau Beach (where two old bridges on the old coast road at Waihau Bay were swept away) to Te Mahanga. At Tatapouri Point, Pouawa and the south side of Turihaua Point, where the tsunami was most pronounced, large breaking waves said to be 10-13 m high, were observed offshore. These locations are marked by the presence along parts of the coast of coastal rock platforms, covered at high tide, but visible at low tide, which would considerably affect the characteristics of the tsunami waves near shore. At the northern end of Pouawa Beach, where seaweed was found 12 m above sea-level in telegraph wires well inland from the beach, and the decking and superstructure of a 16 m span wooden bridge across the Pouawa River was swept about 800m inland, indicate a water height at the maximum inundation limit of about 10 m.

At the southern end of the beach, where the water height at the maximum inundation limit was possibly 6-8 m, three rooms of a 4-roomed cottage were demolished, and the building swept from its foundation. Five people in the cottage survived the tsunami, three trapped within the one room that remained intact, and two by running inland when the first wave was observed. Buildings at Tatapouri and Te Mahanga were also structurally damaged, and water entered others at Makorori, Wainui Beach, and Kaiti Beach. Along the beach south of Te Mahanga, north and south of Young Nick's Head, at Makorori, Tatapouri and Pouawa crops and/or fences were damaged.

Gisborne harbour experienced three large surges, reaching a maximum of 1.5-1.8 m above sea level at the time, followed by other smaller surges, the latter causing the tides to ebb and flow every 8-10 minutes for about two hours. Three large bores and a number of smaller bores surged up the Turanganui River and its tributaries, but the water did not overtop the wharves nor did any damage along the river banks. Bores were also reported in other rivers between Young Nick's Head and Tolaga Bay.Fish were reported washed ashore at Tatapouri and, in large quantities, along the beach between Te Mahanga and Mahia.

Several people observed the arrival of the first wave and none noted any effect that might suggest that the water retreated prior to the first large wave arriving. Hence the tsunami arrived with a leading elevation, or at most, a small depression. According to one observer (at Tatapouri), the retreat of the first wave reduced the impact of the second, but the second wave appeared to be larger when it formed out to sea, possibly because of the depression between. The first two waves at Tatapouri and Pouawa were reported as about 3-4 minutes apart, and water remained at a high level for about ten minutes after the second wave at

Tatapouri. Although accounts of the tsunami suggest arrival times ranging from 8.40 am, that is, eight minutes after the earthquake, to 9.20am, other accounts more reliably indicate an arrival time about 9am or just after.

Two men, who had felt the earthquake at Gisborne Post Office and then travelled north by car, reached Pouawa just before the wave hit there. They estimated the time as just before 9 am, or about 25 minutes after the earthquake. The distance of about 20 km was covered in about 20-25 minutes, that is, at a speed of 48-60kph, which is entirely reasonable given the era. Their arriving five minutes after the earthquake is not.

The Harbourmaster at Gisborne, who was responsible for tidal records, reports the time of arrival of the wave at Gisborne Harbour as 9.05am, and at Mahia, about 9am. Some accounts also record the direction travelled by the wave. From the hill behind Tatapouri Point the wave appeared to come from a little south of east. The waves were also seen to break at Tatapouri Point and then progressively break on beaches to the south. Another observer saw the wave travel across Poverty Bay from Tauhine Point to Young Nick's Head. From the road just north of Tatapouri Point, another observer watched the first wave come in, the second wave forming out in the bay and then surging across the bay to Turihaua Point (presumably following the course of the first wave). His description of the first wave seems to imply that the southern end of the beach was affected before the northern end.

8.3.2 Source Parameters

Time UTC: 20:32 25th May, 1947

Source Location lon/lat: 178.80, -38.85

The 1947 March 25 (UT) March 26 (NZST) earthquake was located about 60 km offshore from the coastline north of Gisborne and 10-15 km west of the Hikurangi Trough. Although described by some as severe and prolonged, the earthquake was not widely felt along the nearest coast and caused no damage. The maximum intensity of MMI IVis considerably less than the expected intensity for its moment magnitude M_W 7.0 - 7.1 and surface wave magnitude M_S 7.2 and even somewhat low for its local magnitude M_L 5.9.

This earthquake's importance lies in the fact that it was followed by one of the largest locally generated tsunamis in NZ's historical record. Like the 1947 May 17 (UT) earthquake (q.v.), it has been identified as a "tsunami earthquake" (Downes et al. 2001; Doser & Webb, 2003). Source parameters (strike, dip, rake, centroid depth) and moment magnitude have been determined by Doser & Webb (2003) waveform modelling studies, using the Downes et al. (2001) epicentre, are shown on the map. They comment that "the earthquake exhibits many characteristics associated with 'tsunami earthquakes' (e.g. Pelayo & Wiens 1992; Satake 1994), including a small intensity and local magnitude compared with M_W and M_S, epicentre location ~50 km [sic, this should be 15 km] from the trench (trough) axis, shallow focal depth, low dip angle, and long rupture time."

Doser & Webb also considered the possibility that the seismograms were produced by a landslide or slumping event with a single-force mechanism, rather than a double couple, commenting that: "the radiation pattern for a single-force oriented at 315° (normal to the strike of the bathymetry near the epicentre) is similar to that of a low-angle reverse fault oriented at 45°, making it difficult to distinguish between single-force and double-couple models using body wave-form data alone.

Hasegawa & Kanamori (1987) have interpreted the 1929 Grand Banks earthquake (Ms ~7.2) as a submarine landslide with a source area of 37 500 km2. This event is similar in Ms to the Poverty Bay event, but no evidence for a submarine landslide of this size has been found along this portion of the Hikurangi Margin, so we conclude that seismic radiation for the Poverty Bay event was from an earthquake source."

Eiby (1982a, b) and de Lange (1997) proposed that the March tsunami was caused by mud diapirism. De Lange & Moon (2004) have since proposed a landslide mechanism for the March event. However, Power et al. (2008) use tsunami source and propagation modelling to demonstrate that by taking into account the unusual source and rupture properties of the March 1947 event, which affect the dimensions of the fault plane and the slip, i.e. slow rupture velocities, long duration times, and low rigidity, deformation caused by the earthquake alone is a feasible source for the observed tsunami.

(Extracted and abridged from the Atlas of Isoseismal Maps of New Zealand Earthquakes 2nd edition (Downes & Dowrick, 2009), which lists key references relevant to this event) Because "tsunami earthquakes" like the 1947 March and May (q.v.) earthquakes are often not strongly felt on land, they pose a problem to warning authorities in the near-field (as people don't feel a particularly strong earthquake), as well as in far-field, because of the short response time and the difficulty in forecasting water heights from a non-standard source mechanism.

8.3.3 Tokomaru Bay

Reported to be furthest extent of wave. Effects diminished rapidly north of Tolaga Bay. (Gisborne Herald 26 March 1947)

Max height reached at inundation limit (m): 0.3

8.3.4 Anaura Bay

Effects extended to here (first report). Later eyewitness report: beaches waterlogged to well above HWM. Speed and height of surges rapidly diminished northwards. (Gisborne Herald 26 March 1947)

Tsunami would have arrived at high tide, which was also a spring tide at about MHWS level. See Tolaga Bay

Max height reached at inundation limit (m): 1

Max observed height of inundation (m): 1.7

8.3.5 Tolaga Bay

A huge swell that reached high up beaches and wharves, No damage. A series of high bores travelled up Uawa River for 2 miles (3.2km) and overflowed banks at low points without serious effects. No damage caused north of Tolaga Bay. (Gisborne Herald 26 March 1947).

Earthquake "followed by tidal wave varying from 6-15 ft, according to locality from 14 miles north of Tolaga Bay to 10 miles south, where two bridges at Waihau bay 10 ft above sea level were swept away. Secondary wave of smaller proportions followed an hour after shock experienced. Both waves were observed in the Uawa River as far as 3 miles inland. (DSIR Seismological Observatory Felt Report).

According to NIWA Tide Forecaster (http://www.niwa.co.nz/services/free/tides), HW was at 08:37 March 26 NZST (0.71) at Tolaga bay. MHWS at Tolaga Bay is 0.7 m above MSL (LINZ Website) suggesting also that the tsunami arrived at the time of Spring Tides.

Max height reached at inundation limit (m): 2.0-3.5

Max observed height at inundation (m): 2.5-4.5

8.3.6 Waihau Beach

Two old bridges on old coastal road (now access to Waihau Station) "destroyed at a level 10-12 ft above the previous highest point reached by sea". (Gisborne Herald 26 March 1947);

Earthquake "followed by tidal wave varying from 6-15 ft, according to locality from 14 miles north of Tolaga Bay to 10 miles south, where two bridges at Waihau bay 10 ft above sea level were swept away. Secondary wave of smaller proportions followed an hour after shock experienced. Both waves were observed in the Uawa River as far as 3 miles inland. (DSIR Seismological Observatory Felt Report).

Estimated run-up for MCDEM: 4

Max height reached at inundation limit (m): 4.0-5.0

Max observed height of inundation (m): 4.5-5.5

Damage built/marine/environmental: 2 old bridges washed away

8.3.7 Pouawa Beach North

[Note: The bridge over the Pouawa River, referred to in the following accounts, was at the northern end of Pouawa Beach, whereas the cottage occupied by the Mr & Mrs Hall, a nephew, and two visitors who had not long arrived, was the only house along the stretch of beach and it was located near the south end of Pouawa Beach, just north of Turihaua Point. There is a separate wave height entry for the latter, but the descriptive data are not separated as some comments apply to both locations.]

Decking & superstructure of 36 yr old wooden truss bridge (54 ft truss span and two 25 ft stringer spans) was lifted bodily and deposited half mile up Pouawa River. The cottage occupied by the Halls at the southern end of Pouawa Beach, in which there were three people, was overwhelmed by first wave. Only one section of house was not demolished. It was moved 10 ft and twisted. The rest of the house was smashed and swept out to sea. Another two people escaped to the road above the cottage before the wave hit. At another location nearby, a man's attention to the wave was drawn by noise and a child's comment. The level of water remained high for some time after the [first?] wave. (Gisborne Herald 26 March 1947).

Telegraph poles in area well inland from the beach [which end of beach not stated] carried strands of debris in cross-arms and wires, taken as indications that waves reached at least 35 ft. Very little development or settlement in the area. Two men travelling by car from Gisborne were approaching Pouawa Bridge just before 9 am, noticed a huge swell developing in the bay and saw it break on the first shelf of rocks. They estimated the height as at least 40 ft above sea level, foam and spray being thrown higher as wave broke. They

drove rapidly to higher ground beyond the bridge. The destruction of the bridge was also observed by shepherd on high ground

Earthquake felt severely by the people in the cottage (clock swinging only effect noted). Clock registered 8.40 am when wave was noticed as Mr. Hall looked towards Tapuwai [note that many details here are inconsistent with Tunnicliffe account (q.v. below)]. The second wave arrived when water had receded enough for people still in the cottage to consider getting out. It was not as high as the first wave. The first wave washed the two people outside up onto the road. (Gisborne Herald 27 March 1947); Mr Hall saw a wave coming in when he looked out the door toward Tapuwai. Another person at the cottage estimated wave to be 15-20 ft. [Other details same as Gisborne Herald.] (Dominion 27 March 1947).

A report from two people from Rotorua travelling by car from Gisborne stated that they reached the hill south of Pouawa at about 9 am, saw a huge swell, realised the danger when the wave hit the first rocks, where it appeared to be about 40 ft high. Foam and spray went higher. On the way back [from their destination] they found fish which had been thrown 30 ft above high tide level. At the Hall cottage, the water reached the eaves and the room the three people were in was turned completely round. The other four rooms and three sheds were demolished. (Daily Telegraph 27 March 1947);

[The following recollections from one of the two people, the nephew, who were outside the Hall cottage when the first wave arrived were published in 1990. Details of who saw what differ from Hall statements in newspapers at the time.].

The house was 6ft below road. The view from the door was north along beach, where "approaching the shore and us, at breakneck speed and roaring like an express train was a wall of dirty coloured water towering a good 30 ft, boiling and curling as it picked up acres of beach sand on its way to engulf us within seconds." Before they could do anything, the wave washed over them sending the other person (Winkfield) who had been outside slightly closer to the sea, hurtling past. They were swept up onto the road, one thrown up against a 6 ft bank, while the other (the author) was caught on a fence under water, and then thrown up onto the road also where the water was a foot deep.

A smaller wave hit him there. He saw the wave careering "up the hills for many hundreds of yards. Smaller waves were still coming in from the sea. As the waves came in they met receding surges with much debris. At this stage the sheds were picked up in the swirl, the roof peak of the house bobbed out of the water. The boathouse was detached and shattered. By the time they pushed towards the house the water was 4 ft deep. People in house escaped to bank above road. The author's estimation of height of the wave about 25ft. (Tunnicliffe 1990); Observations by Mr Bennett from EQC state that debris was thrown 40ft above MSL at Pouawa, but wave estimated to be only about 15 ft. Estimated greatest at Tatapouri, wave reported to have arrived at 9.07 am. (DSIR Seismological Observatory files).

Estimated run-up for MCDEM: 10

Max water elevation at shore (m): 10-12

Max height reached at inundation limit (m): ~10

Max observed height of inundation (m): 12

Damage built/marine/environmental: Bridge swept 800m upstream

8.3.8 Pouawa Beach South

Max water elevation at shore (m): 10

Max height reached at inundation limit (m): ≤10

Max observed height of inundation (m): 11

Damage built/marine/environmental: House almost destroyed, outbuildings destroyed

8.3.9 Tatapouri

See also Turihaua Point South. Mr L Robinson's holiday cottage and motor shed on seaward side of Tatapouri Hotel (which is on ground <20m contour) was smashed. He saw approach of wave and escaped. Note that the earthquake was not felt. Warning of wave given by daughter at Hotel at about 9.20am. (Gisborne Herald 26 March 1947).

Proprietors of Tatapouri Hotel (McLauchlan or McLaughlan) were warned by daughter, they managed to run up a bank at the back of the hotel, saw the second wave coming from the back gate. A short time after running away they looked back to see water around the front and two sides of hotel. The cowshed was destroyed, and a two-room cottage and its contents were carried out by the water as it receded. Mr McL estimated "the height of the wave at that point [which point is unclear, when it hit the hotel or bach?] at 12ft above high water". The water was 3 feet deep when it hit the hotel veranda and stoved it in, and left seaweed and sand in the hotel. (Dominion 27 March 1947);

After the second wave the water remained at a high level for ten minutes before it receded. (Grayland 1978)

Wave arrived "shortly after 8.40" (NZ Herald 27 March 1947).

The first wave was at approximately 9.50 am and the second 3-4 minutes afterwards. They were both 12-15 ft in height." (Harbour Board report in DSIR Seismological Observatory files)

Tide was high at the time; see tides at Gisborne or Tolaga Bay.

Max height reached at inundation limit (m): 2.6-4.5

Max observed height of inundation (m): 4.5-5.5

Damage built/ marine/ environmental: Hotel damaged, cottage and shed destroyed

8.3.10 Makarori

Early report states that there was no damage to buildings at the base of the hill despite being on flat ground near the shore. This report appears to be superseded by the later report: A house (owners Mr & Mrs H Olsen) on low ground on Makorori side of Tatapouri Headland was immersed with only three feet of roof showing [no detail on the source of this report, or whether anyone was inside the house]. (Gisborne Herald 27 March 1947);

Two drovers with cattle and dogs were nearly caught on the beach, some dogs at the rear having to swim. (Dominon 27 March 1947)

Tide was high at the time; see tides at Gisborne or Tolaga Bay.

Max. height reached at inundation limit (m): 4-5

Max. observed height of inundation (m): 5-6

Damage built/ marine/ environmental: House inundated, fences swept away

8.3.11 Tatapouri Point

As seen from Wainui, waves appeared to crash about half-way up the cliffs at Tatapouri Point [From Topo map approx 60m cliff at Point, then lesser gradient to 100m. Max height further inland 186m]. (Gisborne Herald 27 March 1947).

From top of Tatapouri Hill Mr F Whitehead saw the first wave come in and go out. As it receded the second wave, which appeared to be higher than the first, started to come in but the receding waters broke its effect. (Dominion 27 March 1947);

From Secretary of Gisborne Harbour Board, who investigated reports for Seismologocal Observatory, attention to wave drawn by foam well out to sea off Tatapouri; great surge grew larger to 30-40ft as it approached Tatapouri. Appeared to come from a little south of east, breaking at Tatapouri first the progressively breaking on other beaches along the coast to a little south of Young Nick's head. Not noticed north of Gable End [clearly inconsistent with other reports]. One observer saw wave cross bay from Tuahine to Young Nicks Head, speed 40 mph and reaching 30 ft off Muriwai. Another observer saw wave break at Wainui estimated height 30-40ft. (Seismological Observatory files)

Tide was high at the time; see tides at Gisborne or Tolaga Bay.

Max. water elevation at shore (m): 10-12

Max. observed height of inundation (m): 11-13

8.3.12 Gisborne Port

Three large surges of approx. 12 ft in variation (i.e. peak-to-trough) in Gisborne Harbour. No damage. Wave could be seen coming across bay from direction of Muriwai. A bore formed in Turanganui River and in harbour. All lines to boats at wharves held. After first rise water dropped 12 ft to well below LWM. Dredge dragged mooring until retied with help of launch. Two other large bores came up harbour channel, but no damage. Other smaller fluctuations later in the morning (Gisborne Herald 26 March 1947).

In Kaiti Basin tide ran well out below LWM and came in to approx. 5 ft above spring tide level and continued to ebb and flow, "the ebbs and flows alternating at periods of 8 to 10 minutes and running up to 7 or 8 knots". The tides returned to normal after about 2 hours. No structural damage was done to the port (Gisborne Herald 2 April 1947);

Officer of Pukeko did not see wave until it entered the harbour. It struck the concrete harbour entrance with great force and swept up the channel causing a 12 ft lift. The wave did not top the wharf. Another officer saw approach of the second wave - "it was not broken - just a huge wall". It struck the harbour entrance with force and caused a heavy surge and rip. Later there were further minor bores, and tidal fluctuations throughout the morning. (Daily Telegraph 28 March 1947);

"On Wednesday 26 March at 8:30am a prolonged earthquake shock was experienced throughout the district. This was followed at 9.5am by a tidal wave which caused a high bore in the river and inner harbour. The tide ran out to well below low-water mark and came in to approximately 5 feet above spring tide level and continued to ebb and flow, gradually subsiding back to normal about 11am. The dredge "A.C." dragged her working moorings but the launch Takitimu took her in tow and she was berthed at No.6 wharf. On examination there seems to be no structural damage done to the harbour. The tide ebbed and flowed at intervals of approx. 8-10 minutes and ran about 7 to 8 knots, gradually taking [tailing?] off (G. McKenzie Smart, Harbourmaster report.)

"The tide was high and showing 6 ft 6 in on the automatic tide gauge. The wave caused a bore in the harbour channel and the river of a height of from 5 to 6 ft above high-water mark and above the 6ft 6in on the tide gauge. The water then receded to low water mark or zero on the gauge followed by another run in to 7 ft 6 in on the gauge. The tide continued to run in and out at approximately 10 min. intervals, gradually subsiding to normal at 11 am, when the gauge was fairly steady at 6ft." (Observatory files)

Postmaster at Gisborne reported the waves of 12-15 ft (where?) arrived at 9.02 am. (Source??) 5 to 6 ft above high-water mark and above the 6 ft 6 in on the tide gauge. The water then receded to low water mark or zero on the gauge followed by another run in to 7 ft 6 in on the gauge. The tide continued to run in and out at approximately 10 min. intervals, gradually subsiding to normal at 11 am, when the gauge was fairly steady at 6 ft." (Observatory files) Postmaster at Gisborne reported the waves of 12-15 ft (where?) arrived at 9.02 am. (Source??)

According to NIWA Tide Forecaster (http://www.niwa.co.nz/services/free/tides)), HW was at 08:32 March 26 NZST (0.70) at Gisborne. MHWS at Gisborne is 0.76 m above MSL (LINZ Website).

Max. observed effective peak-through (m): 3.6-4.5

Max. height reached at inundation limit (m): 1.5-1.8

Max. observed height of inundation (m): 2.2-2.5

8.3.13 Wainui Beach

Residential area suffered some damage, including washing out of foundations of one cottage and severe structural damage to surf club premises. Caravan floated before being grounded (no detail).

"One report from Wainui referred to huge patch of sea lashed to white froth some miles out from Tuahine Point, where the water remained disturbed and frothy for some time after the last tremors of the morning quake had subsided". (Gisborne Herald 26 March 1947);

Houses along Wainui Beach threatened and if wave had been another 2 ft higher a disaster could have occurred. Considerable amount of damage caused. Both ends of beach where road slopes down were worst hit. At southern end: creek said to have taken the main force of wave. Bank in front of house nearest creek washed away, water swept away fence and entered house. Other houses (or at least gardens) said to be damaged. Eyewitness told of wall of jet-black water advancing up beach, breaking as it hit bank in front of house and washing into house itself. A caravan on the lawn was lifted, turned and deposited on a fence. A wireless pole and fence demolished. As wave receded about 50 yds in front of house it

met an incoming wave and water rose high in air. A series of smaller waves broke over the bank. At northern end of beach: Wave judged to have come up to edge of road at the carpark near Okitu Stream. Surf Club premises badly damaged nearby. Doors forced open, floor subsided, strewn with sand and silt, A shed nearby (or the Surf club shed?) on its side. Eyewitness reported water travelling 50 yds up bank behind clubhouse, before rushing back through it. Parts of bank all along beach washed away (see Weekly News photo). (Gisborne Herald 27 March 1947);

Although high above sea level houses at Wainui were threatened. Windows 30-49 ft above sea level were splashed when wave hit bank in front. All along the beach, banks were seriously eroded. (Dominion 27 March 1947);

Officer from Pukeko reported that a trail of debris was left by waves along beach. Water had entered several cottages, causing some structural damage (no detail). At the point where the road met the beach, there were signs the waves had nearly reached the highway. On the northern part of the beach the waves had crossed the road. (Daily Telegraph Mar 28);

Photograph "Damage to the foreshore at Wainui Beach. Most of the force of the water was taken by the bank. [Erosion evident] (Weekly News Apr 2)

Tide was high at the time; see tides at Gisborne or Tolaga Bay.

Max. height reached at inundation limit (m): 4-6

Max. observed height of inundation (m): 5-7

Damage built/ marine/ environmental: Surf club damaged, houses inundated, fences damaged, caravan floated, beach and stream banks eroded

8.3.14 Muriwai, Poverty Bay

Huge swell came up and "swept inland a considerable distance, and wrecked fences and imperilled stock and crops". Full extent of damage not ascertained. (Gisborne Herald 26 March 1947) See also Waipaoa River entry.

Tide was high at the time; see tides at Gisborne or Tolaga Bay.

Max. height reached at inundation limit (m): 3.5

Max. observed height of inundation (m): 4.5

Damage built/ marine/ environmental: fencing destroyed

8.4 May 1947 Event

8.4.1 Tsunami Impact Summary

The tsunami caused by the 1947 May 17 ML5.6 MS7.2 MW6.9-7.1 offshore Tolaga Bay earthquake was not well observed as it occurred on a stormy winter night about half an hour after the earthquake, which was at 7.06 pm, and so at about 1.5 hours before low tide. Nevertheless, its effects (damage, debris, and inland water penetration) were noticeable the next day from Wainui Beach, near Gisborne, to at least Tolaga Bay, and possibly as far as Tokomaru Bay, spanning 50-80 km of coastline. However, much of the coastline was sparsely inhabited. The greatest damage and height reached above sea level at the time (~6 m) was at Waihau Beach, where logs piled ready to repair the bridge damaged in the tsunami two months previously were washed away. Here, the sea penetrated 400 m inland up a creek, further inland and to a higher level than in the March tsunami. Water swept 50 m inland at Tolaga Bay and the water height was estimated to be 1.8-2.4 m higher than in the March 26 event. Taking the tide level into account suggests the waves may have reached 4-5 m above sea level at the time.

8.4.2 Source Parameters

Time UTC: 7:06 17th May 1947

Source Location lon/lat: 178.87, -38.42

The 1947 May 17 M_L 5.6 M_S 7.2 M_W 6.9 - 7.1 offshore Tolaga Bay earthquake occurred shortly after 7 pm (NZST) just over 50 km offshore from the Tolaga Bay coastline, about 10 -15 km west of the Hikurangi Trough. The earthquake was not widely felt and the maximum intensity of MM V is considerably less than the expected intensity for its moment magnitude M_W 6.9 - 7.1 and surface magnitude M_S 7.2, but is consistent with its local magnitude M_L 5.6.

Like the March 25 (UT) earthquake (q.v.), this earthquake's importance lies in the fact that it has been identified as a "tsunami earthquake". Source parameters (strike, dip, rake, centroid depth) and moment magnitude have been determined by Doser & Webb (2003) waveform modelling studies, using the Downes et al. (2001) epicentre.). Doser & Webb comment that: "both waveform modelling inversions give a low-angle mechanism but differ in strike and rake. The rupture time is long (>25 s) and hence the focal depth is poorly constrained. Our M_w is slightly lower than the M_S estimate of 7.2. Again [i.e. like the March earthquake], the mechanism and focal depth of the earthquake suggest that it occurred on the plate interface.

The May 1947 earthquake also exhibits many features of a 'tsunami' earthquake: low M_L (5.6) compared with M_S (7.2) and M_W (6.9 - 7.1), relatively shallow focal depth, long rupture time and low-angle fault plane." Eiby (1982a,b) and de Lange (1997) have proposed that the March, and by default the May, tsunami were caused by marl diapirism. De Lange & Moon (2004) have since proposed a landslide mechanism for the March event, and again by default, suggested the same mechanism for the May tsunami. However, Power et al. (2008) use tsunami source and propagation modelling to demonstrate that by taking into account the unusual source and rupture properties of the March 1947 event, which affect the dimensions of the fault plane and the slip, i.e. slow rupture velocities, long duration times, and low rigidity, deformation caused by the earthquake alone is a feasible source for the observed tsunami.

The May event was not specifically modelled. (Extracted and abridged from the Atlas of Isoseismal Maps of New Zealand Earthquakes 2nd edition (Downes & Dowrick, 2009), which lists key references relevant to this event) Because "tsunami earthquakes" like the 1947 March and May (q.v.) earthquakes are often not strongly felt on land, they pose a problem to warning authorities in the near-field (as people don't feel a particularly strong earthquake), as well as in far-field, because of the short response time and the difficulty in forecasting water heights from a non-standard source mechanism.

8.4.3 Tokomaru Bay

Believed to have escaped damage (Daily Telegraph 19 May 1947)

Max. height reached at inundation limit (m): 1.5

8.4.4 Tolaga Bay

Along some of the beaches between Tatapouri and Tolaga Bay driftwood was deposited well above high tide level. (Gisborne Herald 19 May 1947); Along the beach near Tolaga Bay township driftwood lines were "high enough to indicate the passing of a substantial wave" (Gisborne Herald 19 may 1947);

6-8ft higher than previous tsunami. Two police officers driving to Tolaga Bay noticed logs and debris on low-lying sections of road before reaching Tatapouri [probably at Makorori]. No further evidence of inundation as far as Tolaga Bay. (Daily Telegraph 19 may 1947);

Postmaster reported driftwood 50 yds from HWM, well beyond limit of previous wave. (DSIR Seismological Observatory Files, 1947)

According to NIWA Tide Forecaster (http://www.niwa.co.nz/services/free/tides)), LW occurred at 2108 NZST (-0.51 m) on May 17 at Tolaga Bay, i.e. the earthquake occurred two hrs before LW, the tsunami probably occurring about 1.5 hrs before LW

Estimated run-up for MCDEM (m): 3.5

Max. height reached at inundation limit (m): 4.0-5.0

Max. observed height of inundation (m): 3.5-4.5

8.4.5 Waihau Beach

Earthquake stopped clocks at Mr N Loisel's, worst shake since Masterton quake. "Water surged up creek at height greater than in March, covering footbridge not reached in previous tsunami. Mr Loisel estimated "water penetrated 400 yds inland and two chains above high water level". A pile of logs were swept across road and deposited in a plantation. (Daily Telegraph 19 May 1947);

Higher than wave in March, lifting heavy timber which lay adjacent to bridge previously damaged. Mr Loisel considered the wave was substantially higher at Waihau than previous wave. The bridge site was 2.5 chains from normal HWM. The furthest point inland reached by the wave was about 400yds from HWM. (Gisborne Herald 19 May 1947)

Estimated run-up for MCDEM (m): 6

Max. height reached at inundation limit (m): 6

Max. observed height of inundation (m): 5.5

Damage built/ marine/ environmental: Timber swept inland

8.4.6 Tatapouri

At Tatapouri Hotel wave reached within a chain and a half [30 m] of the building. Comment by Hotel owner, W D McLaughlan, "But for the fact that the tide was almost right out I think the wave would have come nearly as high as the last one". He estimated wave height must have been 12ft. Mr Robinson, who lost bach and furniture in March, had his boat stoved in where it was moored on the sand above high tide level. (Daily Telegraph 19 May 1947);

Wave left its mark level with top of sand bank in front of hotel. Mr Robinson's flat-bottomed boat was found against the bank with its side stoved in. Wave height estimated to have reached 12 ft above normal HWM and "taking account of average rise and fall of the tide there it probably ranged to 18 or 20 ft [5.5 - 6m] above sea level when it struck the reefs in that locality". (Gisborne Herald 19 May 1947);

Hotel owner heard a rush of water about half an hour after the quake, and went out to find that the sea had reached to the top of the bank in front of the hotel. He estimated the wave to be 12 ft high, taking into account the tide and height of the bank. (Dominion 19 May 1947)

The observation of the hotel owner at Tatapouri is probably more reliable than that published by the Gisborne Herald, and for this reason is assigned here

Estimated run-up for MCDEM: 5

Max. height reached at inundation limit (m): 3.6

Max. observed height of inundation (m): 3.2 - 5.5

Damage built/ marine/ environmental: Boat damaged

8.4.7 Makarori

Along the Makorori Beach road driftwood was deposited on road at several places, without doing damage to the road. (Gisborne Herald 19 May 1947);

Two police officers driving to Tolaga Bay noticed logs and debris on low-lying sections of road before reaching Tatapouri [probably Makorori]. No further evidence of inundation as far as Tolaga Bay. (Daily Telegraph 19 May 1947)

Max. observed effective peak-through

Estimated run-up for MCDEM: 3

Max. height reached at inundation limit (m): 3-4

Max. observed height of inundation (m): 2.5-3.5

Damage built/ marine/ environmental

8.4.8 Gisborne Port

No earthquake damage reported, other than fracture of water supply pipeline at Te Arai bridge at Manutuke [less than 10km SW of Gisborne]. (Daily Telegraph 19 May 1947)

"Followed shortly before 8pm by tidal wave. No damage although main road covered beyond Tatapouri." (DSIR Sesismological Observatory Felt report);

Secretary to Gisborne Harbour Board reported that there were no signs of the wave in Gisborne Harbour. (DSIR Seismological Observatory files)

Estimated run-up for MCDEM: 0

Max. height reached at inundation limit: not observed

8.4.9 Wainui Beach

Severe shake, more severe than earthquake in March. (Daily Telegraph 19 May 1947);

Residents found that "sea-water had washed the lower portions of some sections, but that no damage had occurred". (Gisborne Herald 19 May 1947)

Estimated run-up for MCDEM: 2.5

Max. height reached at inundation limit (m): 1.2-2.0

Max. observed height of inundation (m): 0.8-1.6

8.5 November 1952 Event

8.5.1 Tsunami Impact Summary

The tsunami from the 4 November1952 (1658 UT November 5, 0458 NZST, MS 8.3 Mw 9.0) earthquake reached New Zealand shores late in the evening of November 5. The most affected areas were parts of Northland, Gisborne, Wellington, Greymouth and Lyttelton. However, the effects were mostly minor with the largest zero-to-peak measurements or water heights above sea-level at the time generally less than 1 m.

At many places the tsunami seems to have been too small to be observable on tide gauges or by the casual observer. Severe weather conditions and flooding in South Canterbury and Southland would have prevented small effects being noticed there. The lack of observable effects in Napier, however, cannot be attributed to this.

The tsunami was observed in several rivers and in estuaries, tearing nets in the Ashley River and throwing a dinghy on the rocks at Greymouth. One person was slightly injured at Matapouri when a 0.9 m surge hit the boat he was in. A key feature of the data is the occurrence of unexpectedly strong effects at Greymouth, given the path through New Caledonia, Vanuatu etc. The largest waves seem to have occurred late in the series, but the first waves arrived very shortly after the calculated first arrival.

On the other hand, the first observed arrivals, and strongest effects, at Gisborne were well after the expected first arrivals, and the largest amplitude at Wellington was some 24 hours after the first arrival. The effects in the Chatham Islands are unknown.

8.5.2 Source Parameters

Time UTC: 16:58 4th November 1952

Source Location lon/lat: 159.50, 52.75

The 1952 November 4 1658 (UT November 5 0458, NZST Ms 8.3 Mw 9.0) Kamchatka earthquake generated a tsunami that reached a maximum water height above sea level at the time of 13 m locally. The tsunami was widely observed around the Pacific, the NGDC Tsunami Database recording nearly 300 wave height measurements.

8.5.3 Gisborne

Disturbance in water level in inner harbour from about 08:00 6 November, evident on tide gauge from mid-morning. At 10:05 gauge read 8 ft 3 in, level fell 12 inches in next 20 minutes. At 10:34 a further and much sharper drop recorded, falling to 3 ft 6in on the gauge. Gauge steady for the next hour, and at 11:32 reading was still 3 ft 6 in. Within next 10 minutes, level rose by 2 ft 6 in, and then minor surges and recessions until 12:00. Disturbance was likened to that in 1947 but range was noted to be not as wide, and no bore or crest was observed. Changes in level likened to huge swell banking up and filling tideways, with no surface break. Late on afternoon of 6 November, tide still showing marked fluctuations. In vicinity of No 3 shed rise was 2 ft every 5 minutes. Each maximum was followed by a recession. Fluctuations continuous since about 10:00 on 6 November. (Gisborne Herald 7 November 1952; similar in NZ Herald & Evening Post 7 November 1952).

Max. observed effective peak-through (m): 1.4

8.6 1960 Chile Event

8.6.1 Tsunami Impact Summary

Observations of the tsunami generated by the great 1960 (May 22 1911 UT, May 23 0711 NZST M_W 9.4 - 9.6) Chile earthquake were reported at more than 120 locations In New Zealand. The most affected locations occurred along the whole eastern seaboard of New Zealand from Cape Reinga to west of Bluff and to Stewart Island, but the tsunami was also observed at locations on the west coast of the North Island, notably as far as south as Ahipara in Northland, at Wanganui and Paremata but not at New Plymouth, Foxton or Himatangi Beach. On the western and north-western seaboard of the South Island, the tsunami was observed at Nelson, Motueka, as well as several West Coast towns. The tsunami was also experienced on the Chatham Islands, and Campbell Island, where water heights above sea level at the time were from 3 m to over 5 m at locations only a few kilometres apart in Perseverance Harbour. In the Chatham Islands, heights of 1.8 m (Waitangi) to over 3.6 m (Pitt Island) were reported, with damage to a wharf on Pitt Island, but the heights are only known at three locations.

In the North Island, heights of 2 m or more were reported from a few locations in Northland and Coromandel, from Tokomaru Bay to south of Gisborne, at Napier, Te Awanga and Clifton in Hawke's Bay, and at Lake Ferry in Palliser Bay, with the greatest heights around Poverty Bay and northwards (3 - 4 m) and Napier, Clifton and Te Awanga (3 - 4.5 m). In the South Island, heights of 2 m or more were experienced at Wairau (2 - 2.5 m), Sumner area (3 - 3.6 m), around Banks Peninsula (max. 3.2 - 3.6 m, at Lyttelton) and possibly at Oamaru (estimated 1.5 - 2.1 m). On the West Coast, Hokitika reported a height of 0.9 m.

The first arrivals on the east coast were at night, and in general, only noticed where the larger waves occurred or where smaller waves arrived on top of high tide. The first arrivals that were unmistakeable were within a short time of predicted time. As with the 1868 and 1877 tsunami, the largest waves at Lyttelton and Sumner occurred within 1.5 - 3 hrs of low tide. The time of the largest surges varied around the Peninsula, and some (e.g. Okains Bay) seem to have been closer to high tide, but the earlier waves at a lower tide level may not have reached significantly above high tide mark.

Similarly, the largest surges at Gisborne occurred closer to low tide than to high tide, although there were also large surges some hours later nearer high tide, whereas in Napier, the largest surges seem to have occurred at the later time i.e. within an hour or so of high tide. The largest surges generally occurred within 12 - 15 hours after the first arrival, some within the first 2 - 4 hours. In the most affected areas, houses, roads sheds, and paddocks were inundated, bridges, fences, and sheds damaged, and stock killed.

De Lange & Healy (1986) record that the Earthquake and War Damage Commission (1961) recorded 69 claims for tsunami damage. Most were reported from Banks Peninsula and Napier, although damage claims extended from the mouth of the Catlins River in the South Island to Whangarei in the North Island. The value of the claims was not specified in the Earthquake and War Damage Commission report. The absence of a Pacific-wide Tsunami Warning System at the time meant that the tsunami arrived without an official warning being issued, although some ports seem to have notified each other, and one person heard of the tsunami on short wave radio. Several days after the main event, another large earthquake occurred in Chile (possibly an event listed in ITDB/PAC (2004) M7.5 May 25 0834 UT), about which the Air Department in Wellington received a message suggesting that a tsunami could possibly reach New Zealand. This initiated the broadcast of a nationwide warning on radio.

The warning resulted in the evacuation of many east coast towns. In other places, people ignored the warnings and went down to the sea to watch. The response to the warning is discussed in Johnston et al. (2008). Interestingly, many people interviewed about the 1960 tsunami remember the warning and evacuation and the fact that no tsunami occurred and recall nothing of the significant effects of the main event a few days earlier.

8.6.2 Source Parameters

Time UTC: 19:11 22th May 1960

Source Location lon/lat: -74.50, -39.50

The 1960 May 22 1911 UT May 23 0711 NZST Mw 9.4-9.6 Chile earthquake, the largest earthquake instrumentally recorded (up to May 2009), occurred in southern Chile. The series of large earthquakes that followed ravaged southern Chile and ruptured over a period of days a 1,000 km section of the fault (the plate interface), one of the longest ruptures ever reported. The mainshock generated a tsunami that was not only destructive along the coast of Chile, but also caused numerous casualties and extensive property damage in Hawaii and Japan and was noticeable along the shorelines throughout the Pacific Ocean area. (NGDC Tsunami Database, May 2009)

The magnitude of the earthquake was underestimated at the time, primarily because the surface magnitude scale saturates at magnitudes greater than about 8, and the moment magnitude scale, which can determine the magnitude of earthquakes beyond this limit, was not introduced until the late 1970s. More recent calculations of the moment magnitudes are: Mw 9.4-9.6 (Pacheco & Sykes, 1992); Mw 9.5 (Barrientos & Ward, 1990).

8.6.3 Tokomaru Bay

According to Tolaga Bay Harbourmaster, the Tokomaru Bay-Waima road, on the sea front at northern end of Tokomaru Bay, was flooded during night/morning of May 23/24, and debris and stones were swept across the road. It was open again by morning of May 24. The strongest tidal surge occurred at about 0500 May 24, when the sea reached 8 ft above the normal high-water mark. The surge was accompanied by a heavy roaring sound. Ninety feet of wooden protective sea walling was broken. One dinghy was damaged. The sea reached 40 ft up Waima Creek. The greatest disturbance reportedly took place at high tide. No one was forced to evacuate their homes and no damage was done to stock [live? Or shop?]. At am May 24, surges, although decreasing, continued, reportedly at regular intervals, the "water mark was altering by about 3ft or 4ft in three-quarters of an hour". (Gisborne Herald Tuesday 24 May 1960)

According to NIWA Tide Forecaster (http://www.niwa.co.nz/services/free/tides)), HW at 04:52 NZST May 24 (0.6) at Tokomaru Bay. Higher surges may have occurred before 05:00 May 24 at the time of low tides

Estimated run-up for MCDEM: 3

Max. height reached at inundation limit (m): 2.4

Max. observed height of inundation (m): 3

Damage built/ marine/ environmental: wooden sea wall damaged, one dinghy damaged

8.6.4 Tolaga Bay

The proprietor of the Tolaga Bay motor camp was alerted by the pounding and surging of the sea and its hitting strongly against the breastwork at about 2030 May 23, making him wary. He was aroused at 0415 May 24 by the sound of water against the side of his cottage near one of the boundaries of the camp, on the side facing the harbour board sheds. He transferred his wife and family to higher ground within the camp. The water was up to about the level of the veranda of his cottage and it also went through his store, also on the lower level. The water was also in the cookhouse in the camping grounds. It rose and fell fairly regularly. The proprietor said that the peak of the surging appeared to be past at about 0530 May 24. The camp was flooded by the sea and also by the effects by the surge running back into the Uawa River, which rose and fell sharply during the surge periods.

At the rear of the motor camp was a small creek running out into the Uawa and water rushed up this creek as the sea swept up the Uawa. When he went to work cleaning out the cookhouse in the camp this morning, Mr. Clark found that … had penetrated the … of about a … as a layer … about two … harbour … said that when low water was reached, it was as low a tide as he had seen at Tolaga Bay.

According to Captain Mander, there were surges at intervals of about a quarter of an hour from about 0400 May 24, with the sea pounding up on to the beach. By about 0900 May 24 surges were easing with the receding tide. "A protective wall made up of large trees on the harbour side of the wharf was broken up and trees and other debris were washed up on to the road near the harbour board sheds close to the camp, the sea coming up with a rush. The surge rushed up a creek almost two miles from Tolaga Bay and flooded an orchard, dog kennels becoming awash and the dogs forced to swim until the surge receded. (Gisborne Herald Tuesday 24 May 1960)

According to NIWA Tide Forecaster (http://www.niwa.co.nz/services/free/tides), LW at 22:41 May 23 NZST (-0.53), HW at 04:47 May 24 NZST (0.58), LW at 11:04 May 24 NZST (-0.65), HW at 17:23 May 24 NZST (0.60).

Estimated run-up for MCDEM: 2

Max. height reached at inundation limit (m): 2

Damage built/ marine/ environmental: Camp ground buildings flooded, severe erosion, land flooded 3 km up Uawa River

8.6.5 Pouawa Beach North

At about 2045 May 24, a truck standing on the beach at Pouawa being loaded with sand, nose-down towards the surf, was swamped. At the peak of the succession of surges, water almost filled the cab of the vehicle. When rescued on May 25, the truck was unharmed except for sand in the engine and transmission. (Gisborne Herald Tuesday 25 May 1960).

8.6.6 Tatapouri

A fisherman who experienced the March 1947 tsunami heard over his short-wave radio warnings being issued to ships of possible unusual sea conditions and kept watch during the night of May 23 - 24. He observed a low tide well below normal and a fall of about 9 ft. in about a minute and a half. The sea at Tatapouri* reached the top of retaining banks but did not spill over. (Gisborne Herald Tuesday 24 May 1960) [*Note some confusion over location – said to be at his parent's house at Tatapouri but parent's house was at south end

of Pouawa beach in 1947. However, other accounts (where?) indicate parents moved to Tatapouri after 1947]

Max. observed effective peak-through: 5

Max. observed height of inundation (m): 3-3.5

8.6.7 Gisborne Port

The disturbances were first noted by riverside residents at about 8.30 o'clock May 23, when a 4ft bore raced up the Waimata and Taruheru Rivers with a roar. At 0010 May 24, 365-ton coastal trader rose an estimated 20 ft from being grounded in shallow water in the harbour basin. Disturbances prevented ship departing on schedule. The rate of the rise and ebb said to vary considerably, sometimes going up 8 ft in 15 minutes; sometimes much faster. Peak level shown on photograph

According to fishermen, water at the fishing wharf rose 18 feet in ten minutes at about 0100 May 24, to within 1 ft of top of a harbour wall separating the harbour from the river Then the water level dropped as fast as it had risen with a roar. One observer reported that the worst rise was about 0500 May 24, when it looked as though the water was going to sweep up over the wharf. Some fishermen moved their cars out of the way. Some minor damage done to "planing" on the fisherman's wharf, and to a launch trapped under the wharf by rising levels.

At about 0800 May 24 currents powerful enough to propel large tree trunks upstream. Considerable flotsam in harbour. [Photo caption] Water poured into the shed on the fishermen's wharf in the harbour basin, reaching a height level with the lock on the door. (Gisborne Herald Tuesday 24 May 1960).

Watched by large crowds of people on the evening of May 24, water levels reached their highest in the Gisborne harbour since the surging in the Turanganui River and the harbour basin began on May 23. Although the water was above bank level at some points it did not reach the level of the wharf and the roadway skirting the Kaiti basin. When the peak was reached, the water was about 15 in. from the top of the wharf. Apart from fishing vessels which had been moved from their own wharf to berthages at the main wharves, there was no shipping in the basin at the peak tide.

Late on May 24 people travelling over bridges spanning the Taruheru River heard hear a roar from the receding water. The Turanganui river looked to be well up at 0800 May 25, but later in the morning it appeared to be back to normal. The underground conveyors used in bringing frozen meat from low level chambers up to the lighters at the Gisborne Refrigerating Company were immobilised by the surging waters. Electric motors driving the conveyors were saturated and gratings were clogged with debris. Some departments at the freezing works were immobilised when suction pumps drawing water from the river, sluicing equipment and other equipment were put out of action. At high tide on evening of May 24 water level was 2 ft above normal, remained at its peak for about 20 minutes, and then surged quickly seawards again. At about 1715 May 24 there was some evidence of spill-over in the Taruheru river on to low-lying riverside sections. Water was only about 1ft. from deck level of the Botanical Gardens footbridge. Water swept into the premises of J. Wattie Canneries, Limited, near the junction of the Waikanae Creek and the Turanganui River, but only floor level was reached and there was no interruption to production. At 1730 May 24 a small footbridge over the Waikanae Stream, near the factory, was under water. (Gisborne Herald Tuesday 25 May 1960).

At 2000 May 23, 1960, a 3-foot bore was observed coming up the channel, and a similar bore again at 2200 During the night of May 23 - 24 the period of rise and fall was about 20 minutes. Initial range was 12 - 14 feet and later diminished to 4 feet on May 24. Fluctuations continued through May 25 and tides returned to normal late on May 26. (Berkman & Symons, 1964).

According to NIWA Tide Forecaster (http://www.niwa.co.nz/services/free/tides)), LW at 22:34 May 23 NZST (-0.53), HW at 04:40 NZST (0.57), LW at 10:57NZST (-0.63), HW at 17:15 NZST (0.59) NZST May 24.

Max. observed effective peak-through: 5.4-6.0

Estimated run-up for MCDEM: 3.6

8.6.8 Wainui Beach

Water reached the foot of sandhills on morning of May 24, but there were no reports of any scouring or of any excessive surging by the sea. (Gisborne Herald 24 May 1960)

Max. height reached at inundation limit (m): 2.5

Max. observed height of inundation (m): 3

8.6.9 Muriwai

Slight stock losses were reported from some properties and a road running down to the Muriwai side of the Waipaoa River was reported to be under water on May 24. The level of the Waipaoa River in the vicinity of the large railway bridge at 1700 yesterday was reported to be about 2ft. above normal. (Gisborne Herald Tuesday 25 May 1960)

Damage built/ marine/ environmental: Livestock lost

9 APPENDIX 2: PLOTS OF THE B AND C LEVEL MODELLING GRIDS

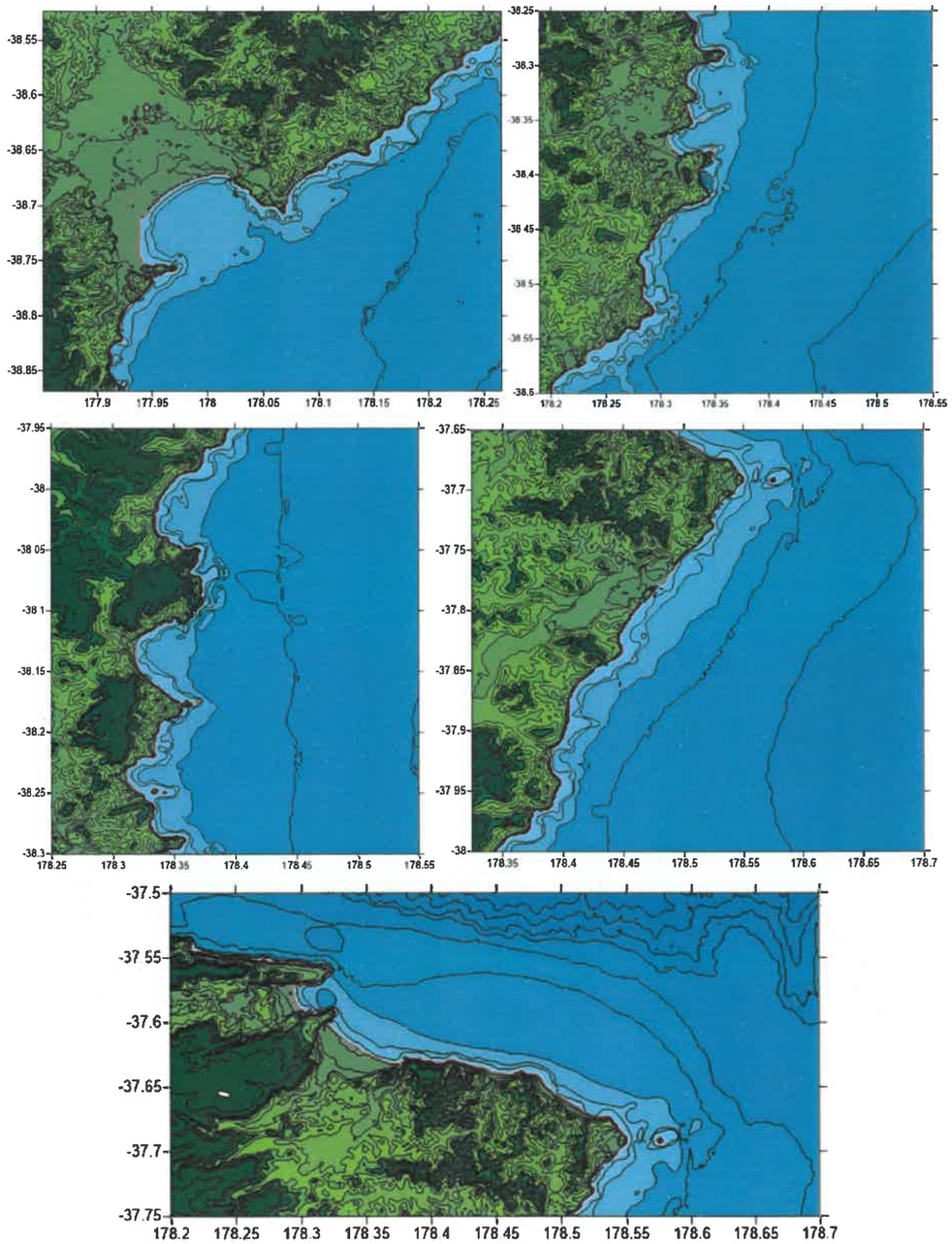

Figure 9.1 The five B-Level modelling grids.

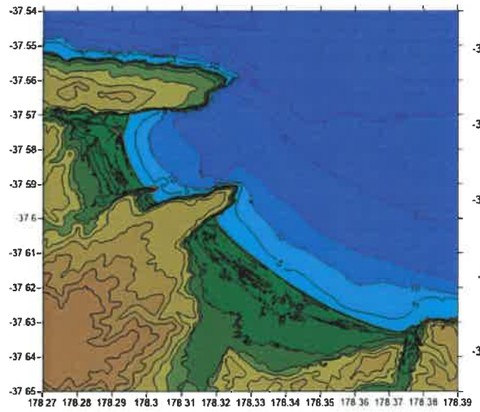

Hicks Bay

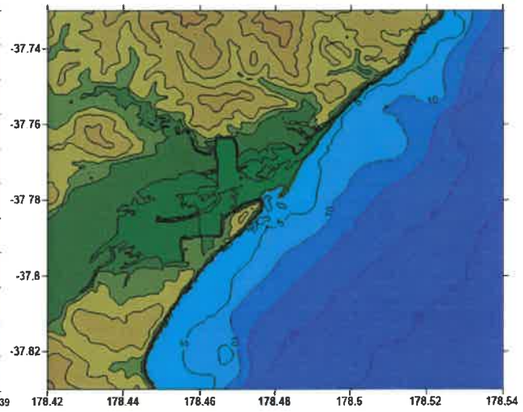

Waiapu

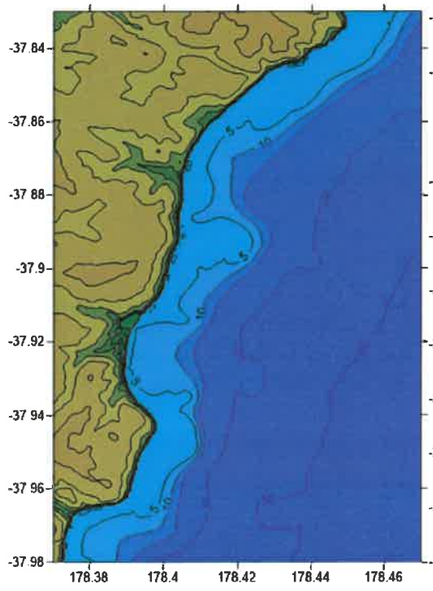

Whareponga

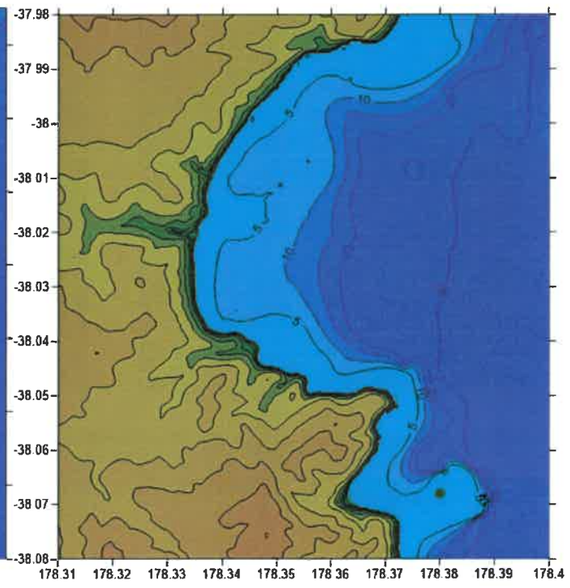

Waipiro Bay

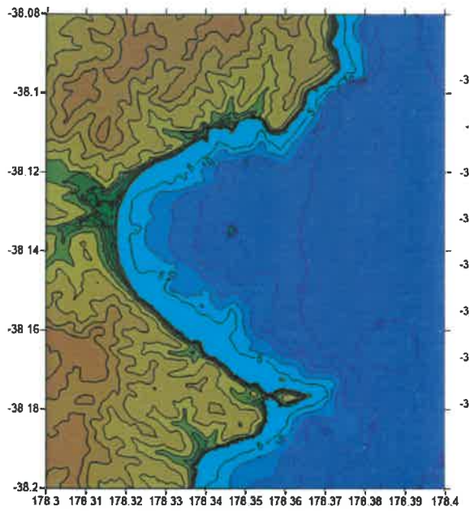

Tokomaru Bay

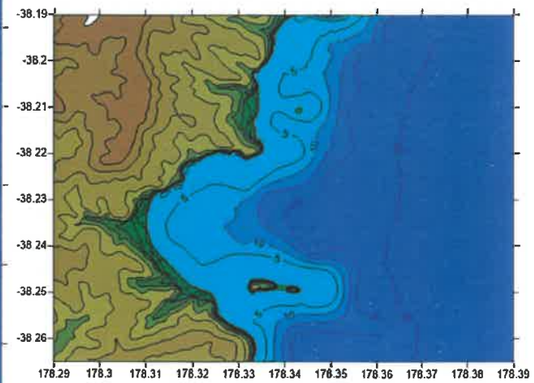

Anaura Bay

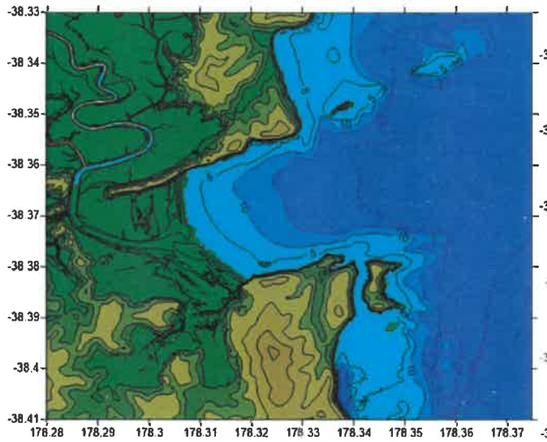

Tolaga Bay

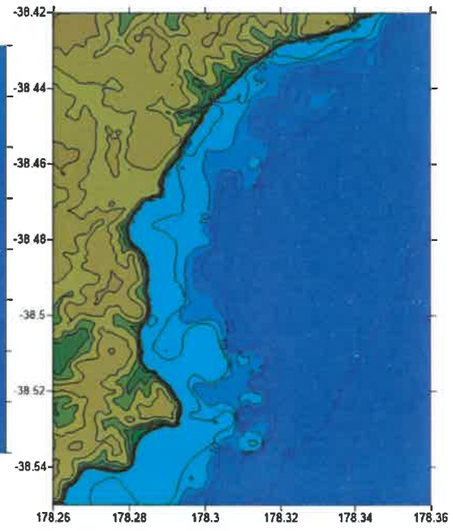

Waihau Bay

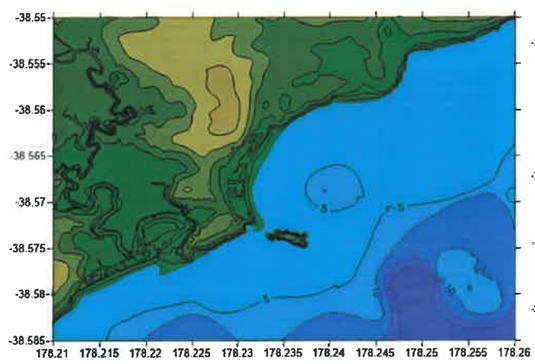

Whangara

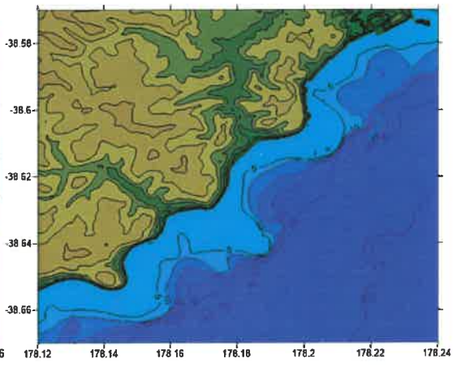

Pouawa

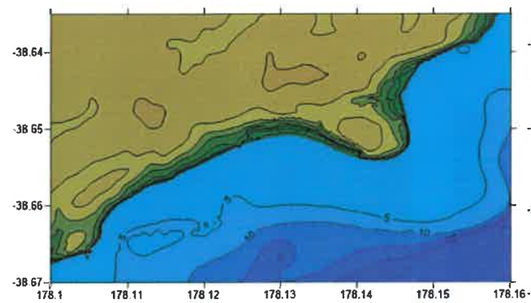

Makorori

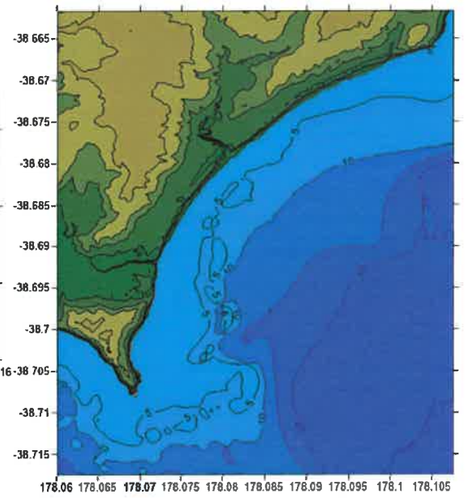

Wainui

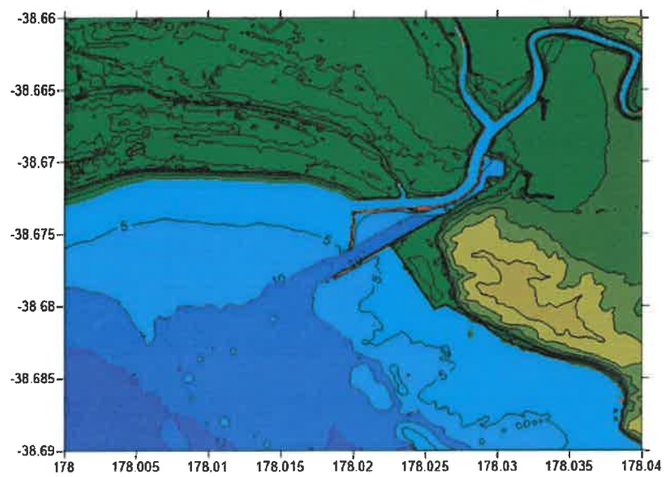

Gisborne Port and Town

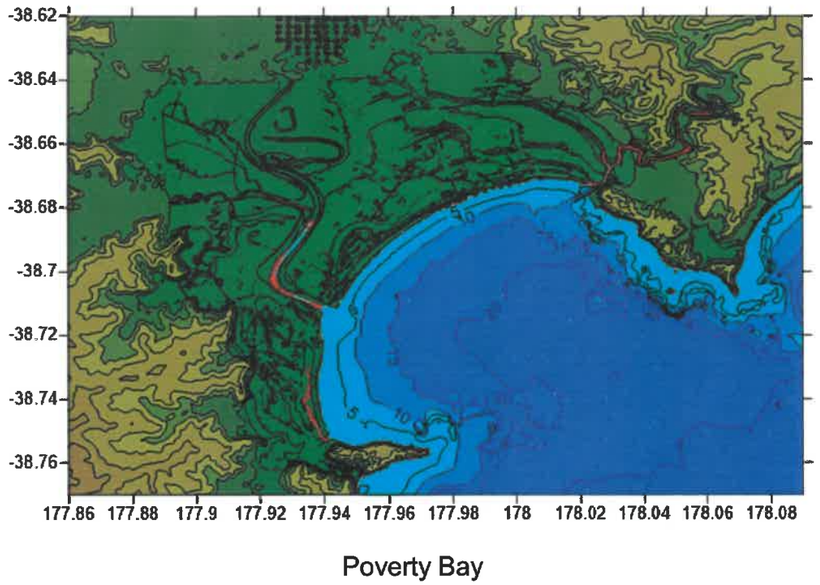

Figure 9.2 The C level numerical modelling grids organised from north to south.

10 APPENDIX 3: WAIHI BEACH: GRID SIZE SENSITIVITY STUDY

Although not part of the project scope, a sensitivity study on the inundation and overland flow depths as a function of model grid resolution was conducted. For this analysis, the 2500-year RI event was run over three model set ups each using the same outer A and B level grids. The innermost C-level grids were run for three different resolutions 50-m, 20-m and 10-m. The model grid details are presented in Table 10.1. The model was run over the mean sea level bathymetry.

Table 10.1 Grid resolutions, time steps and model run-times for the sensitivity study.

Grid	nx	ny	dx	dt	Run time
	(nodes)	(nodes)	(m)	(sec)	(min)
A	458	365	1254.8	6.71	n/a
B	443	389	199.7	2.27	n/a
Waihi Beach					
C: 50 m	222	312	50.0	2.49	26
C: 20 m	554	778	20.1	1.0	86
C: 10 m	1107	1555	10.0	0.5	534

The raw model results are presented in Figure 10.1 showing the computed flow depths over each of the three grid resolutions. In Figure 10.2 we plot the model results along a shore normal transect both for both the original grid spacing (i.e. 10, 20 or 50 m) as well as for grids interpolated to 10 m resolution.

To assess the differences, the results from the coarser (20 and 50-meter grids) were interpolated to a 10 m grid. Then a difference plots were made by subtracting the interpolated gird results from the original 10 m grid, i.e.:

- 10 m results MINUS interpolated 20 m results and
- 10 m results MINUS interpolated 50 m results.

The resulting data set would produce positive numbers where the 10 m flow depths are greater and negative numbers where the 20 or 50 m results were larger. These difference plots are presented in Figure 10.3 and Figure 10.4 for the full grid extents and close-up regions respectively.

The difference plots show that at the shoreline, the model produce higher flow depths on the finer scale grids, but that as the flow proceeds inland, the coarser grids produce greater flow depths

The full set of model results are presented in Figure 10.5 through Figure 10.7 with plots for maximum computed tsunami height, tsunami current speed, overland flow depth and overland flow speed.

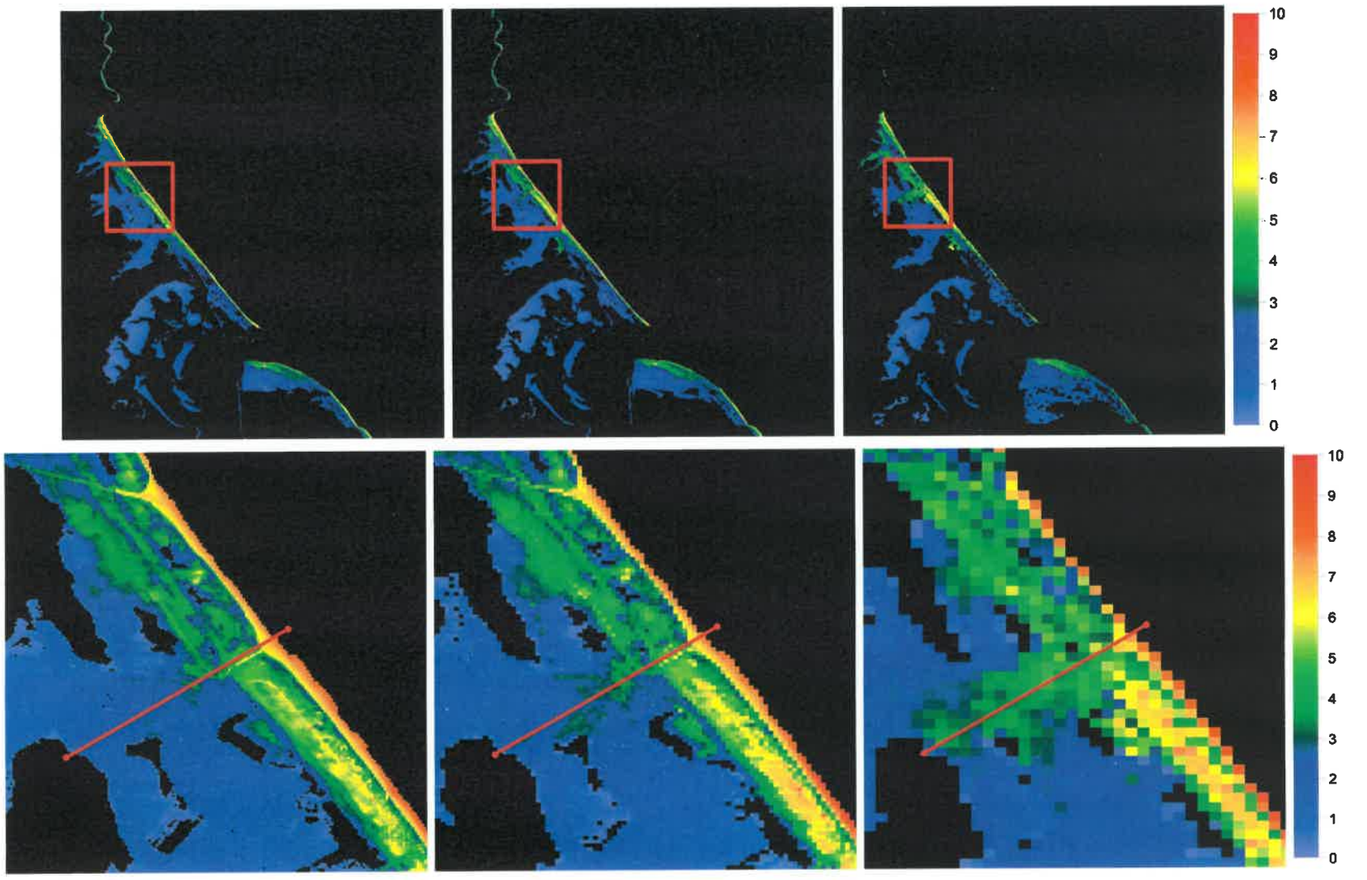

Figure 10.1 Flow depth over the 10 m (left) 20 m (middle) and 50 m (right) grids. Zoomed area is indicated by the red rectangle.

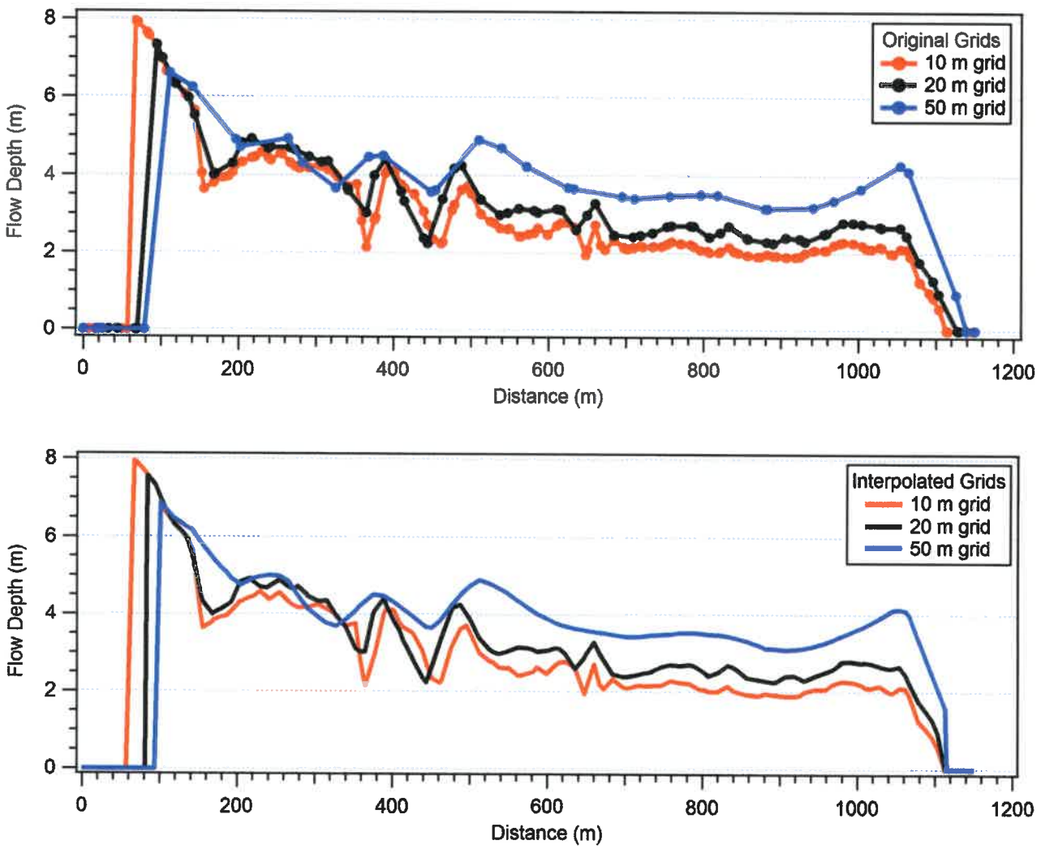

Figure 10.2 Computed maximum flow depths along the transects indicated in Figure 10.1 above.

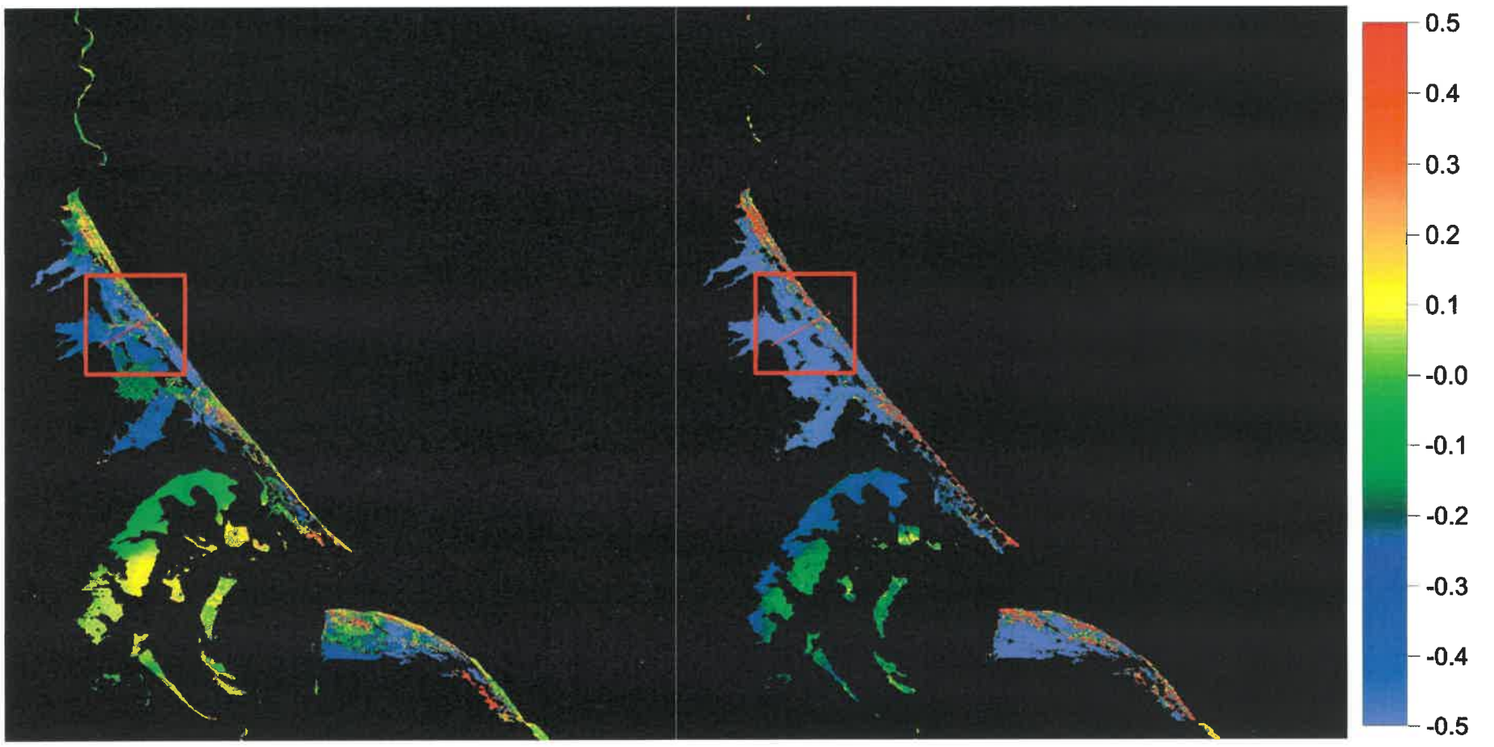

Figure 10.3 Difference in computed flow depth. 10 m results MINUS 20 m results (left) and 10 m results MINUS 50 m results (right). Colour scale is in meters.

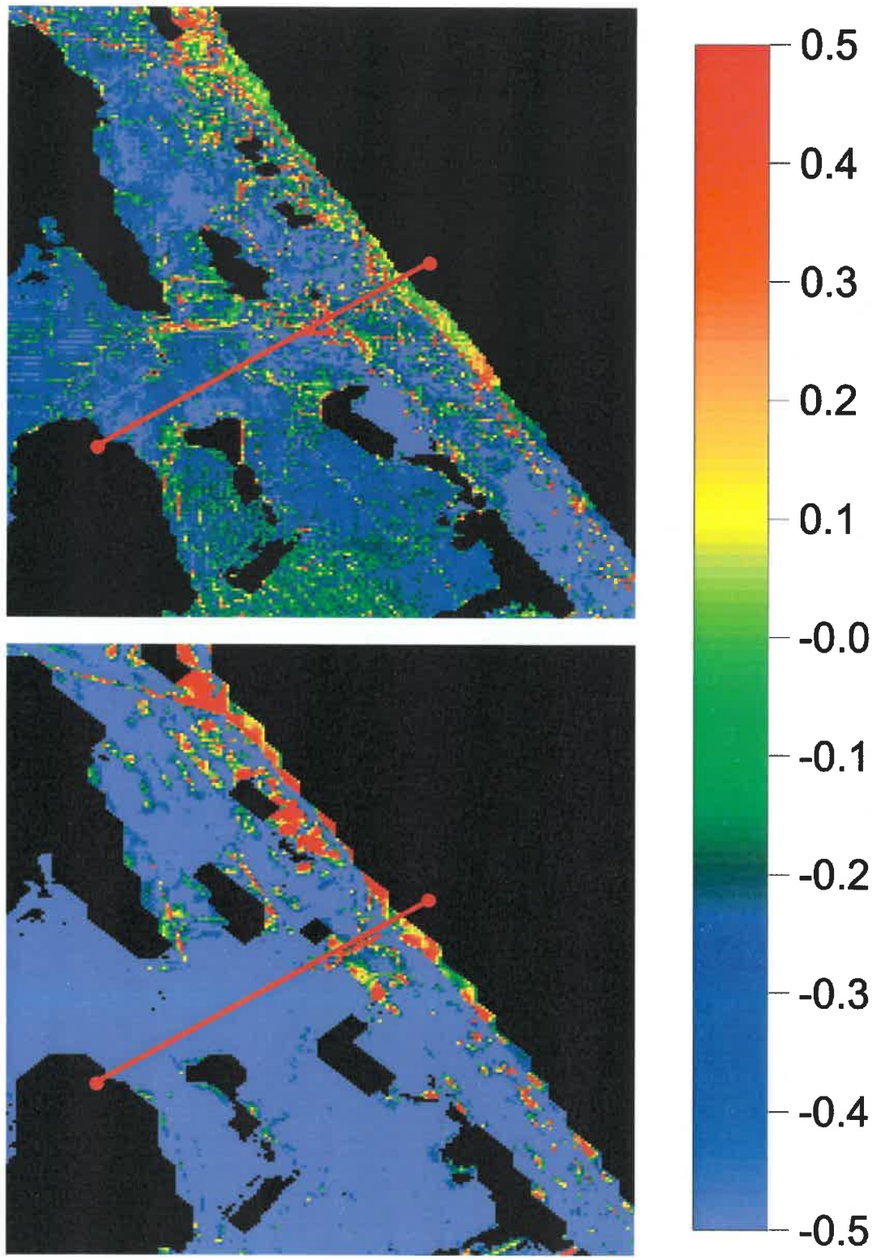

Figure 10.4 Difference in computed flow depth. 10 m results MINUS 20 m results (top) and 10 m results MINUS 50 m results (bottom). Colour scale is in meters.

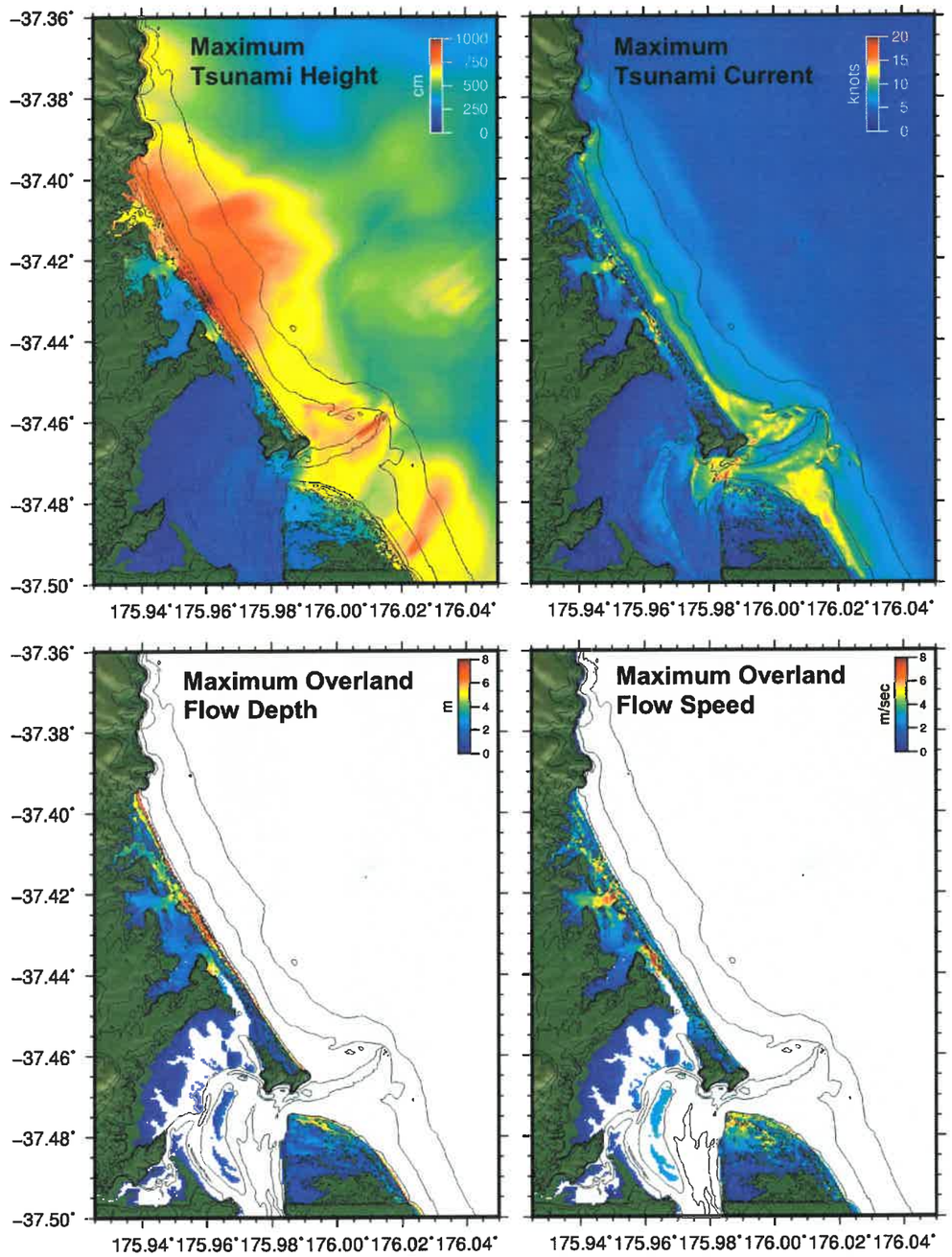

Figure 10.5 Model results for the 50-m C grid

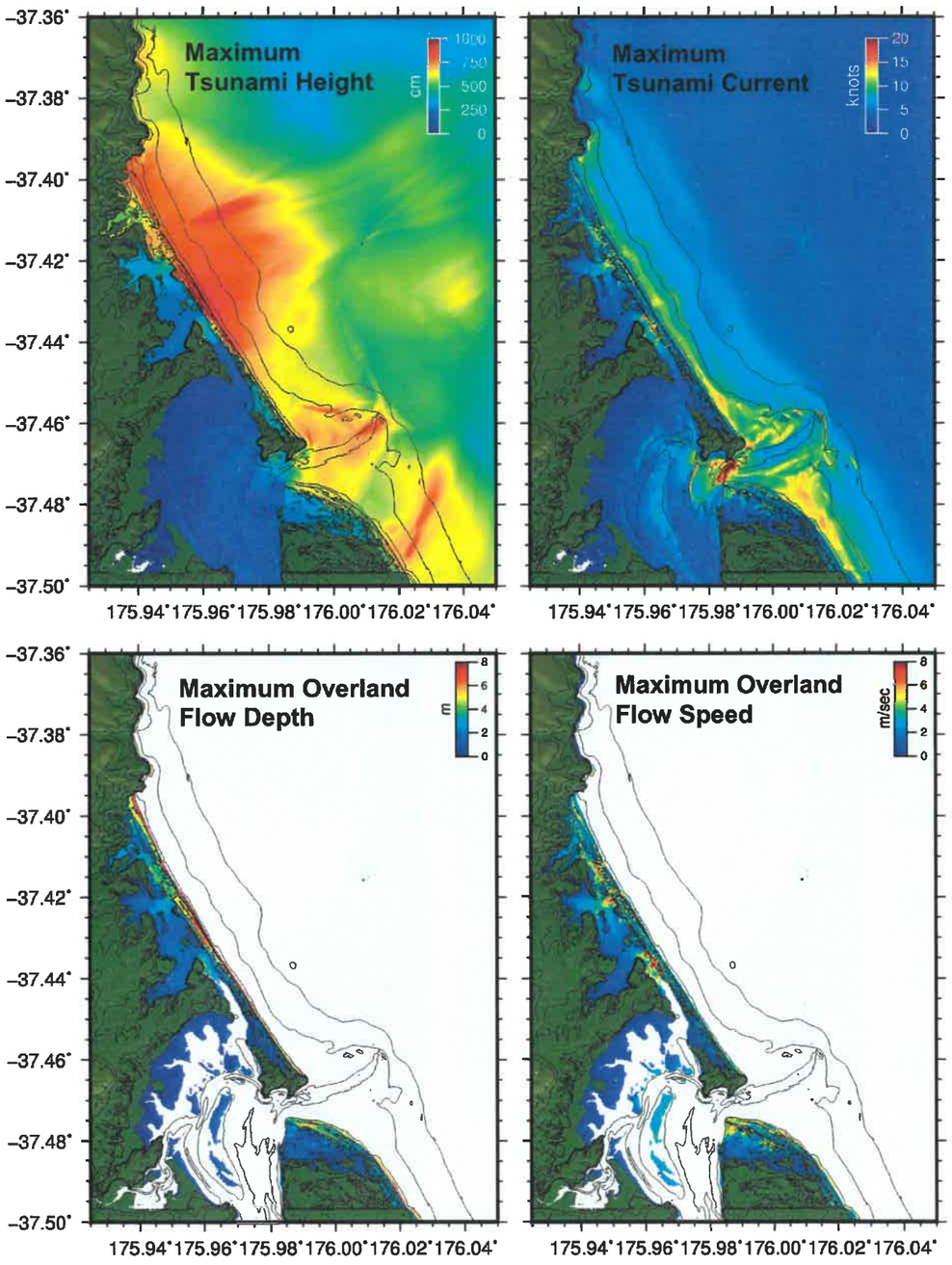

Figure 10.6 Model results for the 20-m C grid

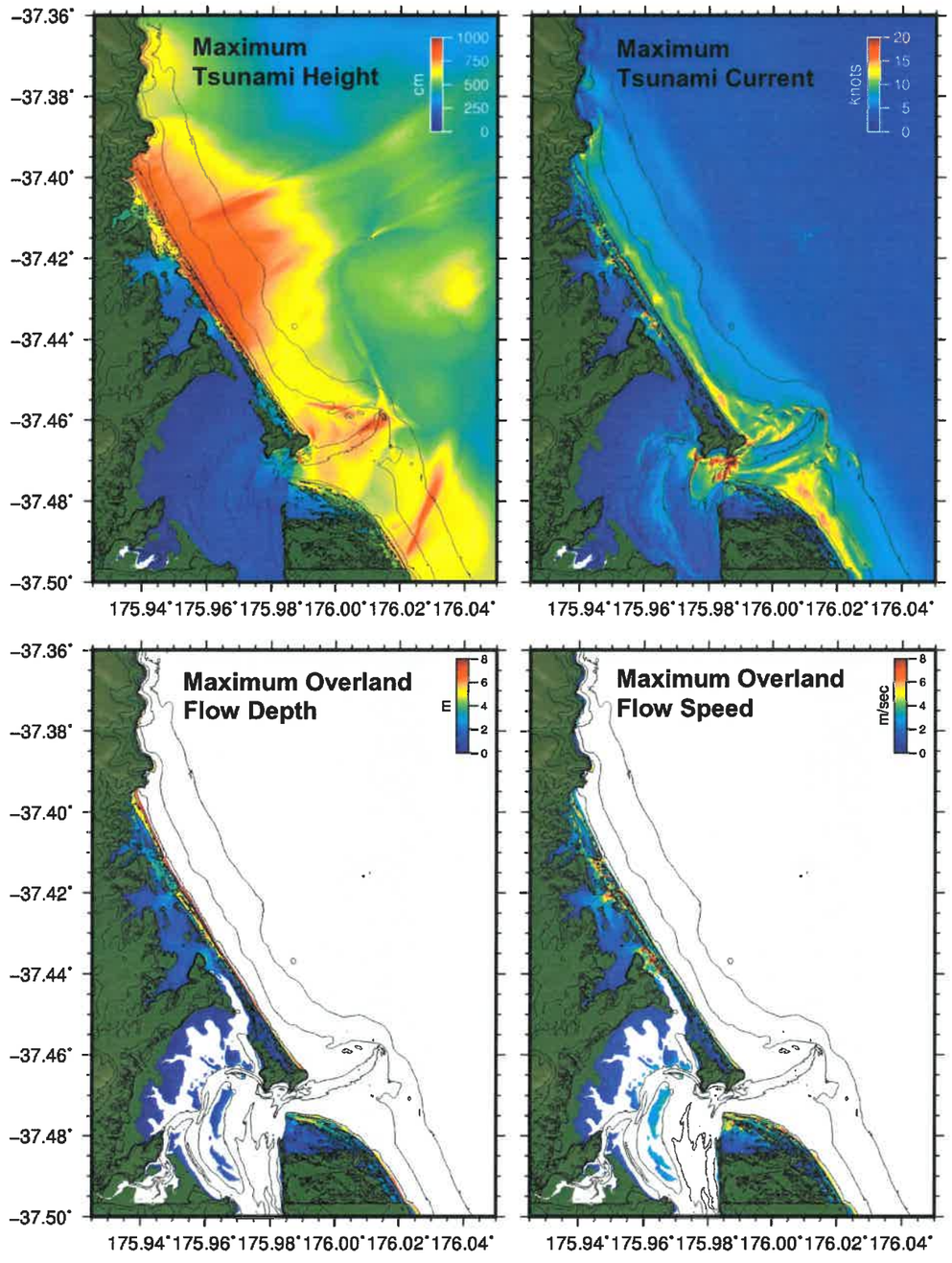

Figure 10.7 Model results for the 10-m C grid